

| REPORT DOCUMENTATION PAGE | | READ INSTRUCTIONS BEFORE COMPLETING FORM |
|---|---------------------------|--|
| 1. REPORT NUMBER NRL Report 8778 | 2. GOVT ACCESSION NO. | 3. RECIPIENT'S CATALOG NUMBER |
| 4. TITLE (and Subtitle) FREQUENCY STABILITY ANALYSIS OF THE GPS NAVSTARS 3 AND 4 RUBIDIUM CLOCKS AND NAVSTARS 5 AND 6 CESIUM CLOCKS | | 5. TYPE OF REPORT & PERIOD COVERED Final report on one phase of the NRL problem. |
| | | 6. PERFORMING ORG. REPORT NUMBER |
| 7. AUTHOR(s) Thomas B. McCaskill, James A. Buisson, and Sarah B. Stebbins | | 8. CONTRACT OR GRANT NUMBER(s) |
| 9. PERFORMING ORGANIZATION NAME AND ADDRESS Naval Research Laboratory Washington, DC 20375 | | 10. PROGRAM ELEMENT, PROJECT, TASK AREA & WORK UNIT NUMBERS X06999CC |
| 11. CONTROLLING OFFICE NAME AND ADDRESS Navy Space Project Naval Electronic Systems Command Washington, DC 20360 | | 12. REPORT DATE December 20, 1983 |
| | | 13. NUMBER OF PAGES 110 |
| 14. MONITORING AGENCY NAME & ADDRESS (if different from Controlling Office) | | 15. SECURITY CLASS. (of this report) UNCLASSIFIED |
| | | 15a. DECLASSIFICATION/DOWNGRADING SCHEDULE |
| 16. DISTRIBUTION STATEMENT (of this Report) Approved for public release; distribution unlimited. | | |
| 17. DISTRIBUTION STATEMENT (of the abstract entered in Block 20, if different from Report) | | |
| 18. SUPPLEMENTARY NOTES | | |
| 19. KEY WORDS (Continue on reverse side if necessary and identify by block number) | | |
| NAVSTAR | Allan variance | Noise process |
| GPS (Global Positioning System) | Smoothed orbit estimation | FM |
| Time domain analysis | Frequency stability | PM |
| Cesium clock | Ensemble average | |
| Rubidium clock | Confidence limits | |
| 20. ABSTRACT (Continue on reverse side if necessary and identify by block number) | | |
| <p>This report describes the on-orbit frequency stability performance analysis of the Global Positioning System (GPS) NAVSTARS 3 and 4 rubidium clocks and the NAVSTARS 5 and 6 cesium clocks. Time domain measurements, taken from the four GPS monitor sites, have been analyzed to estimate the short- and long-term frequency stability performance of the NAVSTAR clocks. The data presented include measurements from 1981, 1982, and the first 100 days of 1983.</p> | | |

LIBRARY
RESEARCH REPORTS DIVISION
NAVAL POSTGRADUATE SCHOOL
MONTEREY, CALIFORNIA 93943

NRL Report 8778

Frequency Stability Analysis of GPS NAVSTARs 3 and 4 Rubidium Clocks and the NAVSTARs 5 and 6 Cesium Clocks

THOMAS B. MCCASKILL, JAMES A. BUISSON, AND SARAH B. STEBBINS

*Space Applications Branch
Aerospace Systems Division*

December 20, 1983



NAVAL RESEARCH LABORATORY
Washington, D.C.

Approved for public release; distribution unlimited.

CONTENTS

| | |
|---|----|
| INTRODUCTION | 1 |
| GPS SYSTEM DESCRIPTION | 2 |
| GPS ON-ORBIT CLOCK ANALYSIS | 3 |
| TIME-DOMAIN CLOCK ANALYSIS | 6 |
| ALLAN VARIANCE SET SELECTION CRITERIA | 7 |
| CLOCK ANALYSIS RESULTS FORMAT | 12 |
| NAVSTAR-3 Clock Results | 18 |
| NAVSTAR-4 Clock Results | 24 |
| NAVSTAR-5 Clock Results | 28 |
| NAVSTAR-6 Clock Results | 32 |
| MONITOR STATION ENSEMBLE CLOCK ANALYSIS | 37 |
| CONCLUSIONS | 47 |
| ACKNOWLEDGMENTS | 48 |
| REFERENCES | 48 |
| GLOSSARY | 50 |
| APPENDIX – NAVSTAR Time-Domain Plots | 53 |

FREQUENCY STABILITY ANALYSIS OF THE GPS NAVSTARs 3 AND 4 RUBIDIUM CLOCKS AND THE NAVSTARs 5 AND 6 CESIUM CLOCKS

INTRODUCTION

The NAVSTAR Global Positioning System (GPS) is a Department of Defense (DOD) space-based satellite system. When operational in the late 1980s, 18 to 24 satellites in six orbital planes will provide accurate navigation information to users anywhere in the world. Examples of GPS use are weapons delivery, point-to-point navigation, search/rescue operations, and passive rendezvous. GPS can provide navigational updates to platforms with other navigational systems.

One role of the Naval Research Laboratory (NRL) in GPS is to provide space-qualified atomic clocks for use in the NAVSTAR spacecraft. The responsibility of NRL includes preflight and postflight frequency stability analyses [1,2] to ensure that on-orbit accuracy and stability requirements are met.

This report describes the on-orbit frequency stability performance analysis of the GPS NAVSTARs 3 and 4 rubidium clocks and the NAVSTARs 5 and 6 cesium clocks. Time-domain measurements, taken from the four GPS Monitor Sites (MS), have been analyzed to estimate the short- and long-term frequency stability performance of the NAVSTAR clocks. The results include long-term (1- to 10-day sample times) results for data collected during 1981, 1982, and the first 100 days of 1983. Short-term (900- to 7200-s sample times) results are presented for data collected during 1982 and the first 100 days of 1983.

The first part of the report briefly describes the NAVSTAR GPS system with emphasis on the clock measurements. Equations are then presented which permit the separation of the orbital signal, and other smaller effects, from the clock offset between a NAVSTAR clock and a GPS MS clock. A time-domain analysis of the NAVSTARs 3, 4, 5, and 6 clocks is then presented. The Allan variance is used as the measure of frequency stability in the time domain. The results presented include a time-domain noise analysis, to identify the random periodic noise processes that are present in the NAVSTAR cesium and rubidium clocks. Readers who are familiar with the mathematical theory of clock analysis may choose to proceed directly to the section on clock analysis results.

GPS SYSTEM DESCRIPTION

The NAVSTAR GPS system comprises three major segments:

(a) Control Segment

The current GPS Control Segment consists of a master control station (MCS), located at Vandenberg, Calif. and four monitor sites. One MS is located adjacent to the MCS at Vandenberg; the remaining three remote monitor sites are located at Hawaii, Alaska, and Guam. These four stations track the GPS space vehicles (SV). Data from these sites are transmitted to the MCS and processed to determine SV orbits and clock offsets. A separate Satellite Control Facility is used to transmit commands and navigational information to the GPS spacecraft.

(b) *Space Segment*

During the period covered in this report, the GPS Space Segment constellation consisted of five NAVSTAR SVs; NAVSTAR-8 was launched on July 14, 1983. The launch dates and clock information are detailed in Table 1:

Table 1—Launch Dates and Frequency Standard Type of NAVSTAR SVs

| GPS SV | Launch Date | Current Frequency Standard |
|--------|-------------|----------------------------|
| NAV-1 | 2/22/78 | Quartz |
| NAV-3 | 10/07/78 | Rubidium |
| NAV-4 | 12/11/78 | Rubidium |
| NAV-5 | 2/09/80 | Cesium |
| NAV-6 | 4/26/80 | Cesium |
| NAV-8 | 7/14/83 | Rubidium |

Each GPS space vehicle continuously broadcasts spread spectrum signals in *L*-band. The center frequency values are at 1227.6 and 1575.42 MHz, which are designated as L_1 and L_2 , respectively. The signal waveform is a composite of two pseudorandom noise (PN), phase-shift-key (PSK) signals transmitted in phase quadrature. These two signals are referred to as the *P*-signal and the *C/A* signal.

The *P*-signal provides the capability for precise navigation, is resistant to electronic countermeasures (ECM) and multipath, and could be denied to unauthorized users by means of transmission security (TRANSEC) devices.

The *C/A* signal provides a ranging signal for users whose navigation requirements are less precise. In addition, this signal serves as an acquisition aid for authorized users to gain access to the *P*-signal. The *C/A* designation indicates the *clear* and *acquisition* functions of this waveform.

Orthogonal binary coded sequences, transmitted from each GPS satellite, provide a capability for identifying each individual satellite. This technique is known as Code Division Multiple Access (CDMA). By means of a correlation detector, one can measure the apparent time difference between transmission of the signal and arrival of the signal as determined by the user's receiver clock. This apparent time difference is composed of two parts—the signal propagation delay from the satellite transmitter to the user and the unknown offset of the user clock. Each GPS spacecraft transmits a navigation message which is modulated onto the signal and may be decoded and used in the calculation of the user's position, velocity, and clock offset.

(c) *User Segment*

The GPS User Segment is composed primarily of users from DOD and the NATO community. Selective civilian use of GPS is being considered, with appropriate restrictions to limit the accuracy.

A high accuracy GPS navigational solution is obtained from four simultaneous measurements of apparent time difference. These measurements are called pseudorange (PR) measurements because the signal must travel from the GPS spacecraft to the user's receiver, a distance of about 20,000 to 25,000 km. Hence this delay is present in addition to the actual clock difference. The time differences are taken between the user receiver clock and each of the NAVSTAR spacecraft clocks. Using a computer-controlled receiver, the GPS user tunes and locks the GPS receiver to signals which are broadcast from the NAVSTAR SVs, and then makes four simultaneous PR measurements. The four

NAVSTAR SV positions are calculated from the GPS navigation message, which is modulated onto each GPS signal. These four PR measurements are then used to calculate a navigational solution [3,4] for the user's latitude, longitude, height, and clock offset. GPS provides a near-instantaneous navigation capability for users on a worldwide basis.

A GPS navigational solution for the user's velocity and clock rate may be computed through the use of four additional simultaneous measurements of apparent frequency difference. These apparent frequency difference measurements are called pseudorange-rate (PR-rate) measurements, because the relative motion between the GPS spacecraft is present in addition to the clock rate difference. The basic GPS navigation solution for user position and clock offset is independent of the user's velocity and clock rate; however, the user's position is required for the velocity solution. Alternately, the solution for velocity and clock rate may be estimated from two or more successive GPS position and clock offset solutions.

GPS ON-ORBIT CLOCK ANALYSIS

The GPS instantaneous navigation capability is possible because each NAVSTAR clock is synchronized to a common GPS time. The clock offset, orbital elements, and spacecraft health parameters of all spacecraft in the GPS constellation are periodically determined at the GPS master control station (MCS). These clock offsets, orbital elements, and spacecraft health parameters are then uploaded to each NAVSTAR SV and inserted into the GPS navigation message. Each NAVSTAR clock must then keep time, to within GPS specifications, until the next clock update. The time stability of a clock is related to its frequency stability; therefore, a fundamental measure of GPS clock performance is the frequency stability of the clock. The Allan variance is the statistical measure of frequency stability that is used for reporting clock performance.

The procedure that has been devised at NRL [5,6] for determining GPS clock performance is presented in Fig. 1. The goal of this technique is to separate the clock offset from the orbital and other effects that are present in the GPS signal. This procedure utilizes a highly redundant set of PR, and PR-rate measurements, that are collected from all four GPS MS during 2-week intervals. This redundant set of measurements allows the determination of clock and orbit states that are independent of the GPS MCS realtime Kalman estimation procedure. A description of this technique follows, with emphasis on the variables related to clock performance analysis.

Measurements of PR and integrated PR-rate are taken between the NAVSTAR SV clock and the MS clock by using a spread spectrum receiver. The MS receivers are capable of making measurements from four GPS SVs, simultaneously, whenever four or more SVs are above the MS horizon. The measurements are taken once every 6 s and then aggregated and smoothed once per 15 min. Figure 2 presents a plot of a typical PR signature obtained from a single NAVSTAR satellite pass over an MS. Each measurement is corrected for equipment delay, ionospheric delay, tropospheric delay, earth rotation, and relativistic effects. The data are then edited and smoothed after subtracting the predicted SV ephemeris and clock offset, which removes most of the signal. Following the smoothing procedure, the predicted values are added to the smoothed values to produce the smoothed measurements. The clock offset is evaluated near the midpoint of the 15-min data span, using a cubic polynomial model and both the PR and the PR-rate measurements.

The PR measurements are resolved to 1/64 of a *P*-code chip, which corresponds to 1.5 ns of time, or 46 cm in range. Nominal values of PR noise levels are $\sigma_{PR} = 1.3$ m for the L_1 measurements, and $\sigma_{PR} = 2.0$ m for the L_2 measurements. The L_1 and L_2 measurements are combined to correct for ionospheric refraction, which results in an increase to $\sigma_{PR} = 4.53$ m for the corrected PR measurements. The accumulated ΔPR measurement noise levels are 0.31 cm for L_1 and 0.56 cm for L_2 .

NAVSTAR GPS LONG-TERM FREQUENCY STABILITY ANALYSIS FLOW CHART

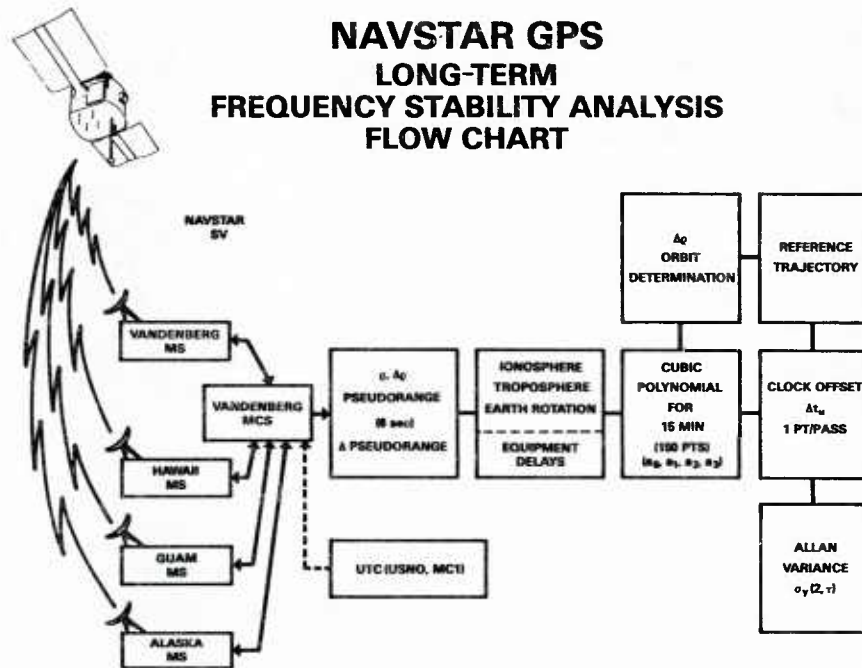


Fig. 1 -- NRL on-orbit clock performance analysis procedure

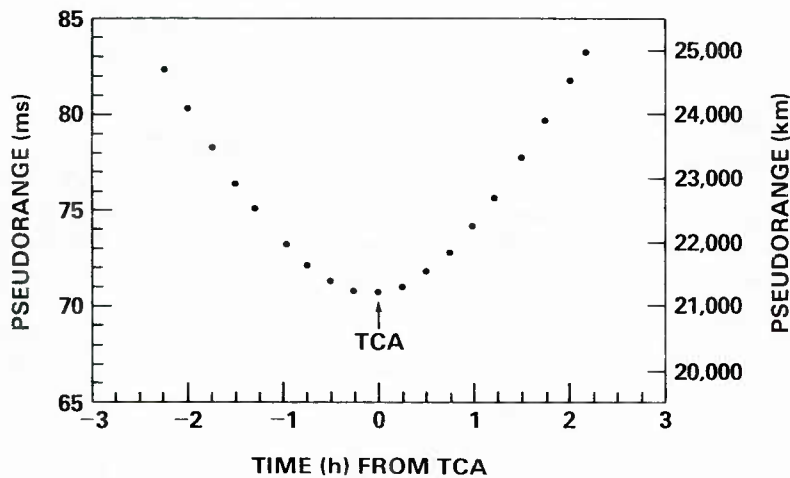


Fig. 2 -- Typical NAVSTAR-4 pseudorange signature

These measurements are also combined to correct for ionospheric refraction. The smoothing procedure uses the PR-rate measurements to aid in the PR smoothing of each 15-min segment of data. This process [7] results in a smoothed PR measurement noise level of 18.5 cm.

The equation that relates the PR measurement to the clock difference between the NAVSTAR SV clock and the MS clock is

$$PR = R + c(t_{MS} - t_{SV}) + ct_A + \epsilon \quad (1)$$

where

- PR is the measured pseudorange,
- R is the slant range (also known as the geometric range) from the SV (at the time of transmission) to the MS (at the time of reception),

c is the speed of light,
 t_{MS} is the MS clock time,
 t_{SV} is the SV clock time,
 t_A is ionospheric, tropospheric, and relativistic delay, with corrections for
 antenna and equipment delays, and
 ϵ is the measurement error.

The clock difference, $(t_{SV} - t_{MS})$, is obtained by dividing by c —the speed of light—and rearranging Eq. (1) into

$$(t_{SV} - t_{MS}) = R/c + t_A + \epsilon/c - PR/c. \quad (2)$$

In Eq. (1), the PR is a measure of distance, typically expressed in km. In Eq. (2), the unit of measure is time, typically expressed in ms.

The clock difference $(t_{SV} - t_{MS})$ may be defined as a new variable, $x(t_k)$, so that

$$x(t_k) = (t_{SV} - t_{MS}). \quad (3)$$

In this report, the subscript k is used to denote the time of measurement as determined by the MS clock. This definition of $x(t_k)$ is made so that the clock difference notation will agree with referenced literature; the clock difference is also denoted by the variable Δt_k , so that

$$\Delta t_k = (t_{SV} - t_{MS}). \quad (4)$$

The variables $x(t_k)$ and Δt_k are equivalent; the choice of variable will be one of convenience.

All of the smoothed PR measurements from the four GPS monitor sites are collected at the GPS MCS. These measurements are processed to produce a real-time estimate of each of the NAVSTAR clock and ephemeris states. These smoothed measurements are further processed in postflight analysis to produce a smoothed estimate of the NAVSTAR ephemerides.

The realtime estimates of the NAVSTAR SV clock and ephemeris states are made using a Kalman [8,9] estimator which has been adapted for GPS use [10]. The success of the estimation technique is critically dependent on the stability of the NAVSTAR SV and MS clocks. For example, Fig. 2 presents the time delay that occurs as the NAVSTAR signal travels from the spacecraft to a GPS MS. This figure indicates a change in apparent time differences of 15 ms (or 15,000,000 ns) during the first 3 h of this NAVSTAR pass. Current GPS specifications call for a maximum clock uncertainty of about 5 ns during the pass. If the NAVSTAR SV clock does not meet this specification, then the Kalman estimator has difficulty in separating the orbit part of the GPS signal from the clock noise. Equation (2) shows that the MS clock has the same weight in the measurement as the NAVSTAR clock; therefore, it is highly desirable to have an MS clock of equal or better time stability at each GPS MS.

Smoothed estimates for the NAVSTAR orbits are routinely made by the Naval Surface Weapons Center (NSWC), using an orbit estimation program [11]. The model includes dynamics of the satellite motion, solar radiation pressure, pole wander, earth tides, and orbit adjust maneuvers. The smoothed orbits are made once per week, using all available observations for a 2-week span from each of the four GPS monitor sites. The PR measurements are differenced to compute Δ PR values which are used as the measured quantity in the NSWC program. The model incorporates a segmented bias parameter solution, with analysis of the resulting residual patterns of the smoothed orbit estimation.

The major advantage of the smoothed orbit estimate, over the Kalman realtime estimate, is the production of a smoothed orbit which is almost completely determined by the data, without restrictive assumptions on the uncertainty in clock and orbit states.

TIME-DOMAIN CLOCK ANALYSIS

GPS operation requires that the on-orbit NAVSTAR SV clocks keep the current GPS time. Because the clocks are periodically updated, it is important to evaluate clock performance as a function of the sample time τ , which is the difference between two successive values of running time.

Given two clock measurements, $x(t_k)$ and $x(t_j)$, which were made at running times t_k and t_j (by the GPS MS clock), the sample time τ is given as

$$\tau = (t_k - t_j). \quad (5)$$

This sample time is varied from 900 s to 10 days (in this report) to evaluate clock performance.

One clock model used to describe the NAVSTAR clock as a function of time is a quadratic equation of the form

$$x(t) = x_0(t_0) + y_0(t_0)(t - t_0) + \frac{\dot{y}_0(t_0)(t - t_0)^2}{2} + \epsilon(t). \quad (6)$$

In Eq. (6), $x_0(t_0)$ is the initial clock offset, $y_0(t_0)$ is the clock rate (also known as the fractional frequency offset), $\dot{y}_0(t_0)$ is the drift in the fractional frequency (also known as the aging rate), and $\epsilon(t)$ is the error term.

By choosing $\tau = (t - t_0)$ and omitting the error term, Eq. (6) can be written as

$$x(t) = x_0(t_0) + y_0(t_0)\tau + \frac{\dot{y}_0(t_0)\tau^2}{2}. \quad (7)$$

By holding the value of τ fixed, and evaluating Eq. (7) for many data samples, the statistical error in the clock coefficients and the error term can be estimated.

The measure of clock performance used in the analysis of this report is the Allan variance [12], which is defined by

$$\sigma_y^2(\tau) = \frac{\langle (\bar{y}_{k+1} - \bar{y}_k)^2 \rangle}{2} \quad (8)$$

where \bar{y}_k denotes the average fractional frequency, τ denotes the sample time, and the brackets $\langle \rangle$ denote the infinite time average. Two other parameters are involved in the Allan variance analysis. The first parameter is the repetition interval T , which is equal to the sample time in Eq. (8). The other parameter is f_h , the system noise bandwidth, which does not explicitly appear in the Allan variance equation. The system noise bandwidth is receiver dependent, and depends upon user dynamics. Information on the GPS MS receivers may be found in Ref. 13.

The fractional frequency, denoted by the variable y , is given by

$$y = \frac{(\nu - \nu_0)}{\nu_0} \quad (9)$$

where ν is the instantaneous frequency, and ν_0 is the reference, or nominal frequency. The average fractional frequency, denoted by y_k , is given by

$$\bar{y}_k = \frac{1}{\tau} \int_{t_k}^{t_k + \tau} y(t) dt. \quad (10)$$

Equation (10) shows that \bar{y}_k depends on t_k and τ , as well as $y(t)$; so \bar{y}_k could be written as $\bar{y}(t_k, \tau)$ to show this dependence. The values for \bar{y}_k used in this report are obtained from values of clock offset $x(t_k)$ computed according to Eq. (3). The average frequency \bar{y}_k may be evaluated in terms of $x(t)$, as given by

$$\bar{y}_k = \frac{1}{\tau} [x(t_k + \tau) - x(t_k)]. \quad (11)$$

The infinite time average required in Eq. (8) for the Allan variance is, of course, unobtainable in the real world. Therefore, a finite approximation of the Allan variance, given by Eq. (12), is used.

$$\sigma_y^2(2, \tau, M) = \frac{1}{(M-1)} \sum_{k=1}^{M-1} \frac{(\bar{y}_{k+1} - \bar{y}_k)^2}{2}. \quad (12)$$

The arguments of the finite approximation, $\sigma_y^2(2, \tau, M)$, are 2, τ , M , respectively. The number 2 specifies that pairs of fractional frequencies are used, τ denotes the sample time, and $(M-1)$ denotes the number of frequency pairs.

The difference between $\sigma_y^2(\tau)$ and $\sigma_y^2(2, \tau, M)$ is that $\sigma_y^2(\tau)$ is the desired quantity defined by an infinite series and $\sigma_y^2(2, \tau, M)$ is a partial series obtained from a finite number of data points. The use of a finite number of data points does not introduce any bias in the estimate of $\sigma_y^2(\tau)$ [14]. The ratio of the variables $\sigma_y^2(2, \tau, M)$ and $\sigma_y^2(\tau)$ is used in establishing confidence limits for $\sigma_y^2(\tau)$.

The convergence of this finite-sample average, $\sigma_y^2(2, \tau, M)$, towards a theoretical limit has been investigated by Lesage and Audoin [14]. The confidence of this quantity as a measure of $\sigma_y^2(\tau)$ has also been investigated by Lesage and Audoin [14] and Barnes [15]. These theoretical results indicate that a high-confidence estimate of $\sigma_y^2(\tau)$ may be obtained through the use of large data bases, which result in a large number of frequency pairs. In practice it is desirable to have a data base length which is at least 10 times larger than the sample time.

The square root of the Allan variance is called the Allan deviation. The Allan deviation is defined as

$$\sigma_y(\tau) = [\sigma_y^2(\tau)]^{1/2}. \quad (13)$$

ALLAN VARIANCE SET SELECTION CRITERIA

The GPS measurements may be aggregated into sets for the short- and long-term frequency stability analysis. Figure 3 presents a flow diagram of this procedure. The smoothed PR measurements are combined with the reference ephemeris to produce smoothed clock offsets. Each smoothed measurement is obtained from up to 150 6-s PR and 149 Δ PR measurements. This procedure includes corrections for ionospheric, tropospheric, and equipment delays, and also for relativity effects. The set selection criteria are then applied to construct subsets of clock offset values, $\{x(t_k)\}$, which are then used to produce the $\sigma_y^2(\tau)$ Allan variance values.

For the short-term frequency stability analysis, the $\sigma_y^2(\tau)$ is computed from the set of smoothed clock offsets, using one or more satellite passes. Figure 3 indicates that sets of 5, 10, or more days have been used to compute one value of $\sigma_y^2(\tau)$.

Figure 4 presents an example of a 5-day set of NAVSTAR-3 observations as recorded at the Vandenberg MS. The plot presents the elevation angle of NAVSTAR-3 as a function of time for 5 days beginning at day 180. The elevation angle is computed every 15 min and is plotted as a dot on Fig. 4. Inspection of this plot indicates that a partial pass may occur at the beginning or end of the 5-day set.

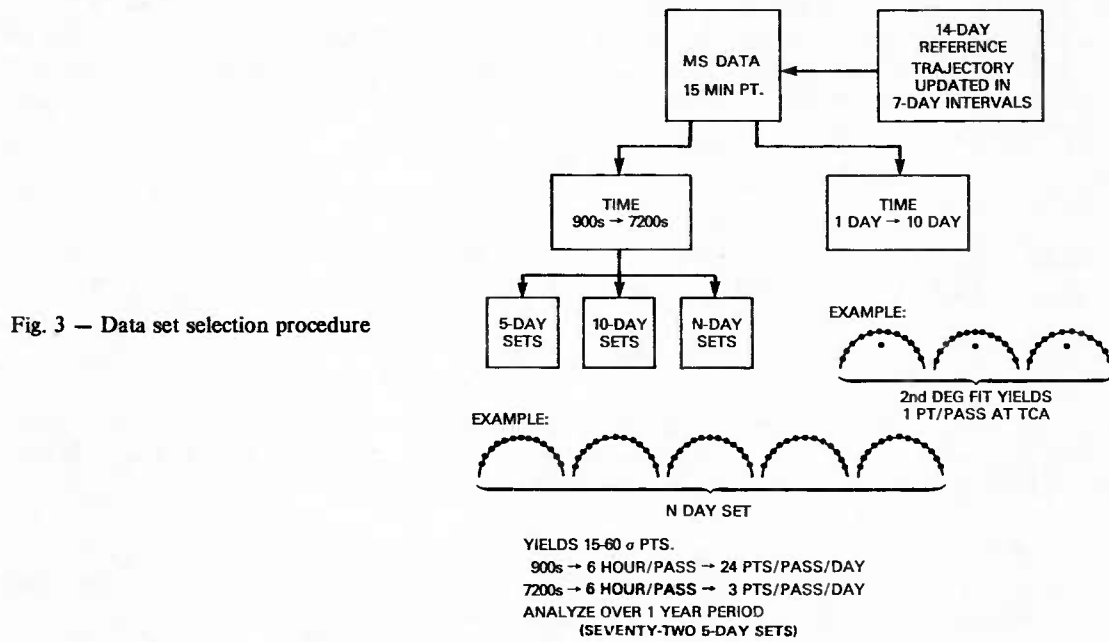


Fig. 3 — Data set selection procedure

GPS
ELEVATION ANGLE vs TIME
NAVSTAR-3 SV VANDENBERG MS

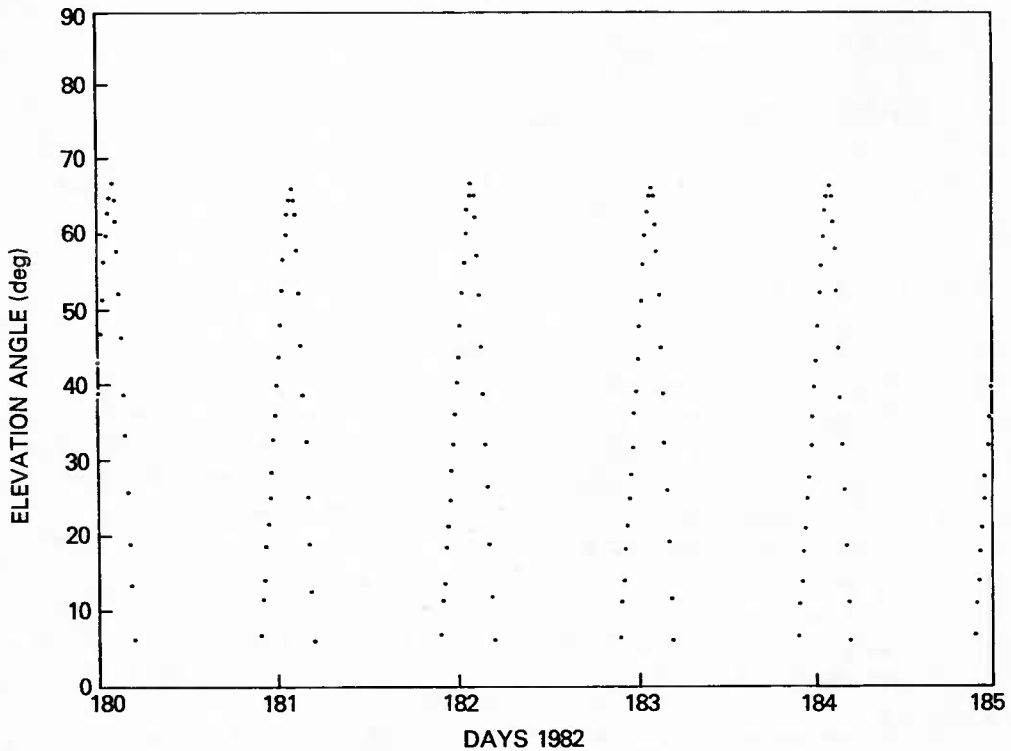


Fig. 4 — NAVSTAR-3 elevation angle vs time for a 5-day set

Note the repeating pass signature in Fig. 4 which is characteristic of all GPS orbits. This repeating signature is a result of the 12-sidereal-h GPS orbits which produce repeating ground tracks. Therefore the number of points-per-pass remains constant. For example, in Fig. 5, 28 sets of 15-min data are available from this NAVSTAR-3 pass over the Vandenberg MS. A 5-day set would contain approximately 140 data segments which could be used to obtain smoothed NAVSTAR clock offset values.

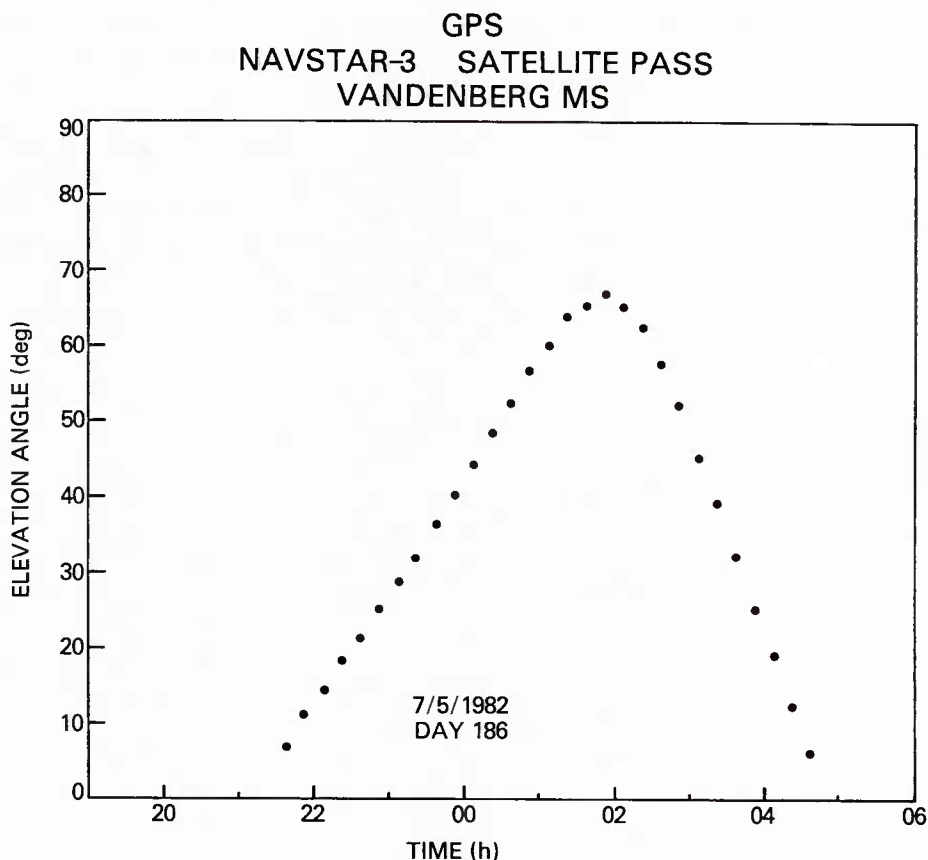


Fig. 5 — NAVSTAR-3 elevation angle vs time, for one pass

The 5-day set has been chosen for use in this report because of a tradeoff between the confidence in the Allan variance and the length of the set. The primary reason for choosing the shortest set possible is to see changes in the NAVSTAR clocks as a function of time. The reason for choosing longer sets is to increase the total number of samples in each $\sigma_y^2(\tau)$ calculation.

The number of $\sigma_y^2(\tau)$ values that are calculated may be maximized, using a procedure based on the one given in Ref. 15. This procedure involves defining a base sampling time τ_0 , which is defined as

$$\tau_0 = \text{MIN} \{ (t_k - t_j): j \neq k \}. \quad (14)$$

For the short-term frequency stability results, a nominal base sampling time of 15 min (or 900 s) will be used. For the long-term frequency stability results, a base sampling time of 1 day will be used. Multiples of the base sampling time may be calculated according to

$$\tau = n\tau_0$$

where the variable n takes on integer values 1, 2, A maximum value of $n = 8$ will be used for the short-term frequency stability analysis, and $n = 10$ for the long-term frequency stability analysis.

The number of clock offsets in a set will be denoted by the variable N . Assuming that all of the clock offsets are equispaced at sample time τ , the total number of Allan variance $\sigma_y^2(\tau)$ values (with maximal use of data) is given by the expression $(N - 2n)$. This is not the case with the data used in this report due to the nature of the GPS orbits. For both the short- and the long-term processing algorithms, each sample time is calculated according to Eq. (5) and each fractional frequency is calculated according to Eq. (11).

A calculation has been performed to produce typical values for the confidence in $\sigma_y^2(\tau)$. The $\sigma_y^2(\tau)$ value is then converted to the Allan deviation $\sigma_y(\tau)$ according to Eq. (13). Most of the reference literature expresses frequency stabilities in terms of $\sigma_y(\tau)$ rather than $\sigma_y^2(\tau)$.

The confidence limits are calculated according to the method outlined in Ref. 15, using a white noise FM process, because this is the dominant noise type that was encountered in the short-term frequency stability values. The confidence limits for a 95% confidence level, calculated for a 5-day set (Fig. 4), are presented in Table 2. These calculations have been made assuming 25 points-per-pass; however, the total number of samples for the 5-day set has been modified to account for the pass-to-pass break in the data which effectively reduces the number of samples that may be computed.

Table 2 — 95% Confidence Limits for a 5-Day Set and a White Noise FM Process

| Sample Time (h) | Confidence Limits | | Number of Samples $\sigma_y^2(\tau)$ | Degrees of Freedom |
|--------------------|-------------------|-------|--|--------------------------|
| | Upper | Lower | | |
| 0.25 | 1.189 | 0.816 | 115 | 76 |
| 0.5 | 1.211 | 0.798 | 105 | 63 |
| 0.75 | 1.253 | 0.772 | 95 | 47 |
| 1.00 | 1.299 | 0.748 | 85 | 36 |
| 1.25 | 1.344 | 0.726 | 75 | 29 |
| 1.5 | 1.403 | 0.702 | 65 | 23 |
| 1.75 | 1.444 | 0.687 | 55 | 20 |
| 2.00 | 1.499 | 0.669 | 45 | 17 |

The typical confidence limits may be used to separate random sampling fluctuations from systematic changes in clock behavior, or other changes in clock performance. For example, if a stability of 1×10^{-12} was computed for a 0.25-h sample time, the upper 95% confidence would be $(1 \times 10^{-12}) \times (1.189) = 1.189 \times 10^{-12}$. A sequence of Allan deviations, computed using successive 5-day sets, could then be analyzed using these 95% confidence limits as a guide to separate random sampling from systematic and other effects. Further inspection of Table 2 indicates that for sample times greater than 2 h, larger sets would be required to produce acceptable confidence limits in $\sigma_y(\tau)$ values.

The $\sigma_y^2(\tau)$ obtained from successive 5-day sets can be further averaged to obtain one value for the entire data span. For a 1-yr data span, seventy 5-day sets would be available for the $\sigma_y^2(\tau)$ calculation. Multiplying the degrees of freedom for a typical 5-day set (Table 2) by seventy 5-day sets per yr results in at least 1000 degrees of freedom for a 2-h sample time, and at least 5000 degrees of freedom for a 15-min sample time. Now, using a sample $\sigma_y(\tau)$ of 1×10^{-12} and the tables from Ref. 15, the 95% confidence limits would be about $\pm 4 \times 10^{-14}$, or better, for the short-term $\sigma_y(\tau)$ values.

For the long-term (1- to 10-day sample times) frequency stability analysis, one pass of a NAVSTAR SV over an MS is used as an operational set-selection criterion. Figure 6 depicts one pass of NAVSTAR-6 as observed from the Vandenberg MS. By using the set of clock offsets from one pass, a single value of clock offset is computed for the pass. The epoch for the calculation is chosen to

GPS
NAVSTAR-6 SATELLITE PASS
VANDENBERG MS

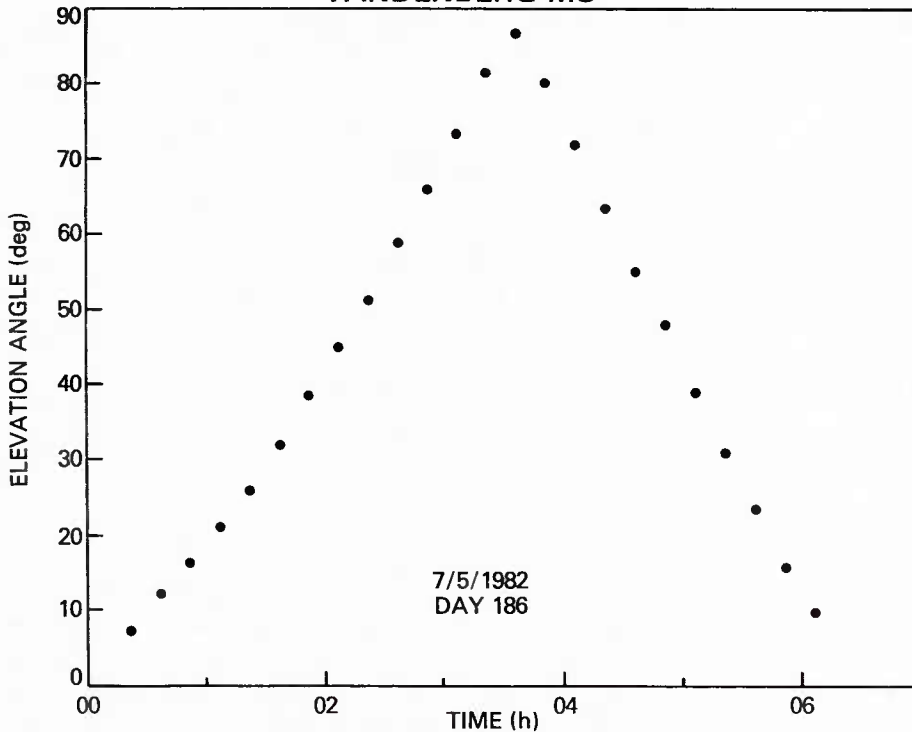


Fig. 6 — NAVSTAR-6 elevation angle vs time, for one satellite pass

be the time of closest approach (TCA) of the spacecraft to the MS. This value of clock offset is denoted as $x(t_{TCA})$. A least square objective function is used with data editing to identify and remove statistical outliers and to limit the set to points within ± 1.5 h of TCA. In addition to this procedure, a pass-to-pass constraint on the sample time τ must be met before $\sigma_y^2(\tau)$ can be computed.

For the long-term frequency stability values, two types of noise processes were encountered—random walk FM for the NAVSTAR rubidium clocks and flicker noise FM for the NAVSTAR cesium clocks. Tables 3 and 4 present the 95% confidence limits for a 1-yr data set, assuming no pass-to-pass break in the data.

Table 3 — 95% Confidence Limits for a 1-yr Set
and a Random Walk FM Noise Process

| Sample Time (days) | Confidence Limits | | Number of Samples $\sigma_y^2(\tau)$ | Degrees of Freedom |
|-----------------------|-------------------|-------|--|--------------------------|
| | Upper | Lower | | |
| 1 | 1.07 | 0.93 | 363 | 364 |
| 2 | 1.09 | 0.91 | 361 | 180 |
| 3 | 1.15 | 0.89 | 359 | 119 |
| 4 | 1.17 | 0.87 | 357 | 88 |
| 5 | 1.20 | 0.86 | 355 | 70 |
| 6 | 1.22 | 0.84 | 353 | 58 |
| 7 | 1.25 | 0.83 | 351 | 49 |
| 8 | 1.27 | 0.82 | 349 | 42 |
| 9 | 1.32 | 0.81 | 347 | 37 |
| 10 | 1.33 | 0.80 | 345 | 33 |

Table 4 — 95% Confidence Limits for a 1-yr Set and a Flicker Noise FM Process

| Sample Time (days) | Confidence Limits | | Number of Samples $\sigma_y^2(\tau)$ | Degrees of Freedom |
|--------------------|-------------------|-------|--------------------------------------|--------------------|
| | Upper | Lower | | |
| 1 | 1.07 | 0.92 | 363 | 315 |
| 2 | 1.08 | 0.91 | 361 | 224 |
| 3 | 1.13 | 0.90 | 359 | 148 |
| 4 | 1.15 | 0.89 | 357 | 110 |
| 5 | 1.17 | 0.87 | 355 | 87 |
| 6 | 1.20 | 0.86 | 353 | 72 |
| 7 | 1.22 | 0.85 | 351 | 61 |
| 8 | 1.24 | 0.84 | 349 | 53 |
| 9 | 1.25 | 0.83 | 347 | 47 |
| 10 | 1.27 | 0.83 | 345 | 42 |

CLOCK ANALYSIS RESULTS FORMAT

Two types of plots are used to present the NAVSTAR time-domain clock data. The first type of plot presents the Allan deviation, $\sigma_y(\tau)$, as a function of sample time, τ . Figure 7 illustrates this type of plot, using typical frequency stability data model curves for the NAVSTAR SV rubidium and cesium clocks, and the MS cesium clocks. The frequency stability model curves do not include the random effects of the orbital dynamics, ionospheric and atmospheric delay, relativistic effects, or the PR measurement system.

The independent variable in Fig. 7 is the sample time, which ranges from 10^3 to 10^6 s. This range covers all but 900 s of the sample times used in this report. The model may be extended to 900 s by extrapolation. The longest sample time used is 10 days (8.64×10^5 s).

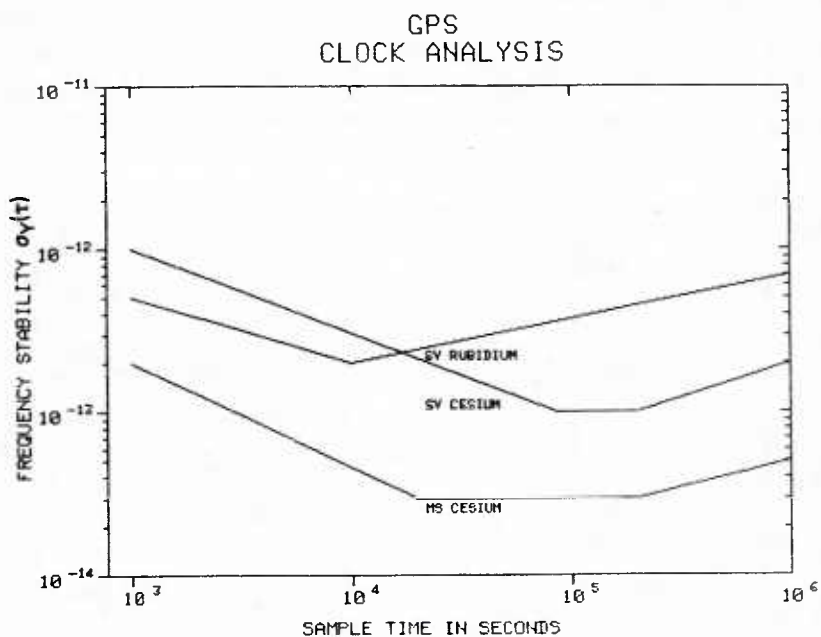


Fig. 7 — Typical frequency stability vs sample time values for rubidium and cesium clocks

The frequency stability model curves may also be used to analyze different noise processes that occur in GPS clocks. In general, five different noise processes are sufficient [16] to describe the random periodic effects encountered in cesium, rubidium, and quartz clocks. These five noise processes are obtained using three types of random noise, and two types of signal modulation. The three noise processes are white noise, flicker noise, and random walk. The two types of modulation are phase modulation (PM) and frequency modulation (FM). The resulting five types of noise processes are white noise PM, white noise FM, flicker noise PM, flicker noise FM, and random walk FM. A time-domain noise process analysis of the on-orbit NAVSTAR clock data will be presented for NAVSTARs 3, 4, 5, and 6.

The second type of plot used presents the $\sigma_y(\tau)$ averaged over consecutive 5-day sets, as a function of running time. Figure 8 illustrates this type of plot, presenting results obtained between the NAVSTAR-3 rubidium clock and the Vandenberg MS clock. Sixty-four 5-day sets were used to produce these $\sigma_y(\tau)$ values for a 900-s sample time.

The 1-yr $\sigma_y(\tau)$ value may be used with the 95% confidence limits to detect changes in clock performance. By using a $\sigma_y(\tau)$, calculated from a 1-yr mean $\sigma_y^2(\tau)$, as a reference point, the 95% confidence limits (from Table 5) are plotted as straight line segments on Fig. 8. Inspection of Fig. 8 indicates that all 5-day $\sigma_y(\tau)$ values are within the 95% limits, except two points between days 244 and 255, 1982.

Both types of time-domain presentations are used to analyze the NAVSTAR clock results.

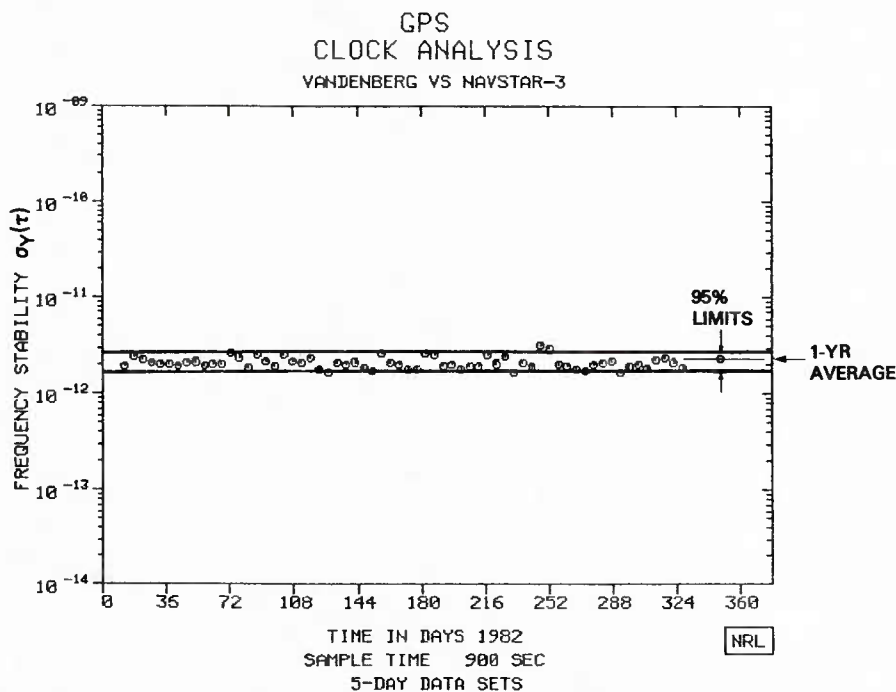


Fig. 8 — Typical frequency stability vs running time values, using 5-day sets

NAVSTAR-3 RESULTS

NRL REPORT 8778

| | τ (HRS) | .25 | .50 | .75 | 1.00 | 1.25 | 1.50 | 1.75 | 2.00 | | |
|-----------|-----------------|------|------|------|------|------|------|------|------|------|------|
| o V82-305 | σ (PP13) | 21.3 | 12.2 | 10.1 | 15.1 | 17.1 | 16.1 | 14.9 | 13.7 | | |
| | AVG PTS | 83 | 83 | 75 | 72 | 64 | 56 | 48 | 40 | | |
| A G82-305 | σ (PP13) | 23.6 | 14.4 | 12.0 | 15.4 | 22.2 | 22.5 | 20.5 | 18.1 | | |
| | AVG PTS | 63 | 53 | 43 | 35 | 26 | 19 | 14 | 9 | | |
| x H82-305 | σ (PP13) | 17.6 | 12.4 | 11.9 | 17.9 | 19.9 | 19.1 | 18.1 | 17.3 | | |
| | AVG PTS | 85 | 85 | 79 | 77 | 70 | 62 | 54 | 47 | | |
| z A82-305 | σ (PP13) | 22.7 | 14.3 | 12.5 | 16.7 | 17.3 | 15.6 | 14.6 | 13.3 | | |
| | AVG PTS | 59 | 55 | 46 | 40 | 32 | 27 | 21 | 16 | | |
| | τ (DAYS) | 1 | 2 | 3 | 4 | 5 | 6 | 7 | 8 | 9 | 10 |
| o VAN-382 | σ (PP14) | 13.0 | 19.0 | 27.0 | 28.0 | 29.0 | 28.0 | 28.0 | 27.0 | 24.0 | 22.0 |
| | TOT PTS | 184 | 184 | 179 | 184 | 190 | 180 | 202 | 177 | 175 | 168 |
| A GUA-382 | σ (PP14) | 12.0 | 17.0 | 15.0 | 13.0 | 12.0 | 11.0 | 10.0 | 9.0 | 8.0 | 7.0 |
| | TOT PTS | 222 | 204 | 196 | 185 | 192 | 182 | 207 | 157 | 155 | 148 |
| x HAW-382 | σ (PP14) | 9.0 | 11.0 | 16.0 | 18.0 | 19.0 | 22.0 | 22.0 | 22.0 | 22.0 | 22.0 |
| | TOT PTS | 147 | 147 | 138 | 141 | 142 | 139 | 156 | 138 | 139 | 122 |
| z ALK-382 | σ (PP14) | 10.0 | 11.0 | 15.0 | 20.0 | 28.0 | 33.0 | 32.0 | 36.0 | 38.0 | 41.0 |
| | TOT PTS | 170 | 144 | 127 | 119 | 118 | 121 | 133 | 118 | 113 | 113 |

GPS
CLOCK ANALYSIS
NAVSTAR-3

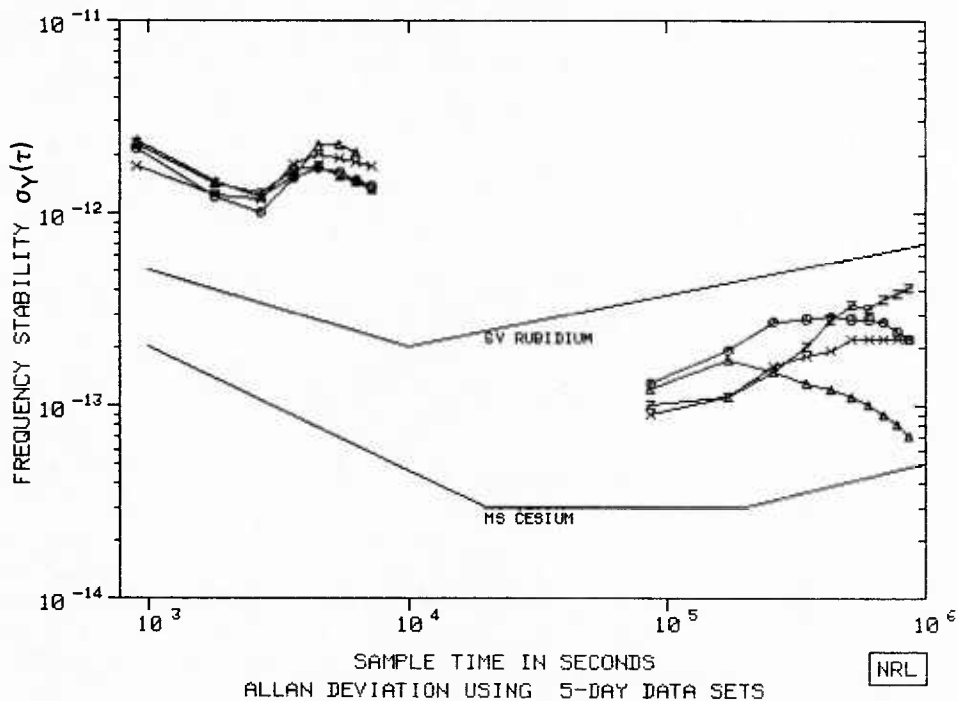


Fig. 9 - NAVSTAR-3 frequency stability vs sample time monitor site composite plot

NAVSTAR-3 Clock Results

The NAVSTAR-3 data for 1982 and part of 1983 are presented in Plots 1 through 19. The clock drift, presented in Eq. (6), has been removed from the data for calculating the long-term results. Plots 1 through 10 reference the Vandenberg MS; Plots 11 through 13, the Guam MS; Plots 14 through 16, the Hawaii MS; and Plots 17 through 19, the Alaska MS.

Plot 1 presents the NAVSTAR-3 frequency stability data for sample times ranging from 900 s to 10 days. The numeric values for every point are tabulated above the plot. The first heading lists the sample times in hours, ranging from 0.25 to 2 h. These times correspond to sample times of 900 to 7200 s, respectively. The 2-row sets of values present the $\sigma_y(\tau)$ in units of parts per 10^{13} , designated as (PP13) and the average number of points per 5-day data set used in the calculation for each sample time. The legend symbol at the beginning of each 2-row set is used to allow easy identification of its plotted values which are connected by solid lines. The set descriptor, V82-305, may be decoded as Vandenberg MS, 1982, NAVSTAR-3 SV, 5-day sets.

Similarly, in Plot 1, the second heading lists the sample times, ranging from 1 to 10 days. Here, the $\sigma_y(\tau)$ is expressed in units of parts per 10^{14} (PP14) and the number of points is the total number in the data set for each sample time. The set descriptor, VAN-382, can be decoded as Vandenberg MS, NAVSTAR-3 SV, 1982.

Plot 2 presents the $\sigma_y(\tau)$ values vs time, for a 900-s sample time, during 1982. Each point was obtained from a 5-day set. The average number points per 5-day set used in the Allan deviation calculation is listed in the third row of Plot 1. For the 1982 data, sixty-four 5-day sets were used. Plot 1 indicates that an average of 83 points per 5-day set was used in the $\sigma_y(\tau)$ calculation. Thus each point in Plot 2 has a nominal confidence corresponding to 83 points, while the $\sigma_y(\tau)$ value in Plot 1 has a confidence corresponding to $83 \text{ points/set} \times 64 \text{ sets} = 5312 \text{ points}$.

The Allan deviation for the 900-s sample time for the entire year of 1982 is listed in the second row of Plot 1. This value is 21.3×10^{13} .

Plot 3 presents stability data for the first 100 days in 1983 with a 900-s sample time. This data is consistent with the 1982 data.

Plot 4 presents the 1800-s sample time stability result obtained during 1982. The stability data for the first half of 1982 appear to have less noise than the remaining half of the year.

Plot 5 presents the 2700-s sample-time frequency stability results for 1982. These data also indicate a slight increase in noise after the first half of 1982.

Plot 6, for a 1-h sample time, indicates an increased noise level for the entire year. Plots 1, 7, 8, 9, and 10 show that the noise increases to a maximum value of 17.1×10^{-13} at a 1.25-h sample time. This increased noise could be due to either the NAVSTAR-3 clock, or the Vandenberg MS clock. Comparisons are made with data from other monitor sites to determine the source.

Plots 11 through 13 present the NAVSTAR-3 $\sigma_y(\tau)$ vs time results, referenced to the Guam MS. For brevity, only plots for the 900-s stability data for 1982 and 1983 are presented. The numeric values for every value of $\sigma_y(\tau)$ are presented in Plot 11. The results are similar, with the anomaly in short-term stability occurring at a sample time of 1.5 h, with a stability of 22.5×10^{-13} .

Plots 14 through 16 present the NAVSTAR-3 $\sigma_y(\tau)$ vs time results, referenced to the Hawaii MS. These results indicate a peak stability of 19.9×10^{-13} for a 1.25-h sample time. The NAVSTAR-3

results, referenced to the Alaska MS, are presented in Plots 17 through 19. The maximum value of the noise is 17.3×10^{-13} at 1.25-h sample time.

Figure 9 presents a 1982 composite of all four monitor sites vs NAVSTAR-3. A station-ensemble plot for each of the four NAVSTAR clocks are included following the NAVSTAR 4, 5, and 6 results referenced to individual monitor sites.

Analysis of Fig. 9 indicates an unexpected increases in the short-term NAVSTAR-3 $\sigma_y(\tau)$ (referenced to all monitor sites) that peaks at a sample time of 1.25 to 1.5 h. Therefore, this increase in noise is due to the NAVSTAR-3 clock rather than to one of the MS clocks.

NAVSTAR-4 RESULTS

| | τ (HRS) | .25 | .50 | .75 | 1.00 | 1.25 | 1.50 | 1.75 | 2.00 | | |
|-----------|-----------------|------|------|------|------|------|------|------|------|------|------|
| o V82-405 | σ (PP13) | 23.2 | 14.9 | 11.7 | 11.2 | 10.8 | 10.7 | 11.1 | 11.3 | | |
| | AVG PTS | 81 | 78 | 64 | 53 | 39 | 25 | 14 | 8 | | |
| A G82-405 | σ (PP13) | 21.6 | 14.0 | 11.6 | 10.6 | 10.3 | 10.1 | 10.1 | 9.8 | | |
| | AVG PTS | 68 | 65 | 57 | 53 | 46 | 39 | 33 | 27 | | |
| x H82-405 | σ (PP13) | 20.1 | 13.6 | 10.8 | 9.8 | 9.2 | 9.0 | 9.3 | 9.3 | | |
| | AVG PTS | 59 | 52 | 39 | 31 | 24 | 19 | 14 | 9 | | |
| z A82-405 | σ (PP13) | 20.0 | 14.2 | 11.3 | 9.6 | 9.2 | 9.3 | 9.6 | 7.9 | | |
| | AVG PTS | 61 | 55 | 44 | 37 | 27 | 17 | 9 | 3 | | |
| | τ (DAYS) | 1 | 2 | 3 | 4 | 5 | 6 | 7 | 8 | 9 | 10 |
| o VAN-482 | σ (PP14) | 16.0 | 18.0 | 20.0 | 22.0 | 22.0 | 24.0 | 23.0 | 22.0 | 22.0 | 21.0 |
| | TOT PTS | 341 | 324 | 320 | 324 | 303 | 301 | 334 | 285 | 289 | 289 |
| A GUA-482 | σ (PP14) | 12.0 | 16.0 | 17.0 | 21.0 | 20.0 | 24.0 | 29.0 | 29.0 | 30.0 | 28.0 |
| | TOT PTS | 105 | 90 | 103 | 87 | 87 | 85 | 92 | 82 | 75 | 79 |
| x HAW-482 | σ (PP14) | 12.0 | 16.0 | 18.0 | 19.0 | 22.0 | 23.0 | 21.0 | 20.0 | 19.0 | 19.0 |
| | TOT PTS | 292 | 271 | 266 | 270 | 263 | 260 | 308 | 268 | 260 | 262 |
| z ALK-482 | σ (PP14) | 13.0 | 19.0 | 23.0 | 28.0 | 31.0 | 29.0 | 28.0 | 28.0 | 30.0 | 28.0 |
| | TOT PTS | 272 | 260 | 248 | 239 | 220 | 208 | 227 | 190 | 195 | 188 |

GPS
CLOCK ANALYSIS

NAVSTAR-4

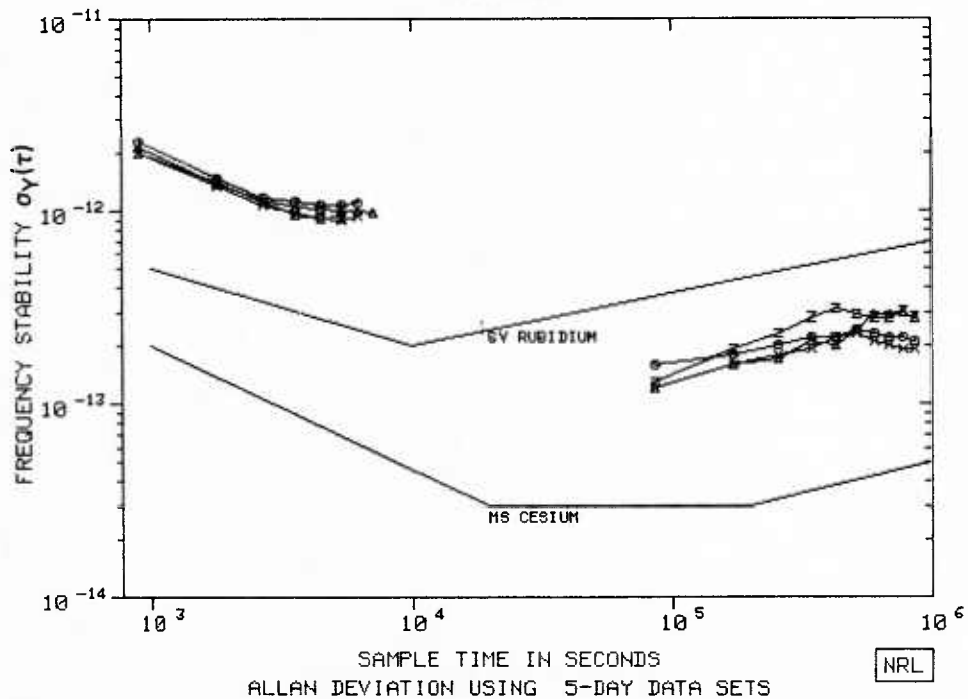


Fig. 10 — NAVSTAR-4 frequency stability vs sample time monitor site composite plot

NAVSTAR-4 Clock Results

The NAVSTAR-4 results are presented in Plots 20 through 38. The clock drift has been removed from the data for the long-term calculations. Plots 20 through 29 reference the NAVSTAR-4 clock to the Vandenberg MS clock. Similarly, Plots 30 through 32 reference the Guam MS; Plots 33 through 35, the Hawaii MS; and Plots 36 through 38, the Alaska MS.

The $\sigma_y(\tau)$, as a function of sample time, referenced to the Vandenberg MS, is presented in Plot 20. Plot 21 presents the $\sigma_y(\tau)$ vs time values for 1982 for the sample time of 900 s. Plot 22 presents the results for the first 100 days of 1983. This plot indicates an anomaly after day 45. Plots 23 through 29 present the 1982 results for sample times of 1800 to 7200 s.

Figure 10 presents a 1982 composite plot of all four monitor sites vs NAVSTAR-4. The small change in slope at 2700 s is the only possible anomaly in the 1982 short-term frequency stability data.

NAVSTAR-5 RESULTS

| | τ (HRS) | .25 | .50 | .75 | 1.00 | 1.25 | 1.50 | 1.75 | 2.00 | | |
|-----------|-----------------|------|------|------|------|------|------|------|------|------|------|
| o V82-505 | σ (PP13) | 26.4 | 17.6 | 14.4 | 12.8 | 11.7 | 10.9 | 10.0 | 9.6 | | |
| | AVG PTS | 78 | 76 | 69 | 63 | 55 | 47 | 39 | 31 | | |
| Δ G82-505 | σ (PP13) | 22.3 | 15.7 | 14.4 | 14.6 | 16.4 | 17.9 | 19.5 | 21.4 | | |
| | AVG PTS | 47 | 44 | 38 | 35 | 29 | 23 | 18 | 13 | | |
| x H82-505 | σ (PP13) | 21.9 | 15.5 | 12.5 | 12.1 | 11.2 | 10.6 | 10.5 | 10.3 | | |
| | AVG PTS | 67 | 65 | 54 | 46 | 35 | 27 | 21 | 13 | | |
| z A82-505 | σ (PP13) | 23.3 | 14.9 | 12.5 | 11.4 | 11.0 | 11.2 | 12.1 | 13.7 | | |
| | AVG PTS | 77 | 71 | 59 | 51 | 39 | 27 | 15 | 9 | | |
| | τ (DAYS) | 1 | 2 | 3 | 4 | 5 | 6 | 7 | 8 | 9 | 10 |
| o VAN-582 | σ (PP14) | 16.0 | 14.0 | 14.0 | 12.0 | 12.0 | 11.0 | 11.0 | 11.0 | 11.0 | 11.0 |
| | TOT PTS | 197 | 200 | 194 | 196 | 193 | 187 | 200 | 179 | 180 | 178 |
| Δ GUA-582 | σ (PP14) | 16.0 | 12.0 | 11.0 | 10.0 | 10.0 | 11.0 | 11.0 | 12.0 | 13.0 | 13.0 |
| | TOT PTS | 99 | 86 | 80 | 73 | 61 | 61 | 67 | 49 | 34 | 30 |
| x HAW-582 | σ (PP14) | 16.0 | 12.0 | 10.0 | 9.0 | 8.0 | 8.0 | 7.0 | 8.0 | 7.0 | 7.0 |
| | TOT PTS | 289 | 271 | 263 | 260 | 244 | 239 | 254 | 238 | 218 | 209 |
| z ALK-582 | σ (PP14) | 15.0 | 12.0 | 10.0 | 10.0 | 10.0 | 10.0 | 10.0 | 9.0 | 9.0 | 9.0 |
| | TOT PTS | 291 | 276 | 265 | 263 | 249 | 238 | 260 | 231 | 224 | 215 |

GPS
CLOCK ANALYSIS
NAVSTAR-5

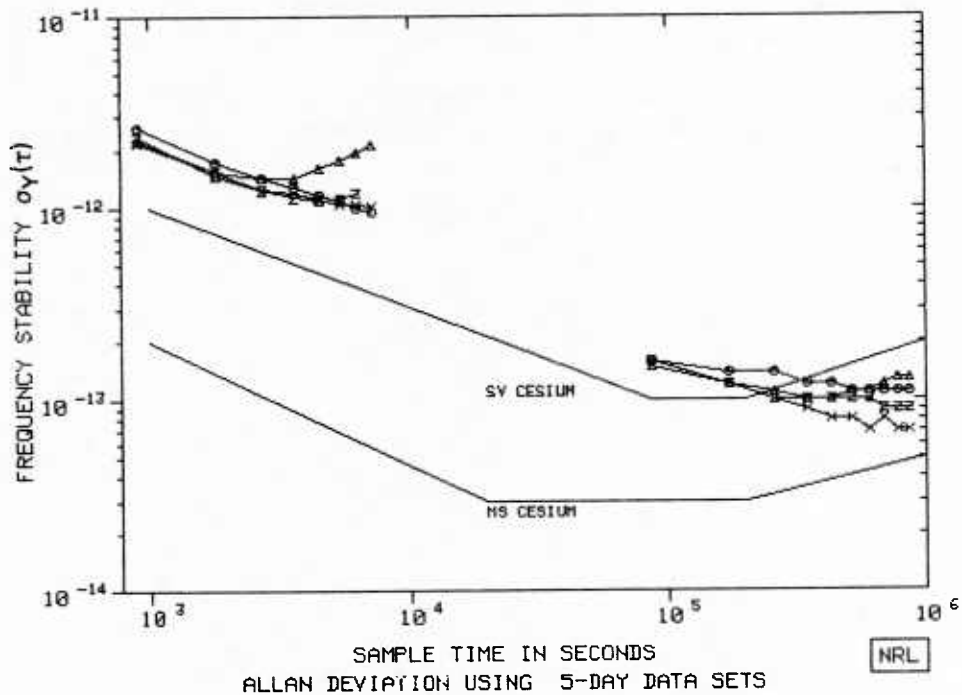


Fig. 11 — NAVSTAR-5 frequency stability vs sample time monitor site composite plot

NAVSTAR-5 Clock Results

The NAVSTAR-5 results are presented in Plots 39 through 64. Plots 39 through 41 reference the NAVSTAR-5 clock to the Vandenberg MS clock. Plots 42 through 58 reference the Guam MS; Plots 59 through 61, the Hawaii MS; and Plots 62 through 64, the Alaska MS.

The $\sigma_y(\tau)$ results, as a function of sample time, referenced to the Vandenberg MS, are presented in Plot 39. Short-term results are presented for 1982 and the first 100 days of 1983. Long-term results are presented for 1981, 1982, and the first 100 days of 1983.

A comparison of the 1982 and 1983 short-term results indicates an increase in noise in 1983 for all sample times between 900 s and 7200 s. This increase in noise can be further analyzed by referring to the $\sigma_y(\tau)$ vs time plots. Plot 40 indicates a small increase in noise at day 180 of 1982. Plot 41, which is a continuation into 1983, indicates the same trend that began during 1982.

The long-term results, referenced to the Vandenberg MS, are also presented in Plot 39. For sample times ranging from 1 to 10 days, all stability values are between a peak of 26×10^{-14} and a minimum value of 11×10^{-14} .

Comparison of the 1981 and 1982 long-term stability values indicates close agreement for sample times of $\tau = 1$ to 3 days. The stability values for 1981 indicate more noise for sample times of 4 to 10 days.

The 1983 stability results indicate more noise for sample times of 1 and 2 days. For 3- to 10-day sample times, the results are in close agreement with the 1982 values.

Figure 11 presents a 1982 composite plot of all four monitor sites vs NAVSTAR-5. The short-term results, referenced to the Guam MS, display a departure from the remainder of the data, beginning at the 2700-s sample time.

NAVSTAR-6 RESULTS

| | τ (HRS) | .25 | .50 | .75 | 1.00 | 1.25 | 1.50 | 1.75 | 2.00 | | |
|-----------|-----------------|------|------|------|------|------|------|------|------|------|------|
| ⊙ V82-605 | σ (PP13) | 23.0 | 14.5 | 12.1 | 10.9 | 10.1 | 9.2 | 8.5 | 7.9 | | |
| | AVG PTS | 60 | 59 | 55 | 56 | 48 | 40 | 33 | 25 | | |
| ▲ G82-605 | σ (PP13) | 22.0 | 14.8 | 13.2 | 12.9 | 13.5 | 14.9 | 16.5 | 17.7 | | |
| | AVG PTS | 57 | 53 | 47 | 42 | 35 | 27 | 21 | 15 | | |
| × H82-605 | σ (PP13) | 19.4 | 12.6 | 9.6 | 8.4 | 8.4 | 8.5 | 8.5 | 8.5 | | |
| | AVG PTS | 94 | 100 | 94 | 89 | 81 | 73 | 64 | 57 | | |
| ⊞ A82-605 | σ (PP13) | 21.9 | 12.9 | 10.5 | 9.4 | 8.9 | 9.1 | 9.9 | 9.9 | | |
| | AVG PTS | 62 | 56 | 47 | 45 | 35 | 30 | 24 | 18 | | |
| | τ (DAYS) | 1 | 2 | 3 | 4 | 5 | 6 | 7 | 8 | 9 | 10 |
| ⊙ VAN-682 | σ (PP14) | 12.0 | 10.0 | 10.0 | 9.0 | 10.0 | 10.0 | 10.0 | 10.0 | 12.0 | 12.0 |
| | TOT PTS | 186 | 194 | 184 | 189 | 185 | 179 | 197 | 177 | 175 | 180 |
| ▲ GUA-682 | σ (PP14) | 12.0 | 10.0 | 9.0 | 8.0 | 13.0 | 12.0 | 14.0 | 10.0 | 10.0 | 12.0 |
| | TOT PTS | 155 | 133 | 126 | 109 | 96 | 90 | 87 | 63 | 52 | 45 |
| × HAW-682 | σ (PP14) | 10.0 | 7.0 | 6.0 | 5.0 | 5.0 | 4.0 | 4.0 | 4.0 | 4.0 | 5.0 |
| | TOT PTS | 175 | 169 | 161 | 157 | 150 | 146 | 158 | 139 | 132 | 128 |
| ⊞ ALK-682 | σ (PP14) | 10.0 | 9.0 | 8.0 | 8.0 | 8.0 | 8.0 | 8.0 | 9.0 | 9.0 | 9.0 |
| | TOT PTS | 235 | 225 | 210 | 203 | 190 | 191 | 211 | 168 | 170 | 159 |

GPS
CLOCK ANALYSIS
NAVSTAR-6

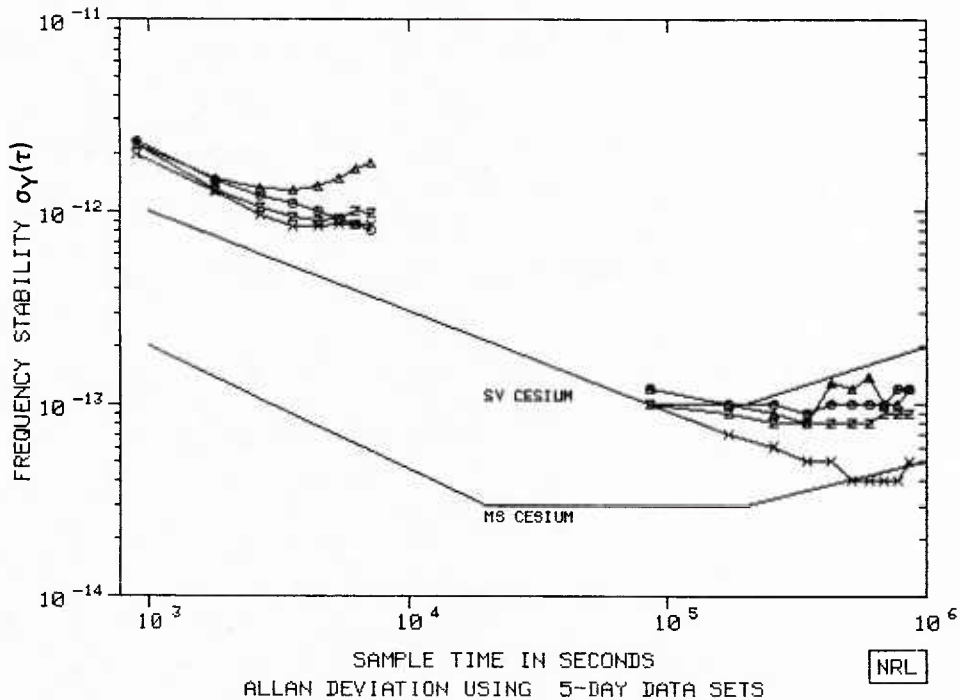


Fig. 12 — NAVSTAR-6 frequency stability vs sample time monitor site composite plot

NAVSTAR-6 Clock Results

The NAVSTAR-6 results are presented in Plots 65 through 90. Plots 65 through 67 reference the NAVSTAR-6 clock to the Vandenberg MS clock. Plots 68 through 84 reference the Guam MS; Plots 85 through 87, the Hawaii MS; and Plots 88 through 90, the Alaska MS.

Plot 65 presents the NAVSTAR-6 frequency stability, referenced to the Vandenberg MS, for sample times ranging from 900 s to 10 days. The NAVSTAR-6 frequency stability results are close to the model values for the SV cesium. The short-term values are larger than the model values by about 1×10^{-12} . The long-term values are in good agreement for sample times of 2 to 3 days. The stability values for 3 to 10 days indicate better performance than the SV cesium model.

A comparison of the NAVSTAR-6 long-term frequency stability results indicates improved stability as a function of year. That is, the 1983 stability is better than that of 1982, and the 1982 stability is better than that of 1981.

Plots 66 and 67 present the $\sigma_y(\tau)$, calculated over 5-day sets, as a function of time. A small increase in noise was first noticed near day 180 of 1982.

Plot 68 presents the NAVSTAR-6 frequency stability referenced to the Guam MS, for sample times ranging from 900 s to 10 days.

The short-term stability values for 900- and 1800-s sample times are in good agreement with the SV cesium model. The values are offset from the model by about 1×10^{-12} .

For sample times of 2700 s to 7200 s, the 1982 and 1983 results indicate an unexpected increase in noise.

The long-term stability values are close to the SV cesium model values for sample times of 1 and 2 days. The NAVSTAR-6 results for sample times of 3 to 10 days indicate better performance than the SV cesium model.

Comparison of the 1982 and 1983 long-term stabilities indicate that the 1983 performance is better than that during 1982.

Plots 69 and 70 present the NAVSTAR-6 $\sigma_y(\tau)$, calculated over 5-day sets, as a function of time. Plots 71 and 72 present the results for a 1800-s sample time. The 2700 through 7200-s sample-time results, presented in Plots 73 through 84, indicate a departure from the slope of the SV cesium model curve.

Plot 85 presents the NAVSTAR-6 frequency stability, referenced to the Hawaii MS, for sample times ranging from 900 s to 10 days.

The short-term stability results are nominal for sample times up to 3600 s. A small change in slope is noted for sample times between 4500 and 7200 s.

The long-term stability values are close to the SV cesium model values for sample times of 1 to 2 days. For sample times of 3 to 10 days, an improvement in stability is observed with respect to the SV cesium model. The 1983 stability results are better than those of 1982.

Plot 88 presents the NAVSTAR-6 frequency stability referenced to the Alaska MS clock. The 1983 performance is better than that of 1982, with a possible anomaly occurring at the 4500-s sample time.

Figure 12 presents a 1982 composite plot of all four monitor sites vs NAVSTAR-6. A similar anomaly in the Gaum MS clock for sample times of 2700 to 7200 s occurs in both the NAVSTARs-5 and 6 analysis. Since it does not occur using NAVSTAR-3 or 4 data, this anomaly is, as yet, unresolved.

MONITOR STATION ENSEMBLE CLOCK ANALYSIS

MONITOR STATION ENSEMBLE CLOCK ANALYSIS

The individual NAVSTAR clock analyses for 1982 may be performed using combined data from all four GPS monitor sites. Ensemble-average values of $\sigma_y(\tau)$ have been calculated to determine correlated effects.

Figures 13 through 16 present the MS ensemble-average $\sigma_y(\tau)$ vs sample time for NAVSTARs 3, 4, 5, and 6, respectively.

Each of the line segments connecting two values of $\sigma_y(\tau)$ may be fitted to an equation of the form given by Eq. (15).

$$\sigma_y^2(\tau) = a(\tau)^\mu. \quad (15)$$

In Eq. (15), the Allan variance, $\sigma_y^2(\tau)$, is modeled as a constant a , which is multiplied by the sample time τ raised to some power μ . The results for a station ensemble vs NAVSTAR-3 are presented in Table 5, using the 1982 data, and six line segments from Fig. 13. Table 5 lists the coefficient a , the exponent μ , and the two pairs of $(\tau, \sigma_y(\tau))$ values that were used to solve for the model values.

For NAVSTAR-4, the 1982 short-term stability results (Fig. 14) indicate two distinct power-law segments, with a possible third segment between 900 s and 1800 s. Table 6 presents the power-law coefficient and exponent values for these three segments plus the two segments for the long-term stability results.

For NAVSTAR-5, the 1982 short-term stability results indicate two distinct segments, with an additional change in slope (exponent μ) occurring at a sample time of $\tau = 1800$ s. Table 7 includes the power-law coefficient and exponent values for the five segments pictured in Fig. 15.

The 1982 NAVSTAR-6 station-ensemble results are presented in Fig. 16. Table 8 lists the model values for three short-term and three long-term stability segments.

Figure 17 presents a stability-vs-sample-time rubidium composite plot of the four-station-ensemble curves for NAVSTARs 3 and 4. Table 9 lists the power-law coefficient, exponent, and data values for the five segments of combined-data values, with a separate tabulation for the NAVSTAR-3 anomaly segments.

A cesium stability-vs-sample-time presentation appears in Fig. 18 which shows the four-station-ensemble curves for NAVSTARs 5 and 6. Table 10 includes the model values for the five combined-data segments.

Figure 19 shows the stability-vs-sample-time composite plot of the station-ensemble curves for NAVSTARs 3, 4, 5 and 6. The three short-term data segments are averaged with the resulting power-law model values listed in Table 11. Also, values for a theoretical segment connecting the 900-s and 1-day sample times are included. It is seen that the calculated values of a and μ are very close to those for the 900- to 1800-s segment, indicating an underlying white noise FM process for sample times ranging from 900 s to 1 day.

Analysis of all NAVSTAR short-term stability presentations indicates that, for sample times of 900 and 1800 s, good agreement exists between measurements from all sites. From 2700 to 7200 s, three unexpected effects are noted. The most obvious is the signal present in NAVSTAR-3 data from all sites, which reaches a maximum value at 1.25- to 1.5-hour sample time as seen in Figs. 9 and 13. The second effect noted in Figs. 11 and 12, for NAVSTARs 5 and 6, is the change in slope of the Guam MS short-term frequency stability measurements. These values were omitted from the ensemble value computation. The third effect is the lack of correlation of this effect with the NAVSTAR-4 data. These last two effects suggest that more than one factor is present.

| | τ (HRS) | .25 | .50 | .75 | 1.00 | 1.25 | 1.50 | 1.75 | 2.00 | | |
|-----------|-----------------|------|------|------|------|------|------|------|------|------|------|
| • E82-335 | σ (PP13) | 21.4 | 13.4 | 11.7 | 15.3 | 19.2 | 18.5 | 17.2 | 15.7 | | |
| | AVG PTS | 290 | 276 | 243 | 224 | 192 | 164 | 137 | 112 | | |
| | τ (DAYS) | 1 | 2 | 3 | 4 | 5 | 6 | 7 | 8 | 9 | 10 |
| • ENS-382 | σ (PP14) | 11.1 | 14.9 | 18.9 | 20.5 | 23.1 | 24.9 | 24.5 | 25.5 | 25.3 | 26.0 |
| | TOT PTS | 723 | 679 | 640 | 629 | 622 | 622 | 698 | 590 | 582 | 551 |

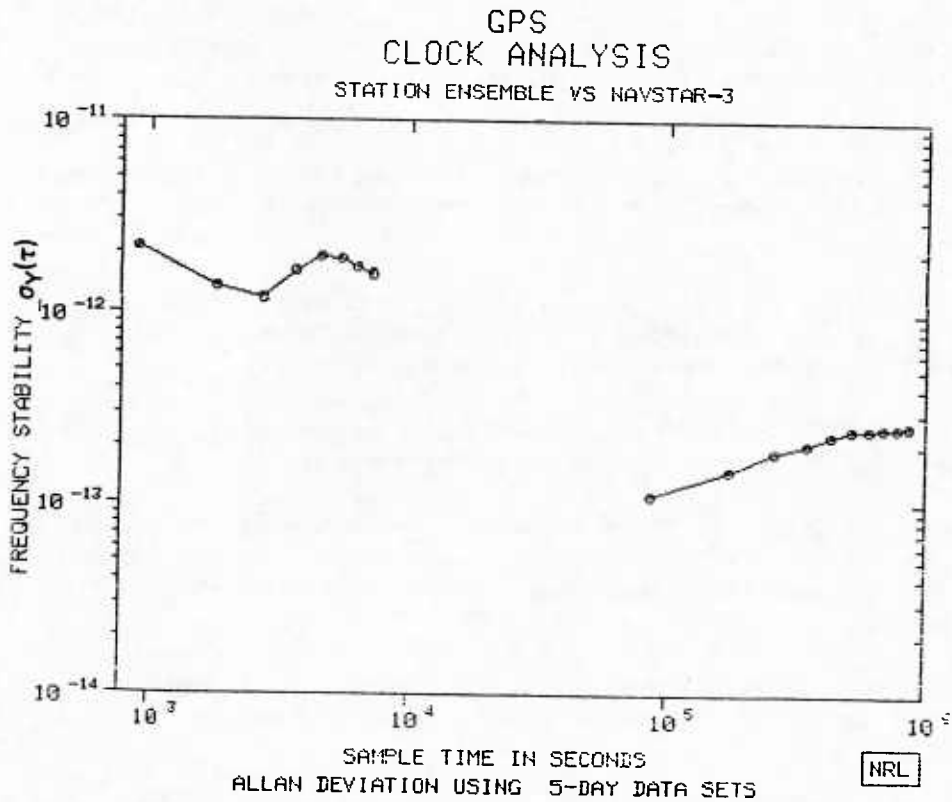


Fig. 13 — NAVSTAR-3 frequency stability vs sample time, monitor site ensemble

| | T(HRS) | .25 | .50 | .75 | 1.00 | 1.25 | 1.50 | 1.75 | 2.00 | | |
|-----------|-----------------|------|------|------|------|------|------|------|------|------|------|
| • E82-485 | σ (PP13) | 21.3 | 14.2 | 11.4 | 10.3 | 9.9 | 9.8 | 10.1 | 9.7 | | |
| | AVG PTS | 269 | 250 | 204 | 174 | 136 | 100 | 70 | 47 | | |
| | T(DAYS) | 1 | 2 | 3 | 4 | 5 | 6 | 7 | 8 | 9 | 10 |
| • ENS-482 | σ (PP14) | 13.4 | 17.3 | 19.6 | 22.8 | 24.1 | 25.1 | 25.5 | 25.0 | 25.7 | 24.3 |
| | TOT PTS | 1010 | 945 | 937 | 920 | 873 | 862 | 961 | 825 | 819 | 818 |

GPS
CLOCK ANALYSIS
STATION ENSEMBLE VS NAVSTAR-4

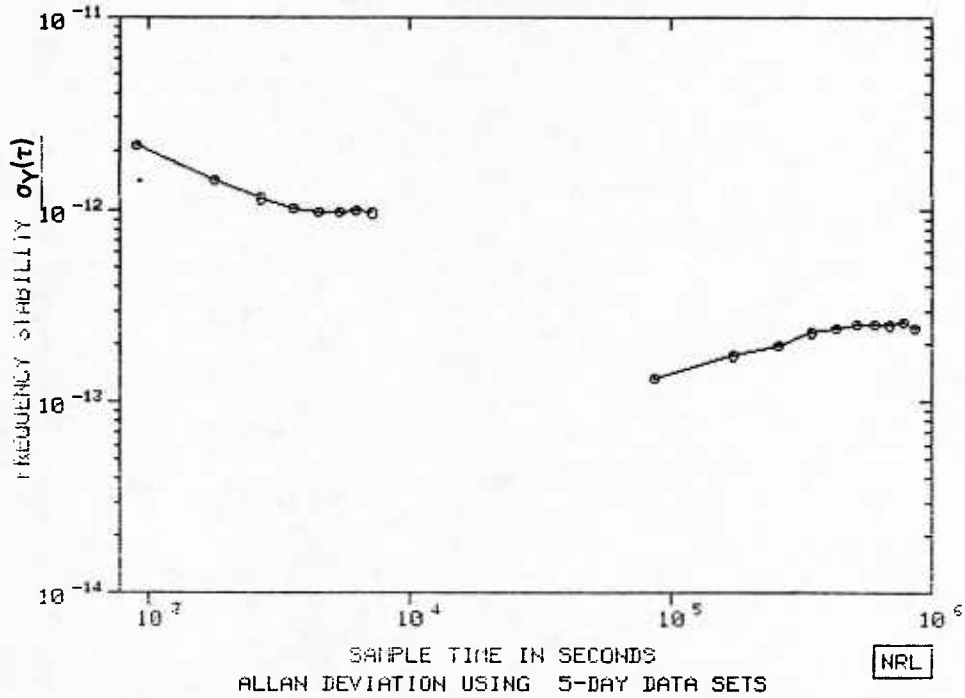


Fig. 14 — NAVSTAR-4 frequency stability vs sample time, monitor site ensemble

| | τ (HRS) | .25 | .50 | .75 | 1.00 | 1.25 | 1.50 | 1.75 | 2.00 | | |
|-----------|-----------------|------|------|------|------|------|------|------|------|------|------|
| • E82-585 | σ (PP13) | 23.5 | 16.0 | 13.5 | 12.1 | 11.3 | 10.9 | 10.9 | 11.3 | | |
| | AVG PTS | 269 | 256 | 182 | 160 | 129 | 101 | 75 | 53 | | |
| | τ (DAYS) | 1 | 2 | 3 | 4 | 5 | 6 | 7 | 8 | 9 | 10 |
| • ENS-582 | σ (PP14) | 15.8 | 12.5 | 11.4 | 10.3 | 10.1 | 10.1 | 9.9 | 10.1 | 10.3 | 10.3 |
| | TOT PTS | 876 | 833 | 802 | 792 | 747 | 725 | 781 | 697 | 656 | 632 |

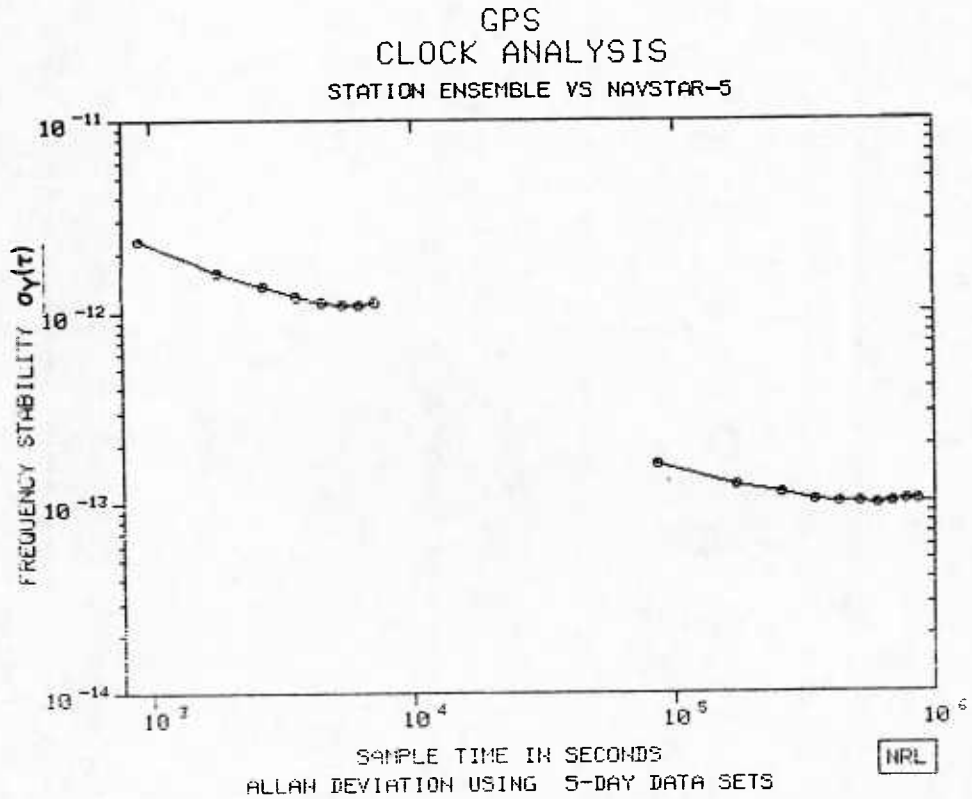


Fig. 15 — NAVSTAR-5 frequency stability vs sample time, monitor site ensemble

| | | | | | | | | | |
|-----------|-----------------|------|------|------|------|------|------|------|------|
| | τ (HRS) | .25 | .50 | .75 | 1.00 | 1.25 | 1.50 | 1.75 | 2.00 |
| • E82-685 | σ (PP13) | 21.6 | 13.7 | 10.8 | 9.6 | 9.2 | 8.9 | 9.0 | 8.8 |
| | AVG PTS | 273 | 268 | 196 | 190 | 164 | 143 | 121 | 108 |
| | τ (DAYS) | 1 | 2 | 3 | 4 | 5 | 6 | 7 | 8 |
| • ENS-682 | σ (PP14) | 11.1 | 9.1 | 8.4 | 7.7 | 9.5 | 9.0 | 9.7 | 8.6 |
| | TOT PTS | 751 | 721 | 681 | 658 | 621 | 606 | 653 | 547 |
| | | | | | | | | | 529 |
| | | | | | | | | | 512 |

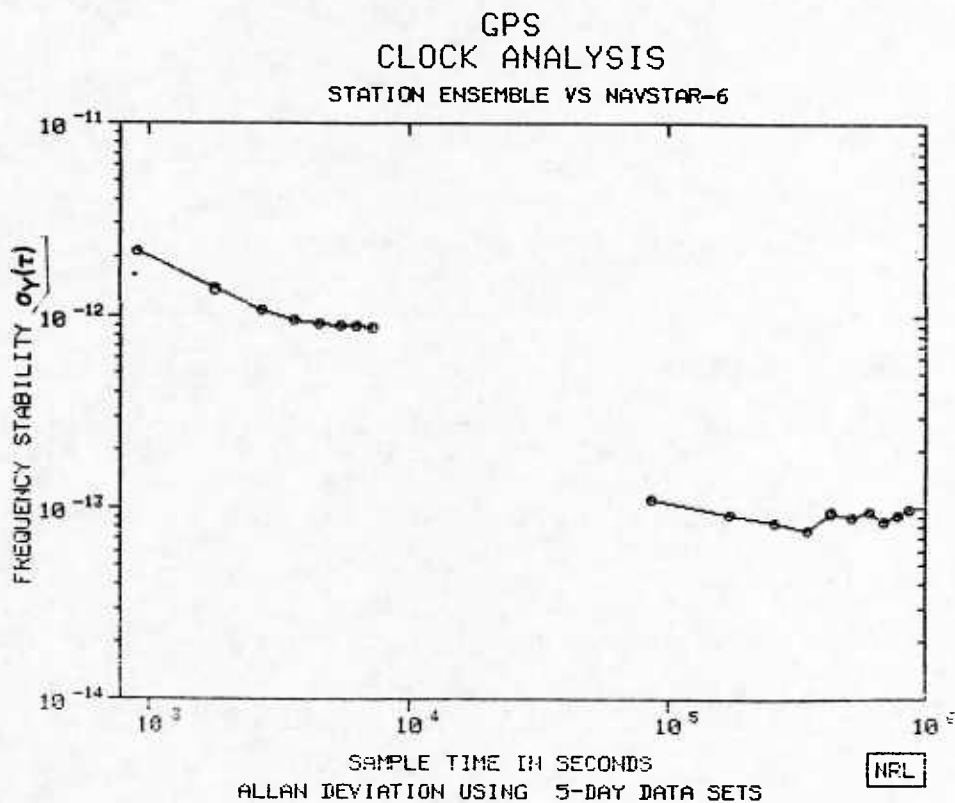


Fig. 16 -- NAVSTAR-6 frequency stability vs sample time, MS ensemble

Table 5 — NAVSTAR-3 vs Station Ensemble—1982.
 Model $\sigma_y^2(\tau) = a(\tau)^\mu$.

| Solution | | Data | | | |
|------------------------|----------|------------------------------|----------|------------------------------|----------|
| Coefficient | Exponent | $(\tau_1, \sigma_y(\tau_1))$ | | $(\tau_2, \sigma_y(\tau_2))$ | |
| a | μ | seconds | PP10(13) | seconds | PP10(13) |
| 4.48×10^{-20} | -1.35 | 900 | 21.40 | 1,800 | 13.40 |
| 2.71×10^{-22} | -0.67 | 1,800 | 13.40 | 2,700 | 11.70 |
| 3.03×10^{-31} | 1.94 | 2,700 | 11.70 | 4,500 | 19.20 |
| 4.96×10^{-21} | -0.86 | 4,500 | 19.20 | 7,200 | 15.70 |
| 4.36×10^{-31} | 0.90 | 86,160 | 1.11 | 516,960 | 2.49 |
| 6.69×10^{-27} | 0.17 | 516,960 | 2.49 | 861,600 | 2.60 |

Table 6 — NAVSTAR-4 vs Station Ensemble—1982.
 Model $\sigma_y^2(\tau) = a(\tau)^\mu$.

| Solution | | Data | | | |
|------------------------|----------|------------------------------|----------|------------------------------|----------|
| Coefficient | Exponent | $(\tau_1, \sigma_y(\tau_1))$ | | $(\tau_2, \sigma_y(\tau_2))$ | |
| a | μ | seconds | PP10(13) | seconds | PP10(13) |
| 1.29×10^{-20} | -1.17 | 900 | 21.30 | 1,800 | 14.20 |
| 7.37×10^{-22} | -0.79 | 1,800 | 14.20 | 3,600 | 10.30 |
| 4.38×10^{-24} | -0.17 | 3,600 | 10.30 | 7,200 | 9.70 |
| 6.26×10^{-30} | 0.70 | 86,160 | 1.34 | 516,960 | 2.51 |
| 3.34×10^{-25} | -.13 | 516,960 | 2.51 | 861,600 | 2.43 |

Table 7 — NAVSTAR-5 vs Station Ensemble—1982.
 Model $\sigma_y^2(\tau) = a(\tau)^\mu$.

| Solution | | Data | | | |
|------------------------|----------|------------------------------|----------|------------------------------|----------|
| Coefficient | Exponent | $(\tau_1, \sigma_y(\tau_1))$ | | $(\tau_2, \sigma_y(\tau_2))$ | |
| a | μ | seconds | PP10(13) | seconds | PP10(13) |
| 1.04×10^{-20} | -1.11 | 900 | 23.50 | 1,800 | 16.00 |
| 7.57×10^{-22} | -0.76 | 1,800 | 16.00 | 4,500 | 11.30 |
| 1.28×10^{-24} | 0.0 | 4,500 | 11.30 | 7,200 | 11.30 |
| 1.38×10^{-23} | 0.56 | 86,160 | 1.58 | 430,800 | 1.01 |
| 4.90×10^{-27} | 0.06 | 430,800 | 1.01 | 861,600 | 1.03 |

Table 8 — NAVSTAR-6 vs Station Ensemble—1982.
 Model $\sigma_y^2(\tau) = a(\tau)^\mu$.

| Solution | | Data | | | |
|------------------------|----------|------------------------------|----------|------------------------------|----------|
| Coefficient | Exponent | $(\tau_1, \sigma_y(\tau_1))$ | | $(\tau_2, \sigma_y(\tau_2))$ | |
| a | μ | seconds | PP10(13) | seconds | PP10(13) |
| 3.55×10^{-20} | -1.31 | 900 | 21.60 | 1,800 | 13.70 |
| 1.27×10^{-21} | -0.87 | 1,800 | 13.70 | 4,500 | 9.20 |
| 4.16×10^{-24} | -0.19 | 4,500 | 9.20 | 7,200 | 8.80 |
| 4.95×10^{-24} | -0.53 | 86,160 | 1.11 | 344,640 | 0.77 |
| 2.22×10^{-37} | 1.88 | 344,640 | 0.77 | 430,800 | 0.95 |
| 1.93×10^{-27} | 0.12 | 430,800 | 0.95 | 861,600 | 0.99 |

Table 9 — NAVSTARs 3 & 4 (Rubidium) vs Station Ensemble—1982.
 Model $\sigma_y^2(\tau) = a(\tau)^\mu$.

| Solution | | Data | | | |
|------------------------|----------|------------------------------|----------|------------------------------|----------|
| Coefficient | Exponent | $(\tau_1, \sigma_y(\tau_1))$ | | $(\tau_2, \sigma_y(\tau_2))$ | |
| a | μ | seconds | PP10(13) | seconds | PP10(13) |
| 2.39×10^{-20} | -1.26 | 900 | 21.35 | 1,800 | 13.80 |
| 4.36×10^{-22} | -0.72 | 1,800 | 13.80 | 4,500 | 9.90 |
| 2.03×10^{-24} | -0.09 | 4,500 | 9.90 | 7,200 | 9.70 |
| 1.87×10^{-30} | 0.79 | 86,160 | 1.23 | 516,960 | 2.50 |
| 4.15×10^{-26} | 0.03 | 516,960 | 2.50 | 861,600 | 2.52 |
| NAVSTAR-3 Anomaly | | | | | |
| 3.03×10^{-31} | 1.94 | 2,700 | 11.70 | 4,500 | 19.20 |
| 4.96×10^{-21} | -0.86 | 4,500 | 19.20 | 7,200 | 15.7 |

| | τ (HRS) | .25 | .50 | .75 | 1.00 | 1.25 | 1.50 | 1.75 | 2.00 | | |
|-----------|-------------------|------|------|------|------|------|------|------|------|------|------|
| ● E82-305 | σ_y (PPL3) | 21.4 | 13.4 | 11.7 | 16.3 | 19.2 | 18.5 | 17.2 | 15.7 | | |
| | AVG PTS | 290 | 276 | 243 | 224 | 192 | 164 | 137 | 112 | | |
| ▲ E82-405 | σ_y (PPL3) | 21.3 | 14.2 | 11.4 | 10.3 | 9.9 | 9.8 | 10.1 | 9.7 | | |
| | AVG PTS | 259 | 250 | 204 | 174 | 136 | 100 | 70 | 47 | | |
| | τ (DAYS) | 1 | 2 | 3 | 4 | 5 | 6 | 7 | 8 | 9 | 10 |
| ● ENS-382 | σ_y (PPL4) | 11.1 | 14.9 | 18.9 | 20.5 | 23.1 | 24.9 | 24.5 | 25.5 | 25.3 | 26.0 |
| | TOT PTS | 723 | 679 | 640 | 629 | 622 | 622 | 698 | 590 | 582 | 551 |
| ▲ ENS-482 | σ_y (PPL4) | 13.4 | 17.3 | 19.6 | 22.8 | 24.1 | 25.1 | 25.5 | 25.0 | 25.7 | 24.3 |
| | TOT PTS | 1010 | 945 | 937 | 920 | 873 | 862 | 961 | 825 | 819 | 818 |

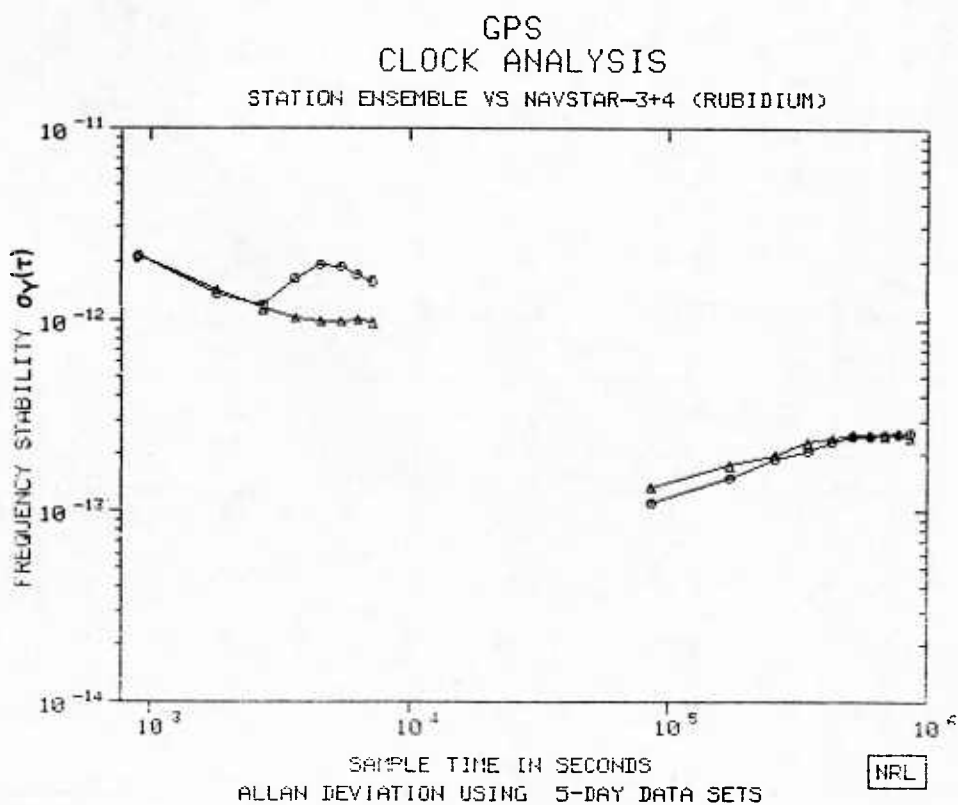


Fig. 17 — NAVSTARs 3 and 4 rubidium frequency stability vs sample time, MS ensemble

| | τ (HRS) | .25 | .50 | .75 | 1.00 | 1.25 | 1.50 | 1.75 | 2.00 | | |
|-----------|-------------------|------|------|------|------|------|------|------|------|------|------|
| ● E82-505 | σ_y (PP13) | 23.5 | 16.0 | 13.5 | 12.1 | 11.3 | 10.9 | 10.9 | 11.3 | | |
| | AVG PTS | 269 | 256 | 182 | 160 | 129 | 101 | 75 | 53 | | |
| ▲ E82-605 | σ_y (PP13) | 21.6 | 13.7 | 10.8 | 9.6 | 9.2 | 8.9 | 9.0 | 8.8 | | |
| | AVG PTS | 273 | 265 | 196 | 190 | 164 | 143 | 121 | 102 | | |
| | τ (DAYS) | 1 | 2 | 3 | 4 | 5 | 6 | 7 | 8 | 9 | 10 |
| ● ENS-582 | σ_y (PP14) | 15.8 | 12.5 | 11.4 | 10.3 | 10.1 | 10.1 | 9.9 | 10.1 | 10.3 | 10.3 |
| | TOT PTS | 876 | 833 | 802 | 792 | 747 | 725 | 781 | 697 | 656 | 632 |
| ▲ ENS-682 | σ_y (PP14) | 11.1 | 9.1 | 8.4 | 7.7 | 9.5 | 9.0 | 9.7 | 8.6 | 9.2 | 9.9 |
| | TOT PTS | 751 | 721 | 681 | 658 | 621 | 606 | 653 | 547 | 529 | 512 |

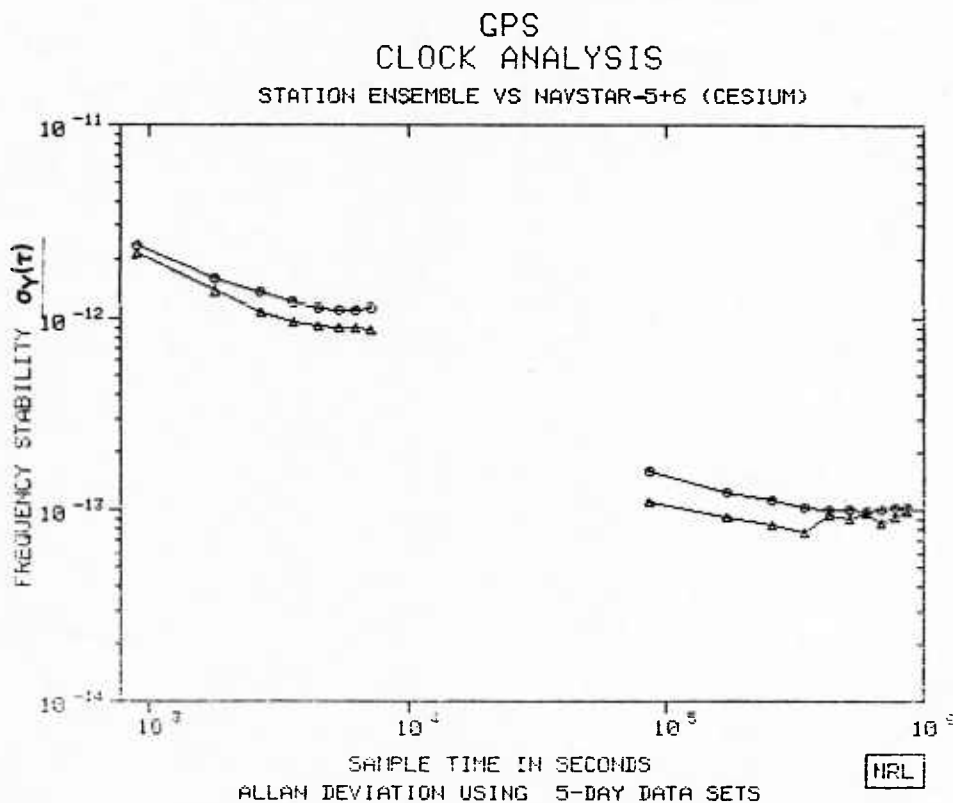


Fig. 18 — NAVSTARs 5 and 6 cesium frequency stability vs sample time, MS ensemble

McCASKILL, BUISSON, AND STEBBINS

| | τ (HRS) | .25 | .50 | .75 | 1.00 | 1.25 | 1.50 | 1.75 | 2.00 |
|-----------|-----------------|------|------|------|------|------|------|------|------|
| o E82-305 | σ (PP13) | 21.4 | 13.4 | 11.7 | 16.3 | 19.2 | 18.5 | 17.2 | 15.7 |
| | AVG PTS | 290 | 276 | 243 | 224 | 192 | 164 | 137 | 112 |
| Δ E82-405 | σ (PP13) | 21.3 | 14.2 | 11.4 | 10.3 | 9.9 | 9.8 | 10.1 | 9.7 |
| | AVG PTS | 269 | 250 | 204 | 174 | 136 | 100 | 70 | 47 |
| x E82-505 | σ (PP13) | 23.5 | 16.0 | 13.5 | 12.1 | 11.3 | 10.9 | 10.9 | 11.3 |
| | AVG PTS | 259 | 256 | 182 | 160 | 129 | 101 | 75 | 53 |
| z E82-605 | σ (PP13) | 21.6 | 13.7 | 10.8 | 9.6 | 9.2 | 8.9 | 9.0 | 8.8 |
| | AVG PTS | 273 | 268 | 196 | 190 | 164 | 143 | 121 | 100 |

| | τ (DAYS) | 1 | 2 | 3 | 4 | 5 | 6 | 7 | 8 | 9 | 10 |
|-----------|-----------------|------|------|------|------|------|------|------|------|------|------|
| o ENS-382 | σ (PP14) | 11.1 | 14.9 | 18.9 | 20.5 | 23.1 | 24.9 | 24.5 | 25.5 | 25.3 | 26.0 |
| | TOT PTS | 723 | 679 | 640 | 629 | 622 | 622 | 698 | 590 | 582 | 551 |
| Δ ENS-482 | σ (PP14) | 13.4 | 17.3 | 19.6 | 22.0 | 24.1 | 25.1 | 25.5 | 25.0 | 25.7 | 24.3 |
| | TOT PTS | 1010 | 945 | 937 | 920 | 873 | 862 | 961 | 825 | 819 | 810 |
| x ENS-582 | σ (PP14) | 15.8 | 12.5 | 11.4 | 10.3 | 10.1 | 10.1 | 9.9 | 10.1 | 10.3 | 10.3 |
| | TOT PTS | 876 | 833 | 802 | 792 | 747 | 725 | 781 | 697 | 656 | 632 |
| z ENS-682 | σ (PP14) | 11.1 | 9.1 | 8.4 | 7.7 | 9.5 | 9.0 | 9.7 | 8.6 | 9.2 | 9.9 |
| | TOT PTS | 751 | 721 | 681 | 658 | 621 | 606 | 653 | 547 | 529 | 512 |

GPS
CLOCK ANALYSIS

STATION ENSEMBLE VS NAVSTAR-3/4/5/6

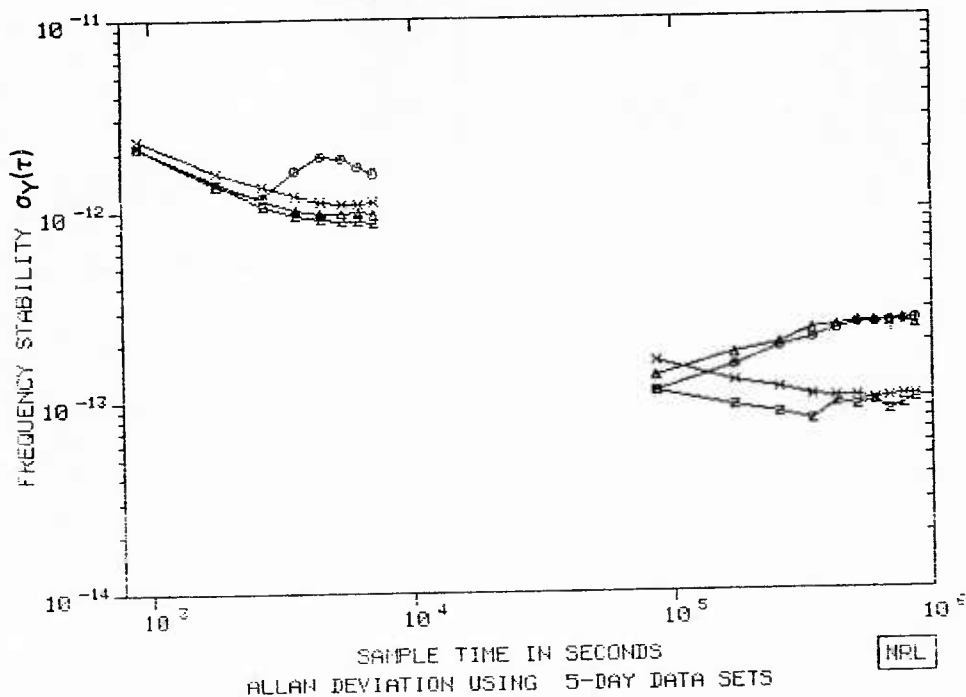


Fig. 19 — NAVSTARs 3, 4, 5, and 6 composite frequency stability vs sample time, MS ensemble

Table 10 — NAVSTARs 5 & 6 (Cesium) vs Station Ensemble—1982.
 Model $\sigma_y^2(\tau) = a(\tau)^\mu$.

| Solution | | Data | | | |
|------------------------|----------|------------------------------|----------|------------------------------|----------|
| Coefficient | Exponent | $(\tau_1, \sigma_y(\tau_1))$ | | $(\tau_2, \sigma_y(\tau_2))$ | |
| a | μ | seconds | PP10(13) | seconds | PP10(13) |
| 1.85×10^{-20} | -1.21 | 900 | 22.55 | 1,800 | 14.85 |
| 9.50×10^{-22} | -0.81 | 1,800 | 14.85 | 4,500 | 10.25 |
| 2.13×10^{-24} | -0.08 | 4,500 | 10.25 | 7,200 | 10.05 |
| 1.68×10^{-24} | -0.40 | 86,160 | 1.35 | 430,800 | 0.98 |
| 3.11×10^{-27} | 0.09 | 430,800 | 0.98 | 861,600 | 1.01 |

Table 11 — NAVSTARs 3/4/5/6 (Cesium & Rubidium) vs Station Ensemble—1982.
 Model $\sigma_y^2(\tau) = a(\tau)^\mu$.

| NAVSTARs Used | Solution | | Data | | | |
|--------------------------------------|------------------------|----------|------------------------------|----------|------------------------------|----------|
| | Coefficient | Exponent | $(\tau_1, \sigma_y(\tau_1))$ | | $(\tau_2, \sigma_y(\tau_2))$ | |
| | a | μ | seconds | PP10(13) | seconds | PP10(13) |
| 3/4/5/6 | 2.08×10^{-20} | -1.23 | 900 | 21.95 | 1,800 | 14.33 |
| 4/5/6 | 5.98×10^{-22} | -0.76 | 1,800 | 14.33 | 4,500 | 10.13 |
| 4/5/6 | 1.44×10^{-24} | -0.04 | 4,500 | 10.13 | 7,200 | 9.93 |
| Postulated Measurement Noise Process | | | | | | |
| 3/4/5/6 | 2.31×10^{-20} | -1.25 | 900 | 21.95 | 86,160 | 1.28 |

The long-term stabilities for the four NAVSTAR clocks are in close agreement for a 1-day sample time with a composite average of 1.3 parts per 10^{13} (PP13).

CONCLUSIONS

- The NAVSTARs 3 and 4 rubidium clock (with drift removed) long-term stability values agreed closely. A random walk FM noise process was present for sample times of 1 to 10 days. These measurements are in good agreement with the expected rubidium long-term performance.
- The NAVSTAR-3 rubidium frequency had a significant departure, from expected performance, at a sample time of 1.25 h. A possible cause is thermal fluctuations with a 2.5-h period. Performance is nominal for 900- and 1800-s sample times.
- For sample times of 1 to 5 days, the NAVSTAR-6 clock exhibited better performance than the NAVSTAR-5 clock. The NAVSTARs 5 and 6 cesium clock long-term stability values agreed closely for sample times of 6 to 10 days. A flicker noise FM process was present, in both cesium clocks, for sample times of 1 to 10 days.

- For sample times of 2 to 10 days, the NAVSTARs 5 and 6 cesium clocks have better frequency stability results than the NAVSTARs 3 and 4 rubidium clocks.
- White noise FM was measured, for both rubidium and cesium clocks, for short-term sample times of 900 and 1800 s. For sample times of 2700 s to 2 h, a gradual transition to an apparent, as yet unexplained, flicker noise FM was observed.
- The 1-day sample time frequency stability measurements, for both cesium and rubidium clocks, were in close agreement with an average value of 1.3×10^{-13} . This average value agrees closely with the projection of the 900- to 1800-s segment, indicating an underlying white noise FM process for sample times ranging from 900 s to 1 day.

ACKNOWLEDGMENTS

The authors express their appreciation to Mr. C. A. Bartholomew, NRL GPS Program Manager, for guidance and support of this work; to Mr. Robert Hill, Dr. James O'Toole, Mr. Jack Carr and Mr. Pat Beveridge of the Naval Surface Weapons Center for the smoothed ephemeris calculations; to Mr. Art Satin and Mr. William Feess of the Aerospace Corporation for technical consultation and assistance in acquiring the data; to Dr. Dave Allan for technical consultation; to Mr. Clarence Carson, Ms. Yvonne Vance and Ms. Anne Gattis of the Bendix Corporation for their assistance in processing the data; and to Mrs. Stella Scates and Ms. Suzane Beauchamp for manuscript preparation.

REFERENCES

1. C.A. Bartholomew, "Satellite Frequency Standards," *Nav.: J. of the Inst. of Nav.*, **25**(2), 113-120 (Summer 1978).
2. T.B. McCaskill, S.B. Stebbins, C.E. Carson, and J.A. Buisson, "Long Term Frequency Stability Analysis of the GPS NAVSTAR-6 Cesium Clock," NRL Report 8599, Sept. 1982.
3. J.A. Buisson and T.B. McCaskill, "TIMATION Navigation Satellite System Constellation Study," NRL Report 7389, June 1972.
4. T.B. McCaskill, J.A. Buisson and D.W. Lynch, "Principles and Techniques of Satellite Navigation Using the TIMATION II Satellite," NRL Report 7252, June 1971.
5. T.B. McCaskill and J.A. Buisson, "NTS-1 (TIMATION III) Quartz- and Rubidium-Oscillator Frequency-Stability Results," NRL Report 7932, Dec. 1975.
6. J.A. Buisson, T.B. McCaskill, O.J. Oaks, M.M. Largay, S.B. Stebbins, "GPS NAVSTAR-4 and NTS-2 Long Term Frequency Stability and Time Transfer Analysis," NRL Report 8419, June 1980.
7. *GPS System Critical Design Review* (Oct. 1981) Book 2, Section 4.3, Title 5.1, p. 3.
8. R.E. Kalman, "A New Approach to Linear Filtering and Prediction Problems," *Trans. ASME Eng. J. Basic Eng. Series D*, **82**, 35-45 (Mar. 1960).
9. Bernard Friedland, "A Review of Recursive Filtering Algorithms," *Proc. of the Spring Joint Comp. Conf.*, AFIPS Conference Proc. **40** 1972, pp. 163-180.

10. S.S. Russell and J.H. Schaibly, "Control Segment and User Performance," *J. of the Inst. of Nav.*, 25(6), 166-172, Summer 1978.
11. J.W. O'Toole, "CELEST Computer Program for Computing Satellite Orbits," NSWC/DL TR-3565, Oct. 1976.
12. D.W. Allan, J.H. Shoaf and D. Halford, "Statistics of Time and Frequency Data Analysis," in *Time and Frequency: Theory and Fundamentals*, Nat. Bur. of Stand. Monograph 140, May 1974, Ch. 8. pp. 151-204.
13. G. Haefner and J. Moses, "NAVSTAR GPS X-Set Receiver Performance Flow Down Specifications," Magnavox reference number R-5227, Dec. 1975.
14. P. Lesage and C. Audoin, "Estimation of the Two-sample Variance with a Limited Number of Data," *Proc. of the 31st Ann. Sym. on Frequency Control*, 1977, pp 311-318.
15. J.A. Barnes, National Bureau of Standards, Boulder, Colo., "Notes on Confidence of the Estimate and Overlapping Samples," unpublished.
16. J.M. Luck, "Construction and Comparison of Atomic Time Scale Algorithms," TR#32, Division of National Mapping, Canberra, Australia, 1983.

GLOSSARY

Allan deviation — measure of frequency stability equal to the square root of the Allan variance

Allan variance — time domain measure of frequency stability behavior adopted by the IEEE to evaluate clock performance

Cesium clock — atomic clock regulated by the natural vibration frequency of atoms in cesium beam resonator

Clock offset — time difference between a clock and a reference clock

Confidence limits — extreme values on interval estimated to contain true value

Ephemeris — calculated positions of a satellite at regular time intervals

Epoch — reference time for a calculation

Fractional frequency — ratio of the frequency minus the reference frequency to the reference frequency

FM — frequency modulation

GPS — Global Position System

L-band — area of radio frequency spectrum between 390 and 1550 MHz

Long-term frequency stability — calculated value based on sample times of 1 to 10 days

MCS — master control station

MS — ground monitor site

NAVSTAR — GPS constellation satellite name

Noise — variation of data from true values

NSWC — Naval Surface Weapons Center

P-code chip — the pulse of shortest duration in the GPS P-code sequence, which is equal in length to the code sequence clock period. For GPS, the P-code chip is equal to $1/10.23 \text{ MHz} = 97.75 \text{ ns}$

PM — phase modulation

Pseudorange — measured distance from SV to MS, including clock offset and delay due to signal travel time (apparent time difference)

Range — actual distance from SV to MS

Rubidium clock — atomic clock based on gas cell containing mixture of rubidium vapor and neutral buffer gas

Sample time (τ) — time interval between two measurements used in calculating the Allan variance

Short-term frequency stability — calculated value based on sample times of 900-7200 s.

Station ensemble — combination of monitor sites to produce average stability values

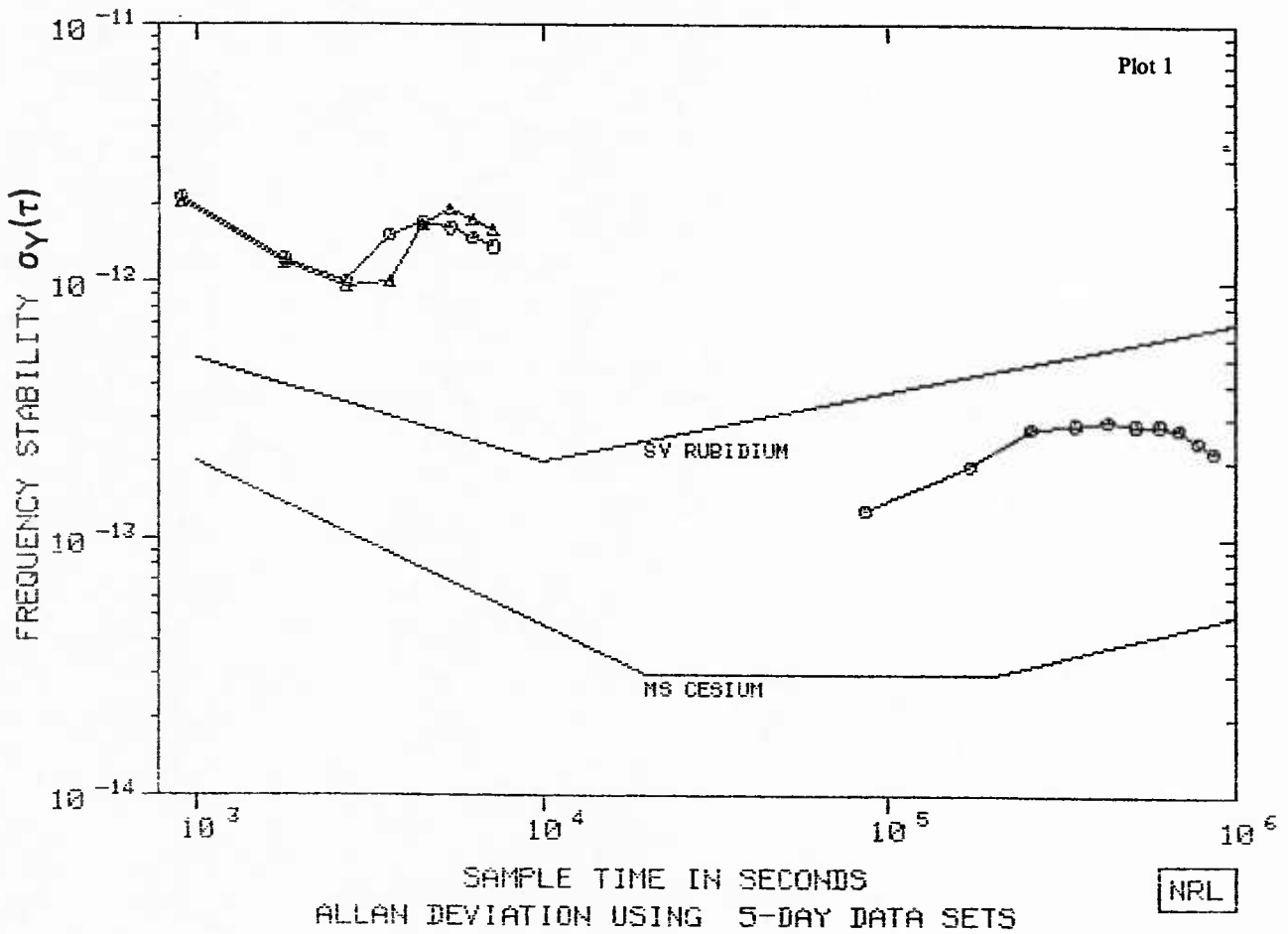
SV — space vehicle

Time domain analysis — analysis with the independent variable being the sampling time rather than the running time

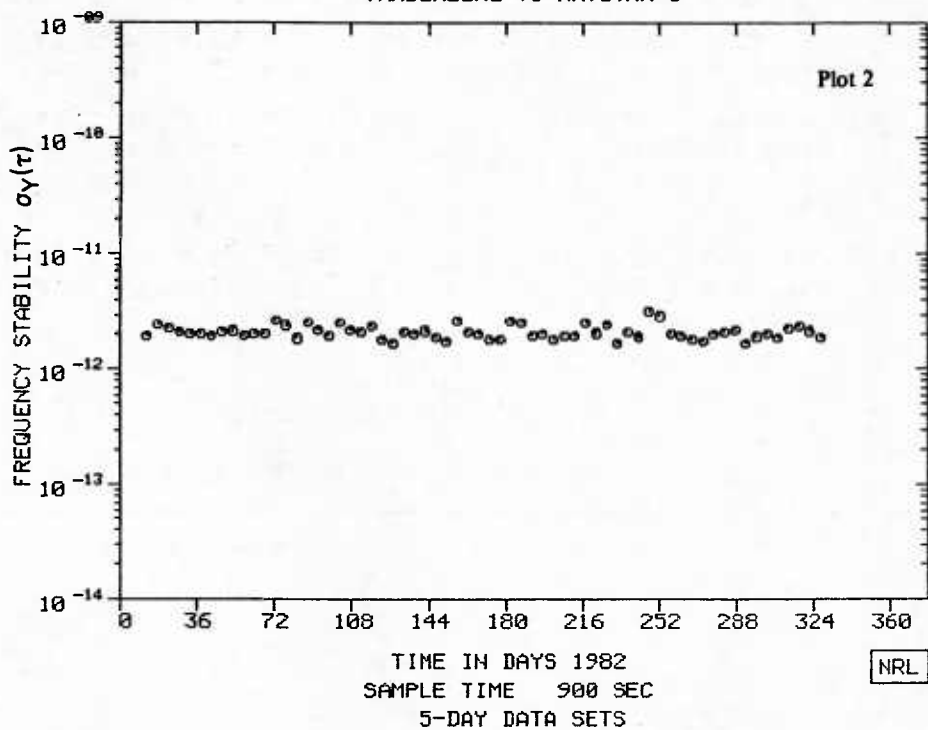
APPENDIX
NAVSTAR TIME-DOMAIN PLOTS 1-90

| | τ (HRS) | .25 | .50 | .75 | 1.00 | 1.25 | 1.50 | 1.75 | 2.00 | | |
|-----------|-----------------|------|------|------|------|------|------|------|------|------|------|
| ● V82-305 | σ (PP13) | 21.3 | 12.2 | 10.1 | 15.1 | 17.1 | 16.1 | 14.9 | 13.7 | | |
| | AVG PTS | 83 | 83 | 75 | 72 | 64 | 56 | 48 | 48 | | |
| ▲ V83-305 | σ (PP13) | 20.6 | 11.9 | 9.7 | 10.1 | 16.7 | 19.2 | 17.5 | 15.9 | | |
| | AVG PTS | 78 | 78 | 72 | 68 | 61 | 54 | 46 | 39 | | |
| | τ (DAYS) | 1 | 2 | 3 | 4 | 5 | 6 | 7 | 8 | 9 | 10 |
| ● VAN-382 | σ (PP14) | 13.0 | 19.0 | 27.0 | 28.0 | 29.0 | 28.0 | 28.0 | 27.0 | 24.0 | 22.0 |
| | TOT PTS | 184 | 184 | 179 | 184 | 180 | 180 | 202 | 177 | 175 | 168 |

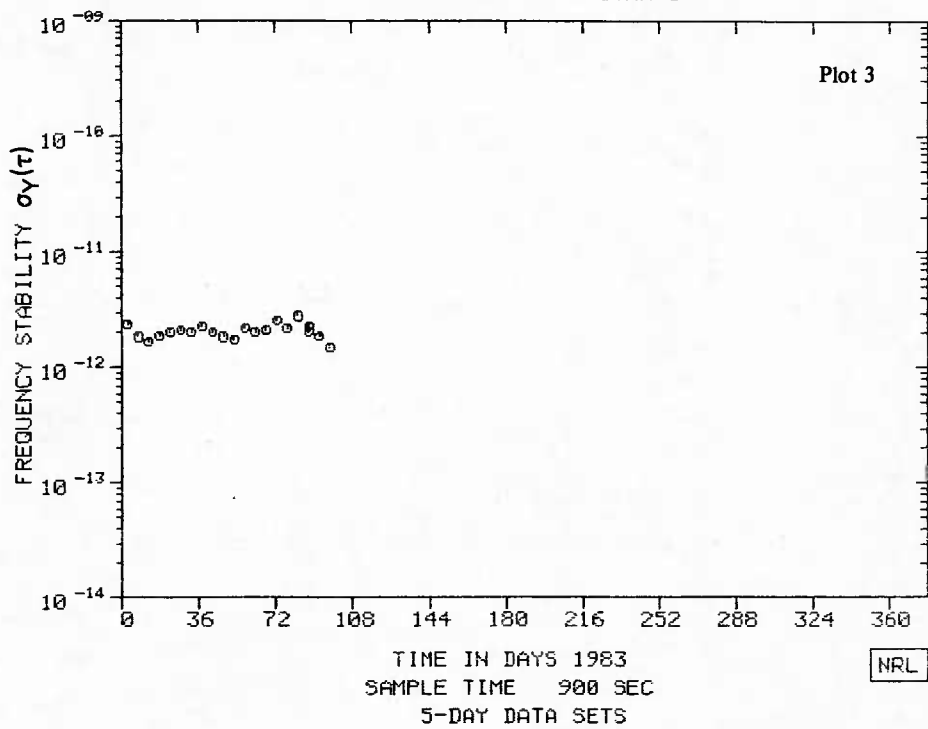
GPS
CLOCK ANALYSIS
VANDENBERG VS NAVSTAR-3



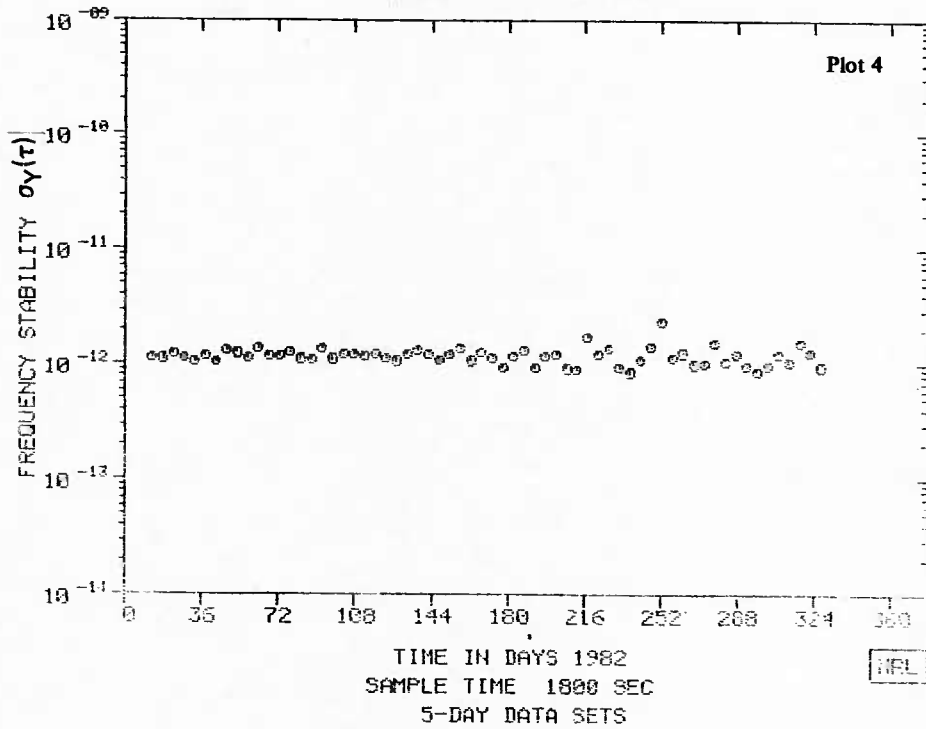
GPS
CLOCK ANALYSIS
VANDENBERG VS NAVSTAR-3



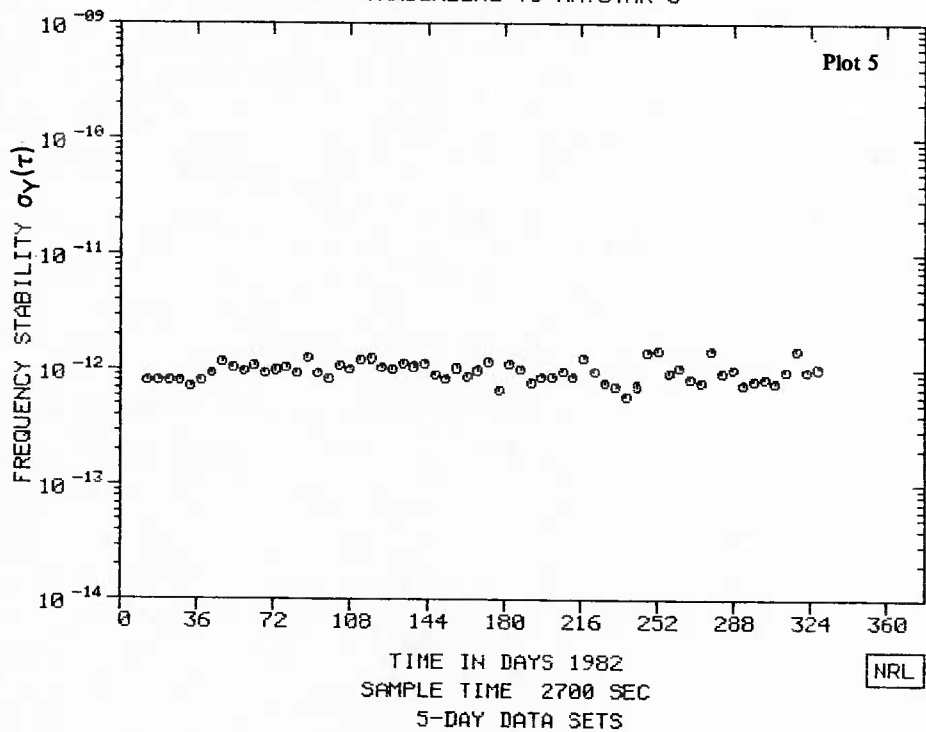
GPS
CLOCK ANALYSIS
VANDENBERG VS NAVSTAR-3



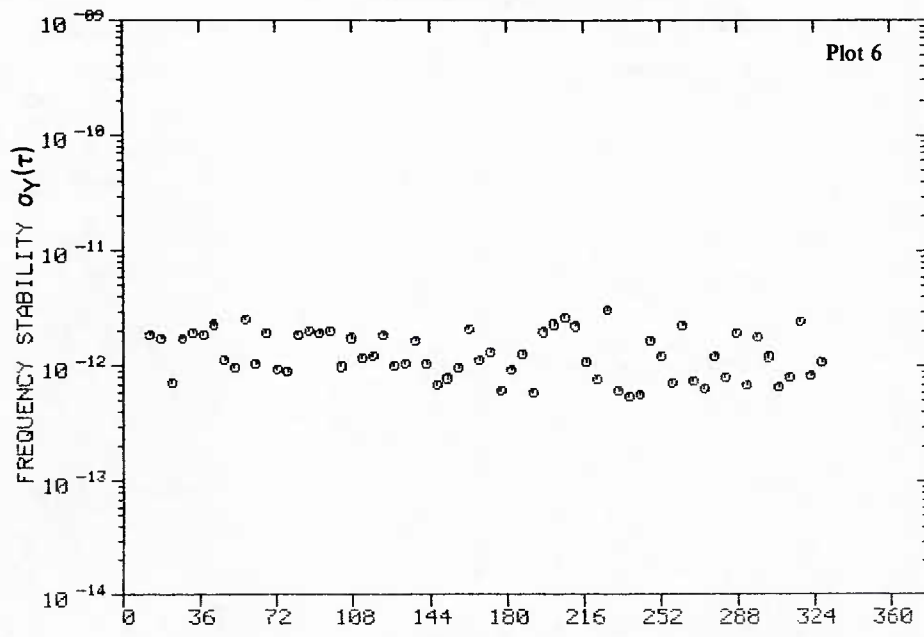
GPS
CLOCK ANALYSIS
VANDENBERG VS NAVSTAR-3



GPS
CLOCK ANALYSIS
VANDENBERG VS NAVSTAR-3



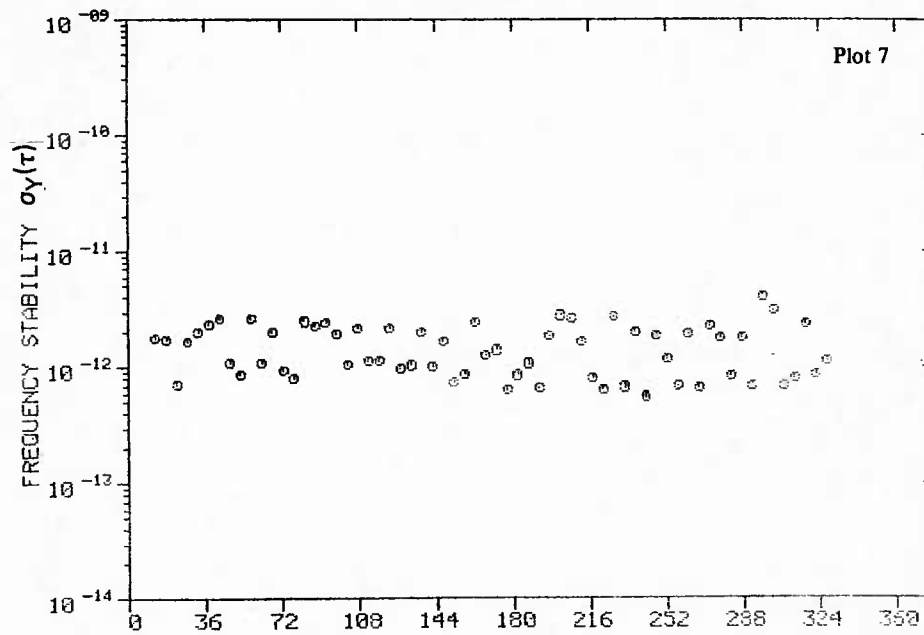
GPS
CLOCK ANALYSIS
VANDENBERG VS NAVSTAR-3



SAMPLE TIME 3600 SEC
5-DAY DATA SETS

NRL

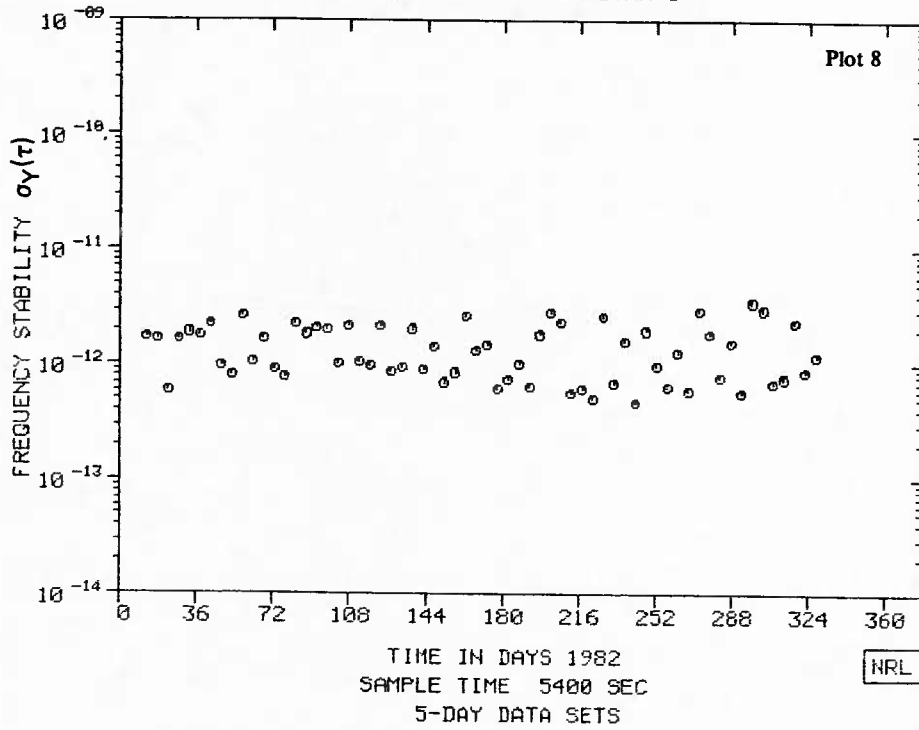
GPS
CLOCK ANALYSIS
VANDENBERG VS NAVSTAR-3



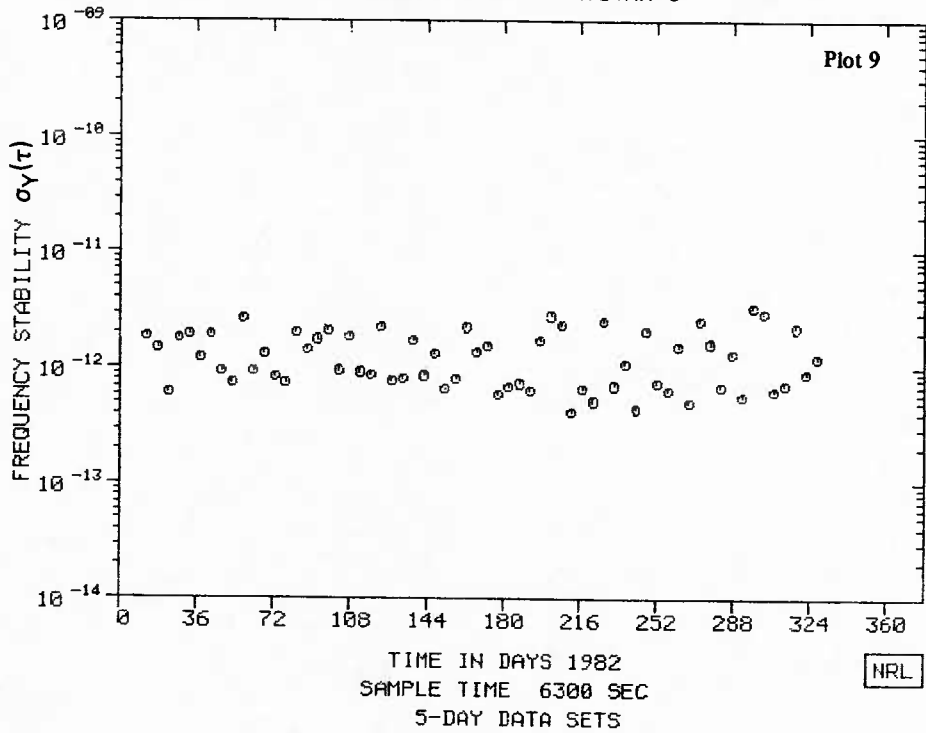
SAMPLE TIME 4500 SEC
5-DAY DATA SETS

NRL

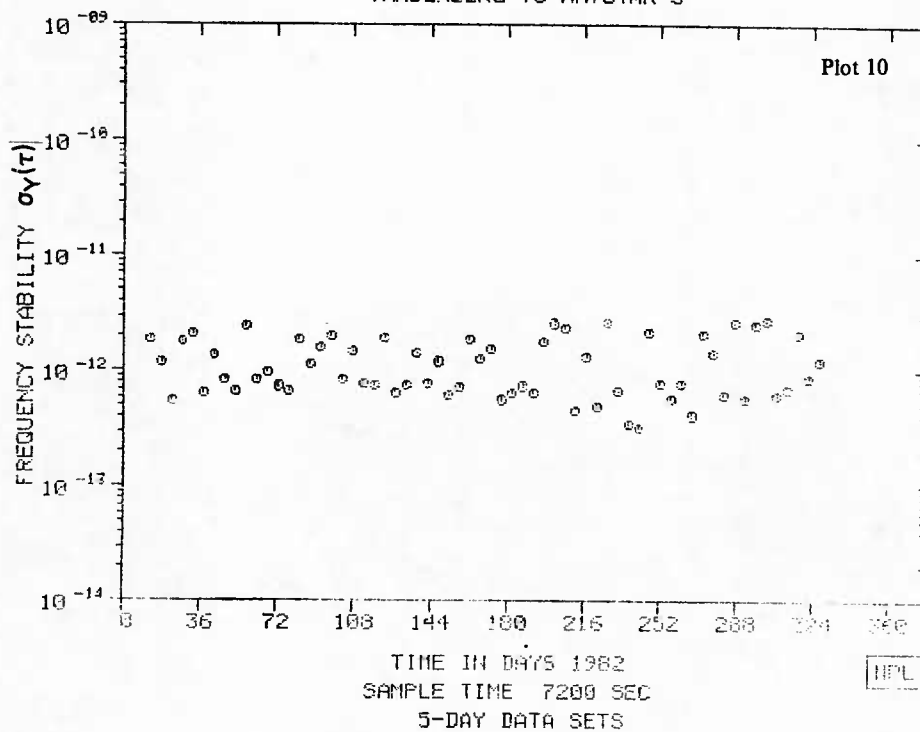
GPS
CLOCK ANALYSIS
VANDENBERG VS NAVSTAR-3



GPS
CLOCK ANALYSIS
VANDENBERG VS NAVSTAR-3



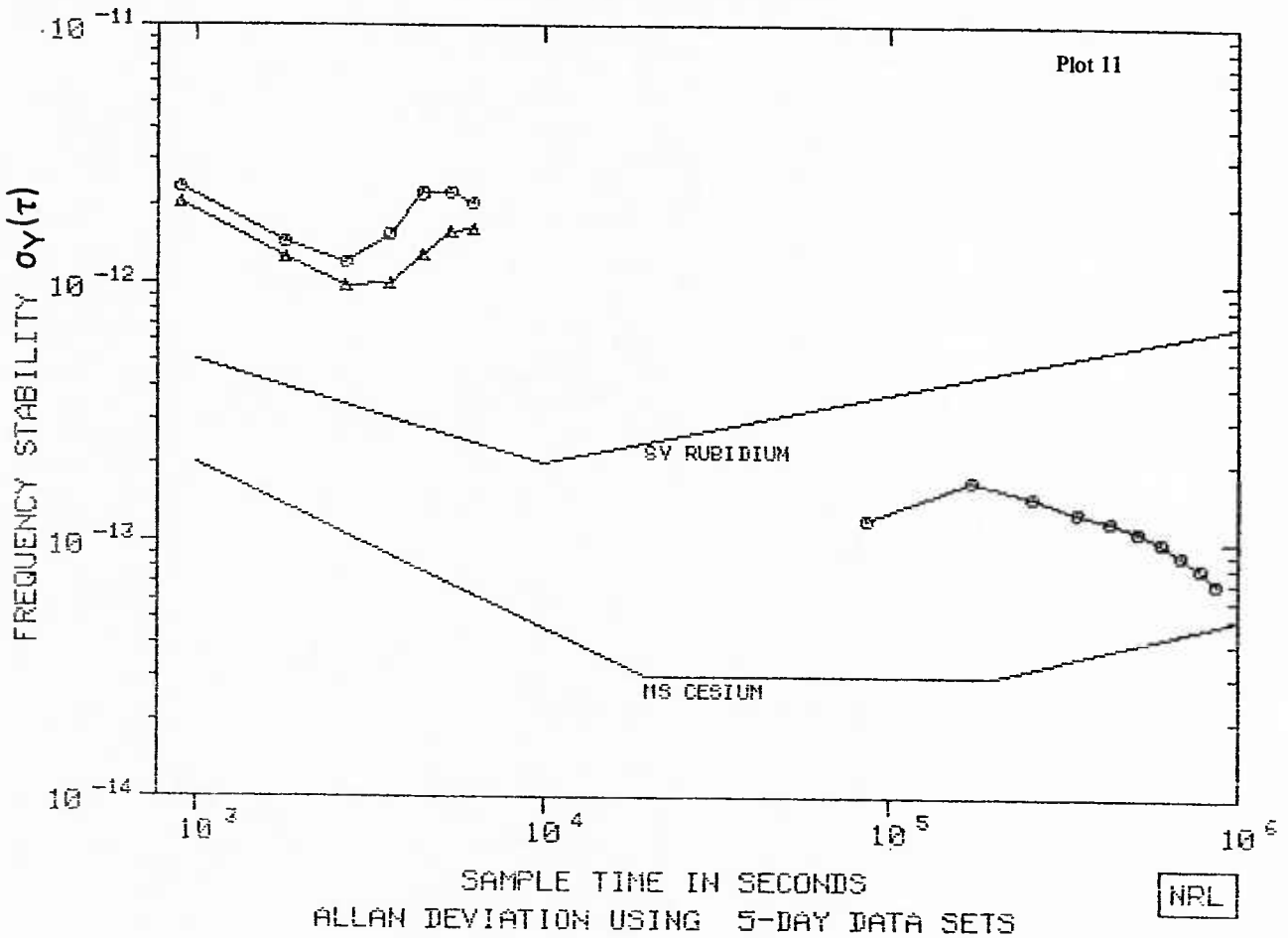
GPS
CLOCK ANALYSIS
VANDENBERG VS NAVSTAR-3



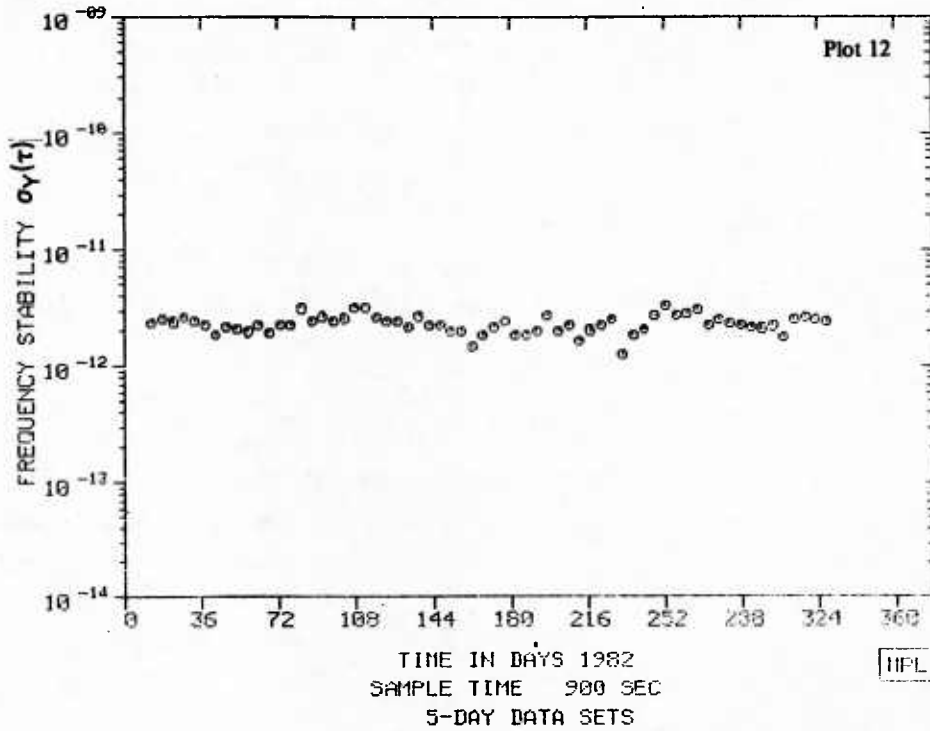
| | τ (HRS) | .25 | .50 | .75 | 1.00 | 1.25 | 1.50 | 1.75 | 2.00 | | |
|-----------|-----------------|------|------|------|------|------|------|------|------|-----|-----|
| ○ G82-395 | σ (PP13) | 23.6 | 14.4 | 12.0 | 15.4 | 22.2 | 22.5 | 20.5 | 18.1 | | |
| | AVG PTS | 63 | 33 | 43 | 35 | 26 | 19 | 14 | 9 | | |
| △ G93-395 | σ (PP13) | 20.5 | 12.6 | 9.9 | 10.0 | 12.9 | 15.8 | 16.3 | 13.2 | | |
| | AVG PTS | 46 | 39 | 32 | 27 | 20 | 15 | 11 | 7 | | |
| | τ (DAYS) | 1 | 2 | 3 | 4 | 5 | 6 | 7 | 8 | 9 | 10 |
| ○ GUA-382 | σ (PP14) | 12.0 | 17.0 | 15.0 | 13.0 | 12.0 | 11.0 | 10.0 | 9.0 | 8.0 | 7.0 |
| | TOT PTS | 222 | 204 | 195 | 185 | 182 | 182 | 207 | 157 | 155 | 148 |

GPS CLOCK ANALYSIS

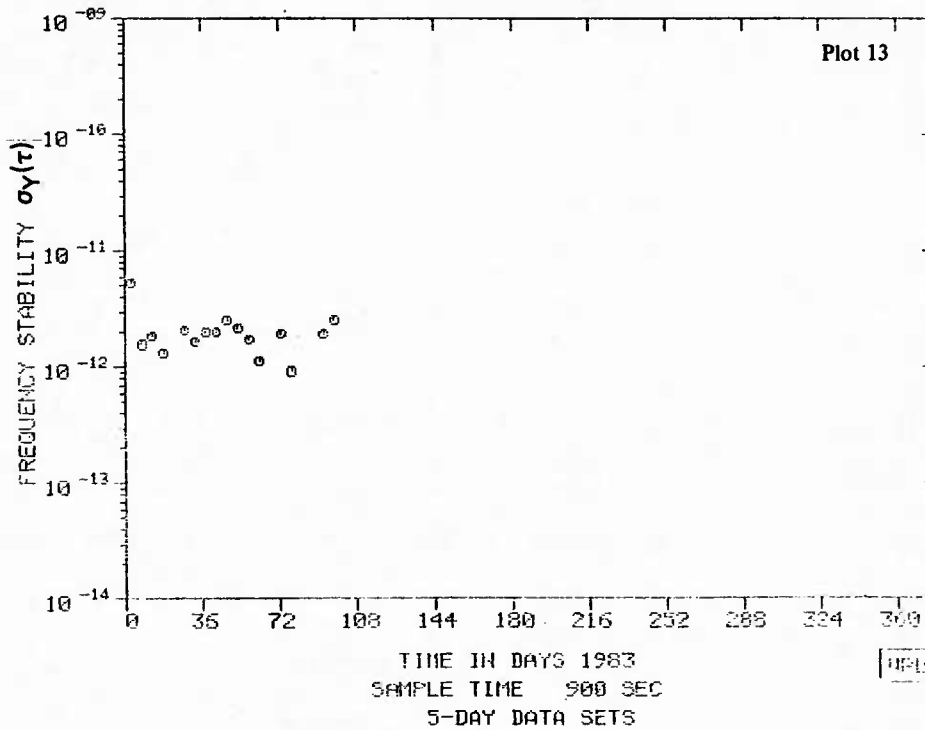
GUAM VS NAVSTAR-3



GPS
CLOCK ANALYSIS
GUAM VS NAVSTAR-3

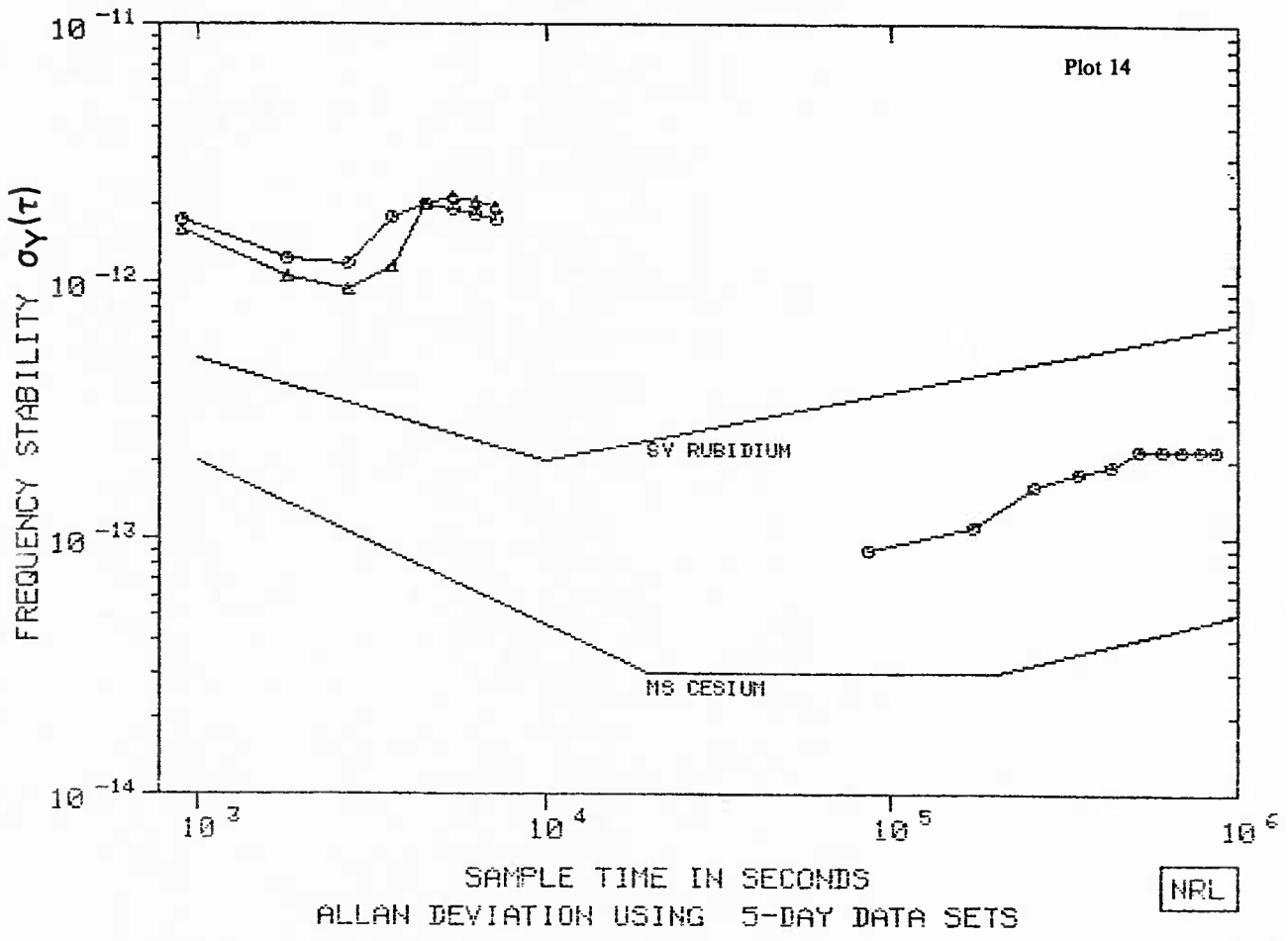


GPS
CLOCK ANALYSIS
GUAM VS NAVSTAR-3

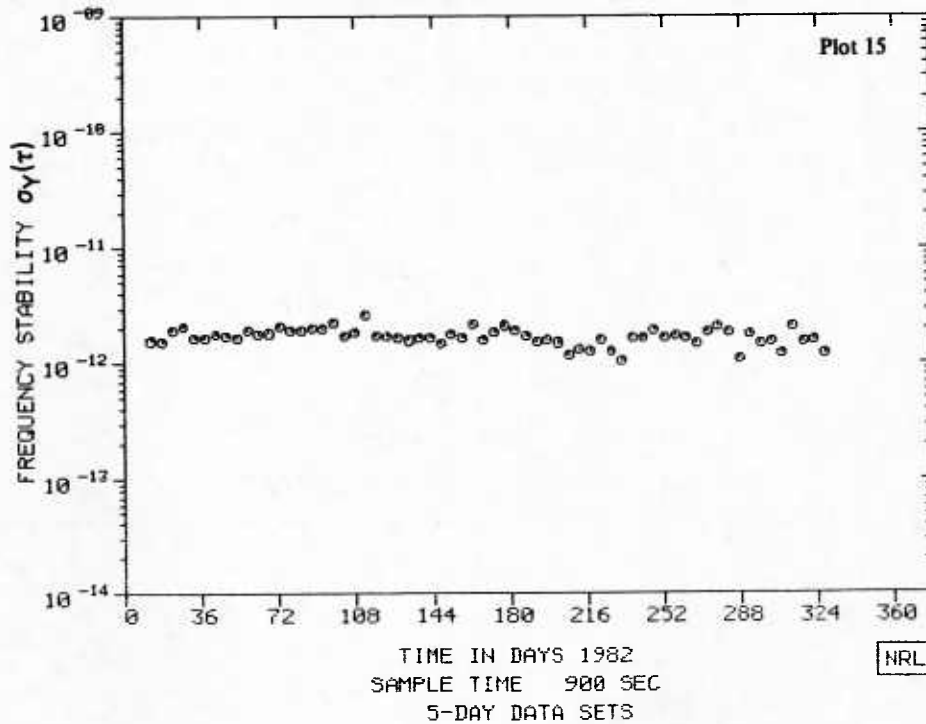


| | τ (HRS) | .25 | .50 | .75 | 1.00 | 1.25 | 1.50 | 1.75 | 2.00 | | |
|-----------|-----------------|------|------|------|------|------|------|------|------|------|------|
| ○ H82-305 | σ (PP13) | 17.6 | 12.4 | 11.9 | 17.9 | 19.9 | 19.1 | 18.1 | 17.3 | | |
| | AVG PTS | 85 | 85 | 79 | 77 | 70 | 62 | 54 | 47 | | |
| △ H83-305 | σ (PP13) | 15.8 | 10.5 | 9.4 | 11.5 | 20.1 | 21.5 | 20.3 | 19.6 | | |
| | AVG PTS | 82 | 82 | 75 | 73 | 68 | 61 | 54 | 46 | | |
| | τ (DAYS) | 1 | 2 | 3 | 4 | 5 | 6 | 7 | 8 | 9 | 10 |
| ○ HAW-382 | σ (PP14) | 9.0 | 11.0 | 16.0 | 18.0 | 19.0 | 22.0 | 22.0 | 22.0 | 22.0 | 22.0 |
| | TOT PTS | 147 | 147 | 138 | 141 | 142 | 139 | 156 | 138 | 139 | 122 |

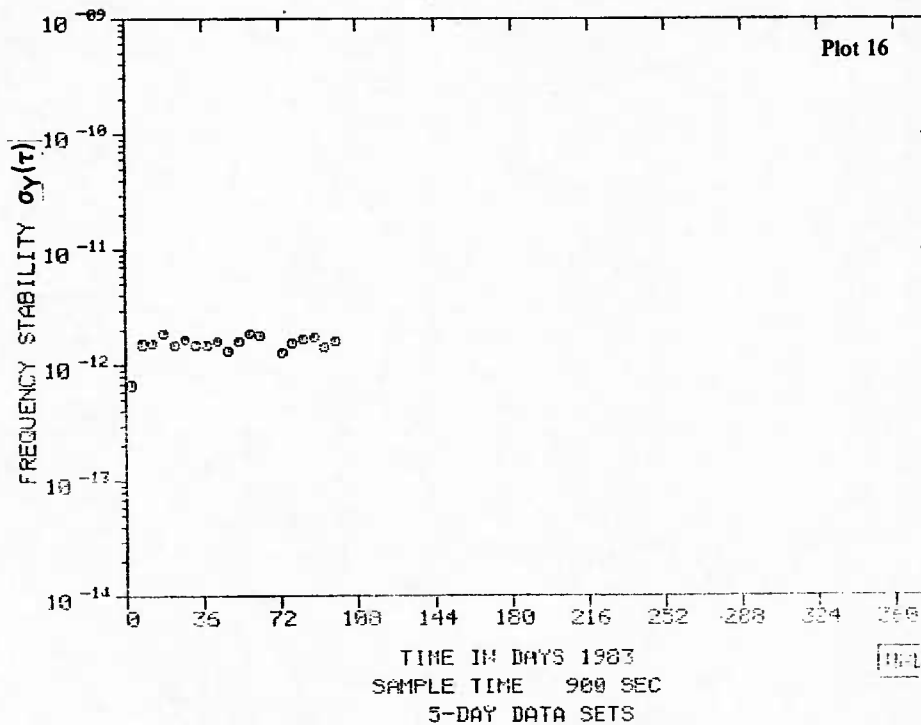
GPS
CLOCK ANALYSIS
HAWAII VS NAVSTAR-3



GPS
CLOCK ANALYSIS
HAWAII VS NAVSTAR-3

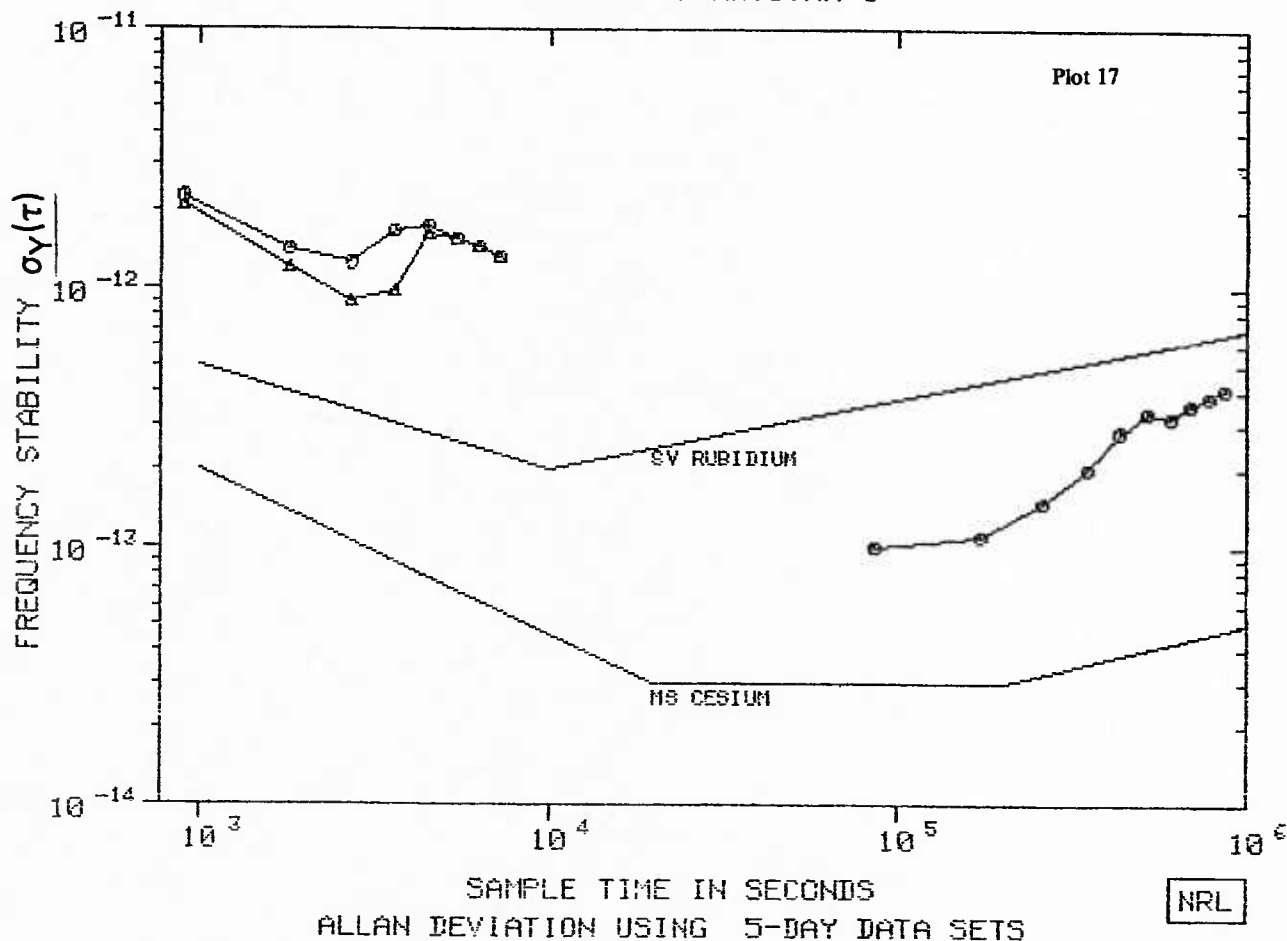


GPS
CLOCK ANALYSIS
HAWAII VS NAVSTAR-3

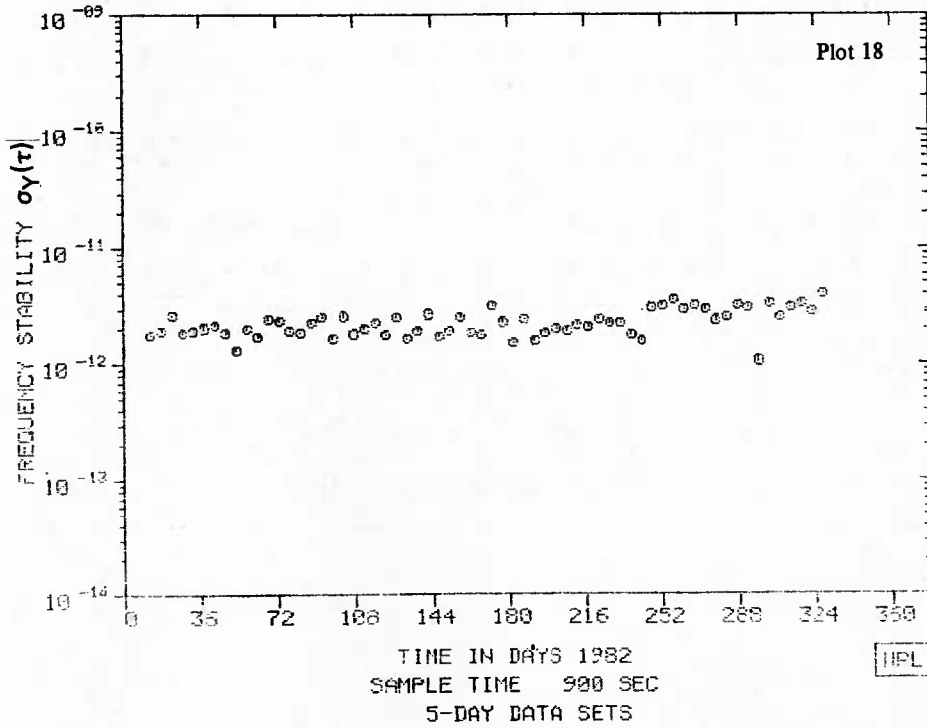


| | τ (HRS) | .25 | .50 | .75 | 1.00 | 1.25 | 1.50 | 1.75 | 2.00 | | |
|-----------|-----------------|------|------|------|------|------|------|------|------|------|------|
| ⊙ A82-305 | σ (PP13) | 22.7 | 14.3 | 12.5 | 16.7 | 17.3 | 15.6 | 14.6 | 13.3 | | |
| | AVG PTS | 59 | 55 | 45 | 40 | 32 | 27 | 21 | 16 | | |
| △ A83-305 | σ (PP13) | 20.8 | 12.1 | 9.0 | 9.8 | 16.4 | 15.6 | 14.6 | 13.1 | | |
| | AVG PTS | 67 | 68 | 59 | 54 | 46 | 39 | 31 | 24 | | |
| | τ (DAYS) | 1 | 2 | 3 | 4 | 5 | 6 | 7 | 8 | 9 | 10 |
| ⊙ ALK-382 | σ (PP14) | 10.0 | 11.0 | 15.0 | 20.0 | 28.0 | 33.0 | 32.0 | 36.0 | 38.0 | 41.0 |
| | TOT PTS | 170 | 144 | 127 | 119 | 118 | 121 | 133 | 118 | 113 | 113 |

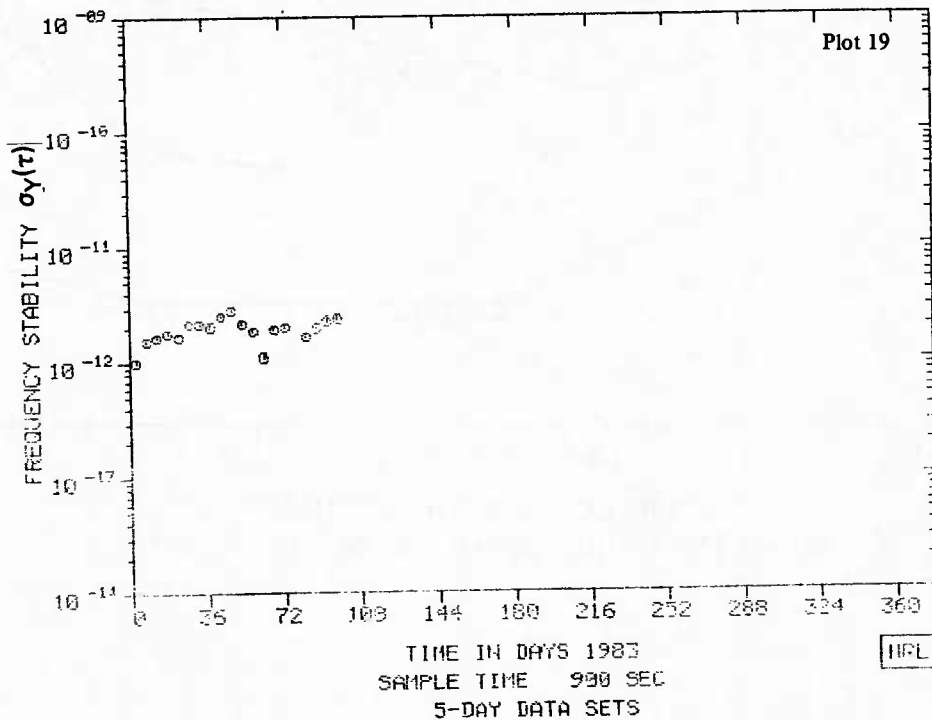
GPS
CLOCK ANALYSIS
ALASKA VS NAVSTAR-3



GPS
CLOCK ANALYSIS
ALASKA VS NAVSTAR-3

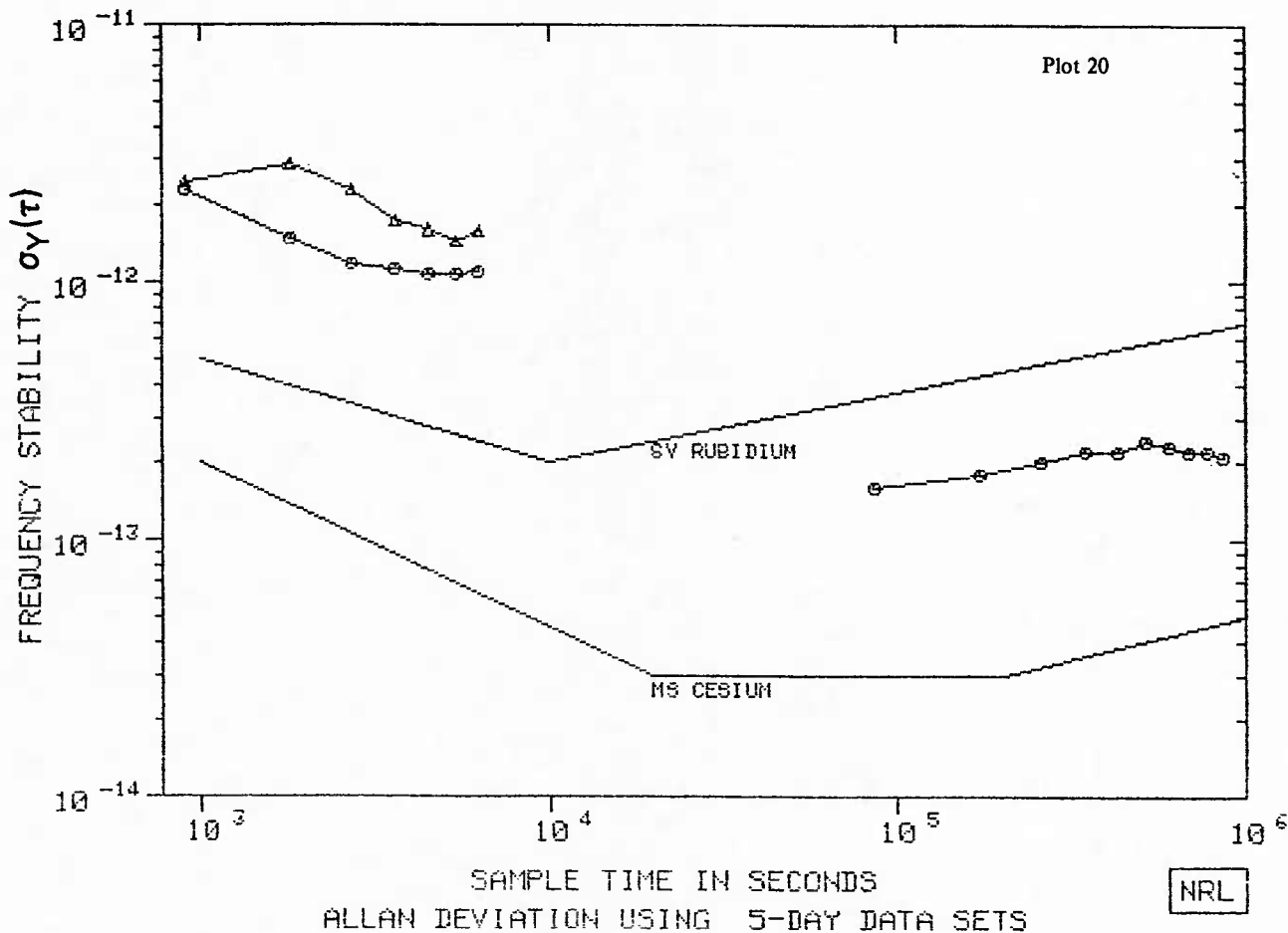


GPS
CLOCK ANALYSIS
ALASKA VS NAVSTAR-3

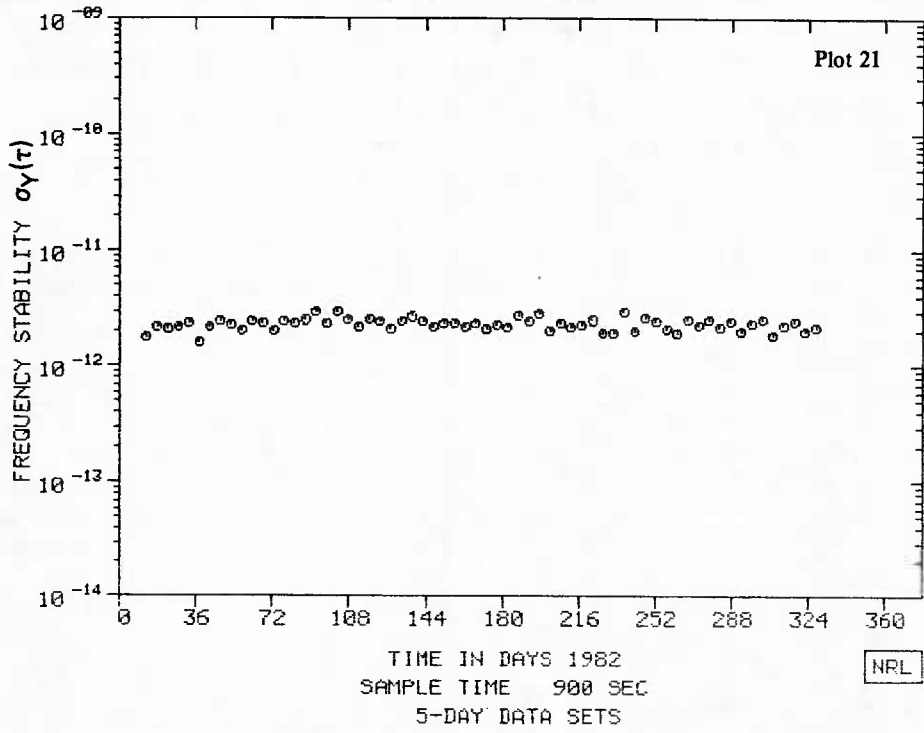


| | τ (HRS) | .25 | .50 | .75 | 1.00 | 1.25 | 1.50 | 1.75 | 2.00 | | |
|-----------|-----------------|------|------|------|------|------|------|------|------|------|------|
| ○ V82-405 | σ (PP13) | 23.2 | 14.9 | 11.7 | 11.2 | 10.8 | 10.7 | 11.1 | 11.3 | | |
| | AVG PTS | 81 | 78 | 64 | 53 | 39 | 25 | 14 | 8 | | |
| △ V83-405 | σ (PP13) | 24.8 | 28.7 | 23.0 | 17.5 | 16.1 | 14.5 | 16.0 | 14.8 | | |
| | AVG PTS | 67 | 65 | 55 | 47 | 36 | 23 | 15 | 8 | | |
| | τ (DAYS) | 1 | 2 | 3 | 4 | 5 | 6 | 7 | 8 | 9 | 10 |
| ○ VAN-482 | σ (PP14) | 16.0 | 18.0 | 20.0 | 22.0 | 22.0 | 24.0 | 23.0 | 22.0 | 22.0 | 21.0 |
| | TOT PTS | 341 | 324 | 320 | 324 | 303 | 301 | 334 | 295 | 289 | 289 |

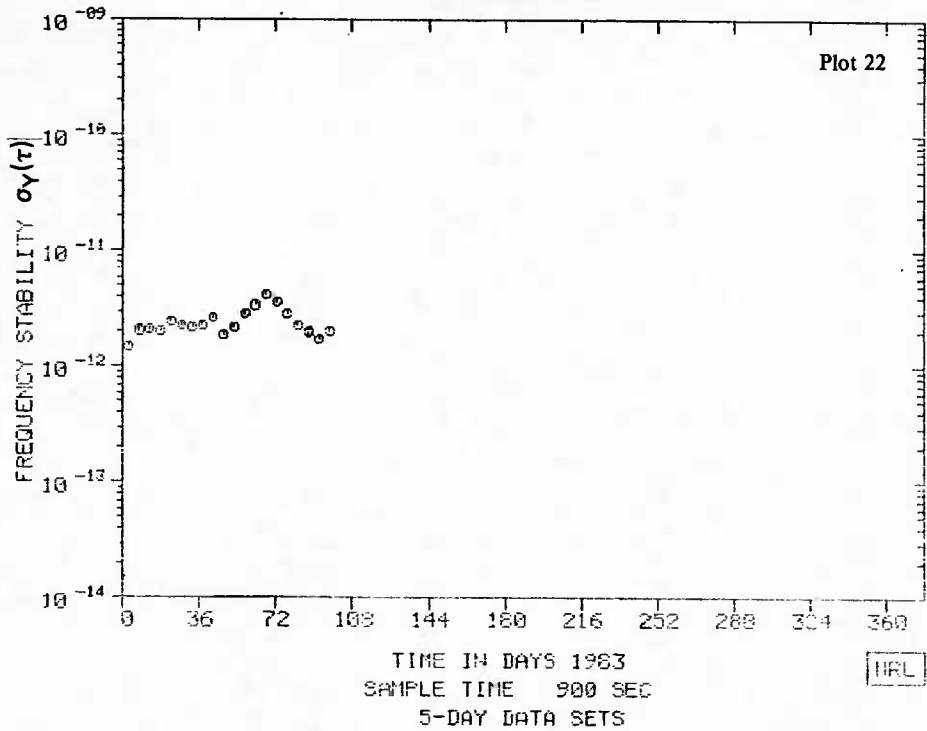
GPS
CLOCK ANALYSIS
VANDENBERG VS NAVSTAR-4



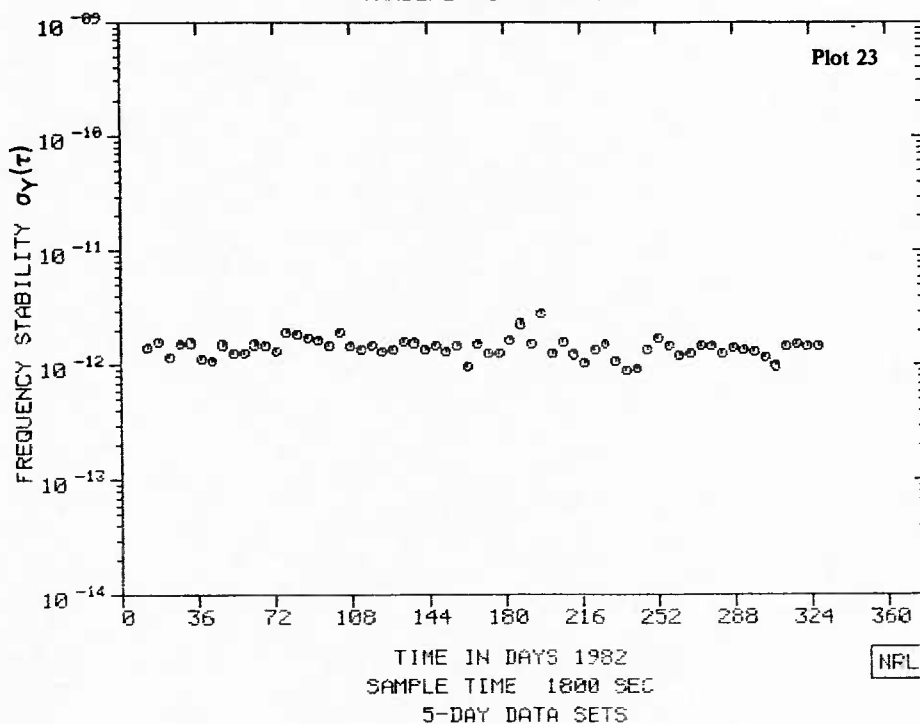
GPS
CLOCK ANALYSIS
VANDENBERG VS NAVSTAR-4



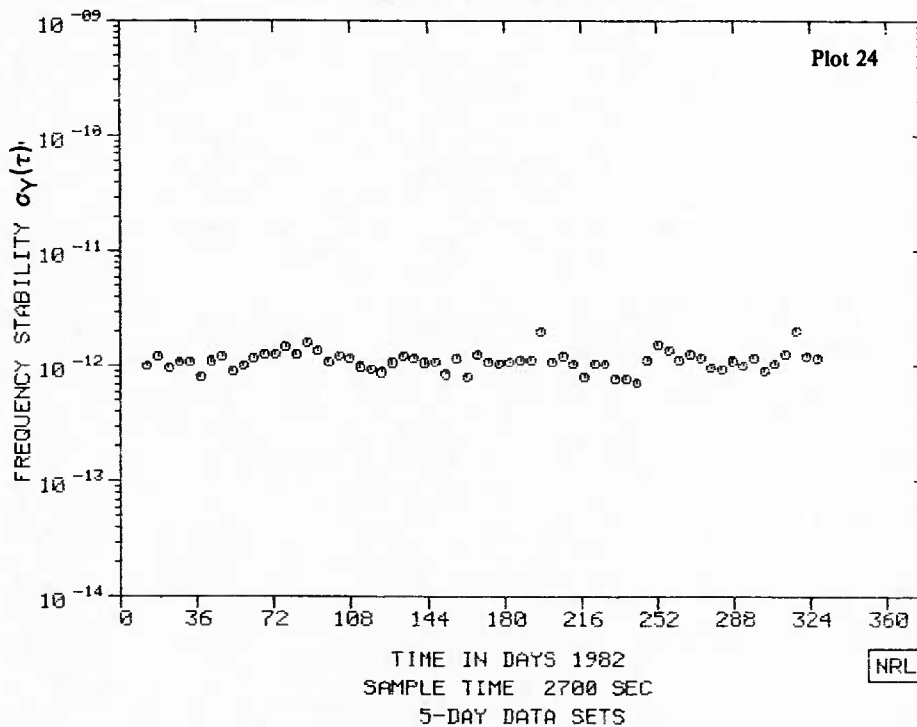
GPS
CLOCK ANALYSIS
VANDENBERG VS NAVSTAR-4



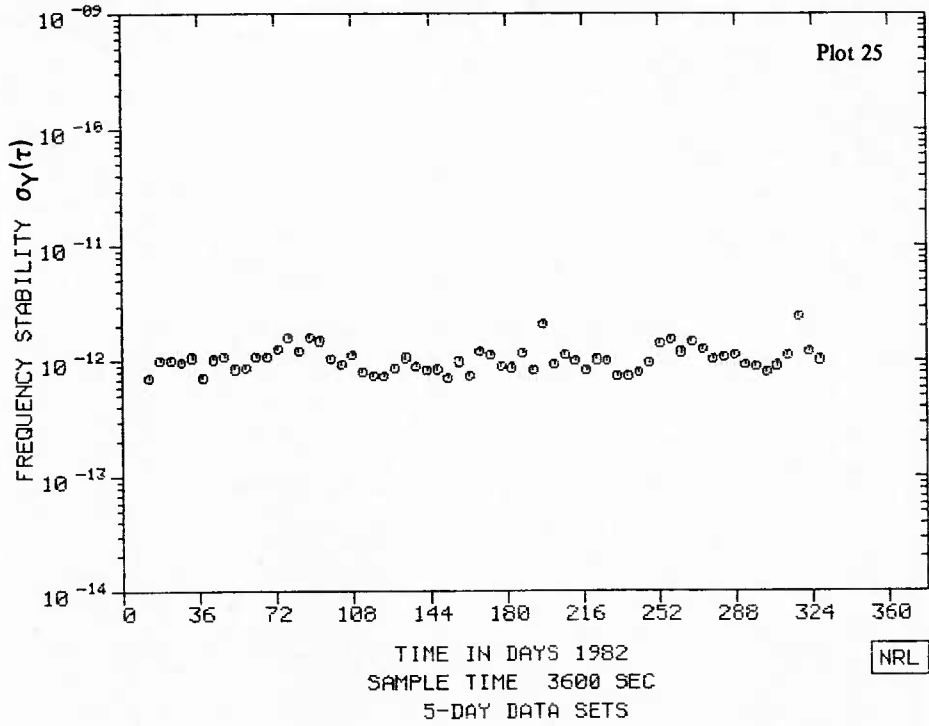
GPS
CLOCK ANALYSIS
VANDENBERG VS NAVSTAR-4



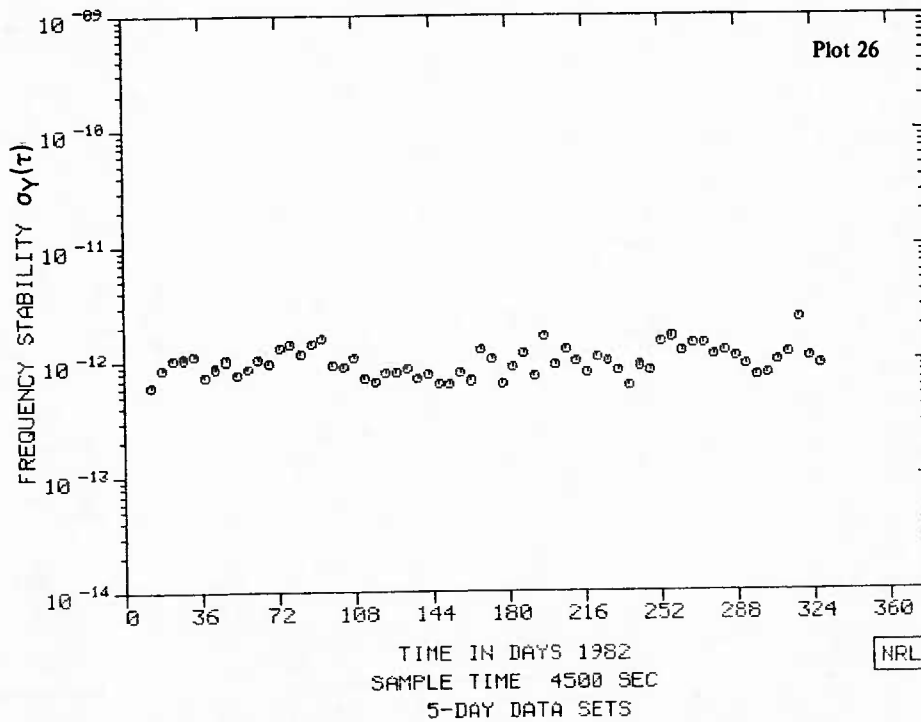
GPS
CLOCK ANALYSIS
VANDENBERG VS NAVSTAR-4



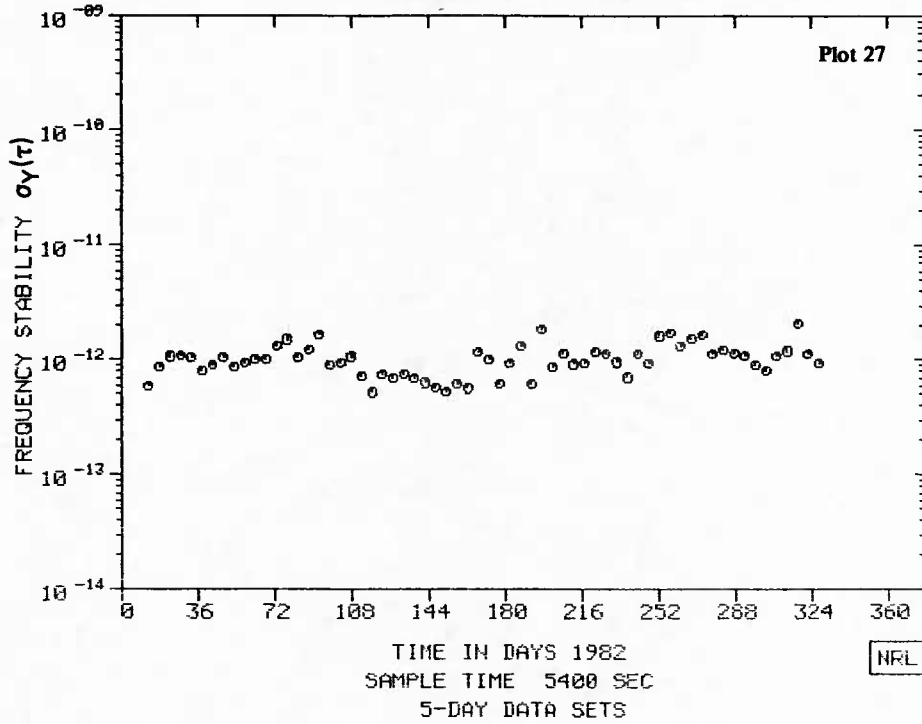
GPS
CLOCK ANALYSIS
VANDENBERG VS NAVSTAR-4



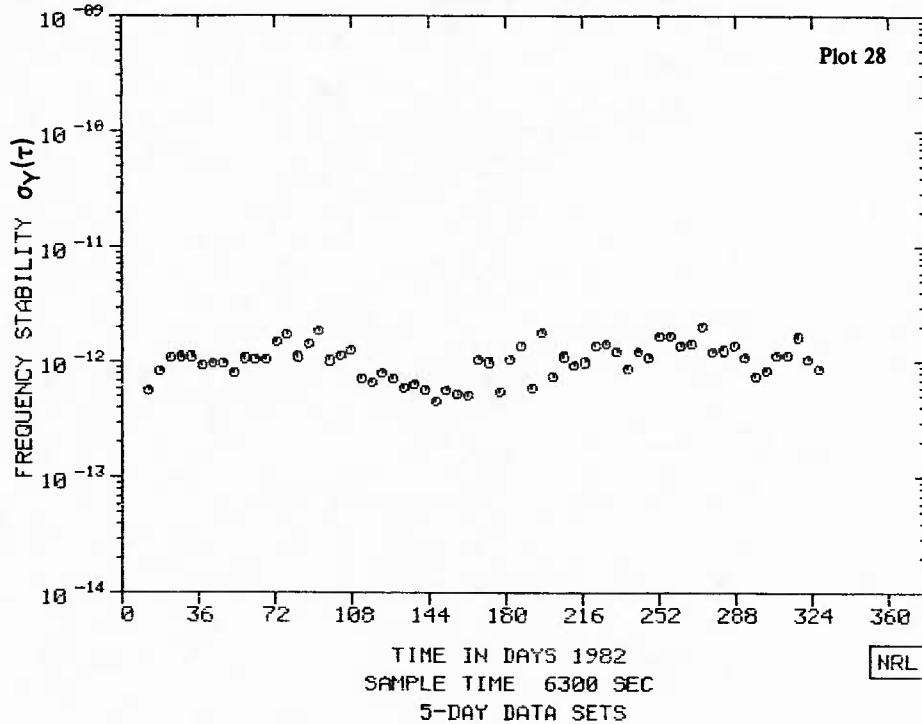
GPS
CLOCK ANALYSIS
VANDENBERG VS NAVSTAR-4

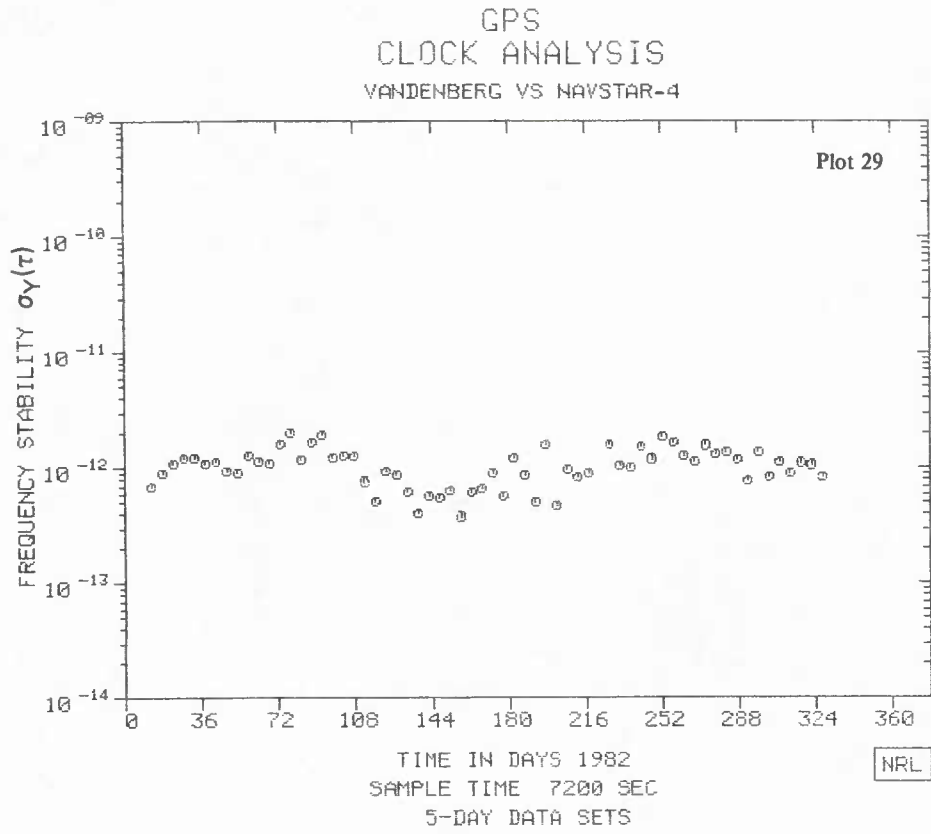


GPS
CLOCK ANALYSIS
VANDENBERG VS NAVSTAR-4



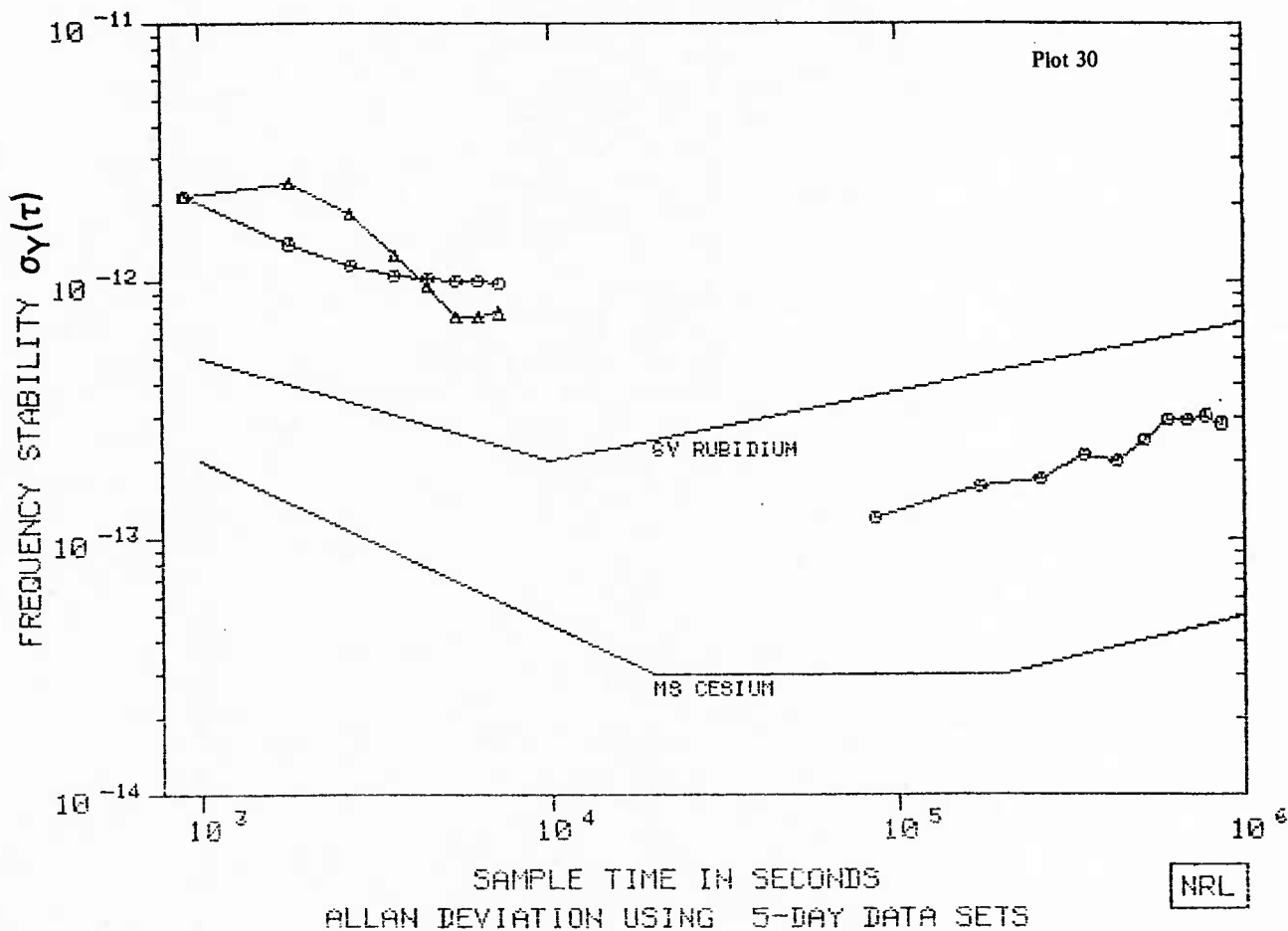
GPS
CLOCK ANALYSIS
VANDENBERG VS NAVSTAR-4



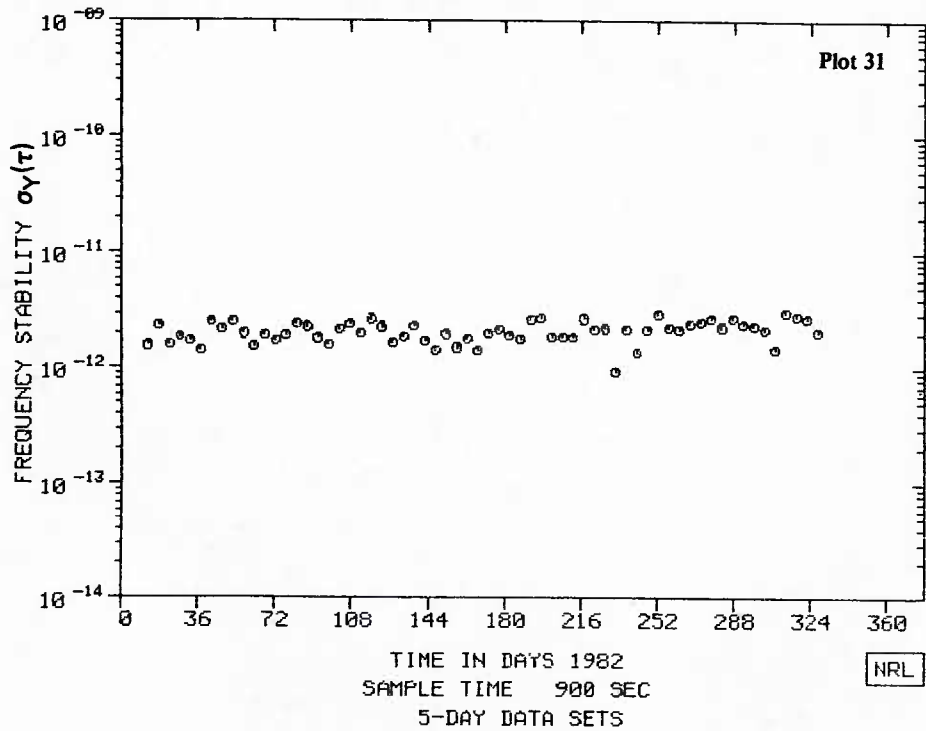


| | τ (HRS) | .25 | .50 | .75 | 1.00 | 1.25 | 1.50 | 1.75 | 2.00 | | |
|-----------|-----------------|------|------|------|------|------|------|------|------|------|------|
| ● G92-405 | σ (PP13) | 21.6 | 14.0 | 11.6 | 10.6 | 10.3 | 10.1 | 10.1 | 9.8 | | |
| | AVG PTS | 68 | 65 | 57 | 53 | 46 | 39 | 33 | 27 | | |
| ▲ G93-405 | σ (PP13) | 21.5 | 24.0 | 18.2 | 12.6 | 9.6 | 7.3 | 7.3 | 7.5 | | |
| | AVG PTS | 43 | 43 | 38 | 35 | 29 | 24 | 20 | 17 | | |
| | τ (DAYS) | 1 | 2 | 3 | 4 | 5 | 6 | 7 | 8 | 9 | 10 |
| ● GUA-482 | σ (PP14) | 12.0 | 16.0 | 17.0 | 21.0 | 20.0 | 24.0 | 29.0 | 29.0 | 30.0 | 28.0 |
| | TOT PTS | 165 | 90 | 103 | 87 | 87 | 85 | 92 | 82 | 75 | 79 |

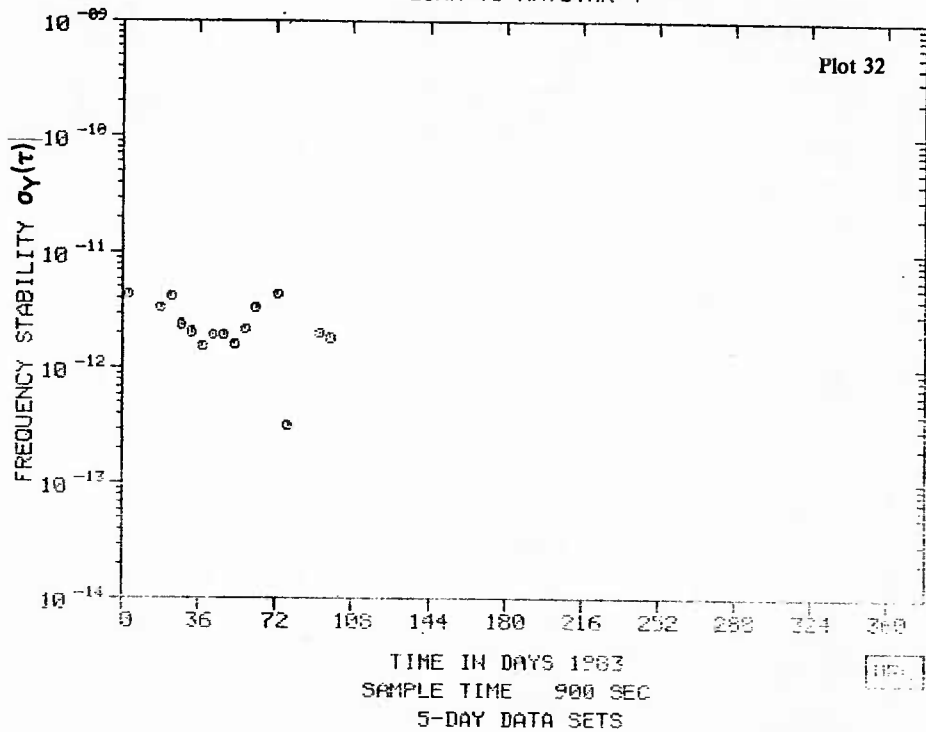
GPS
CLOCK ANALYSIS
GUAM VS NAVSTAR-4



GPS
CLOCK ANALYSIS
GUAM VS NAVSTAR-4

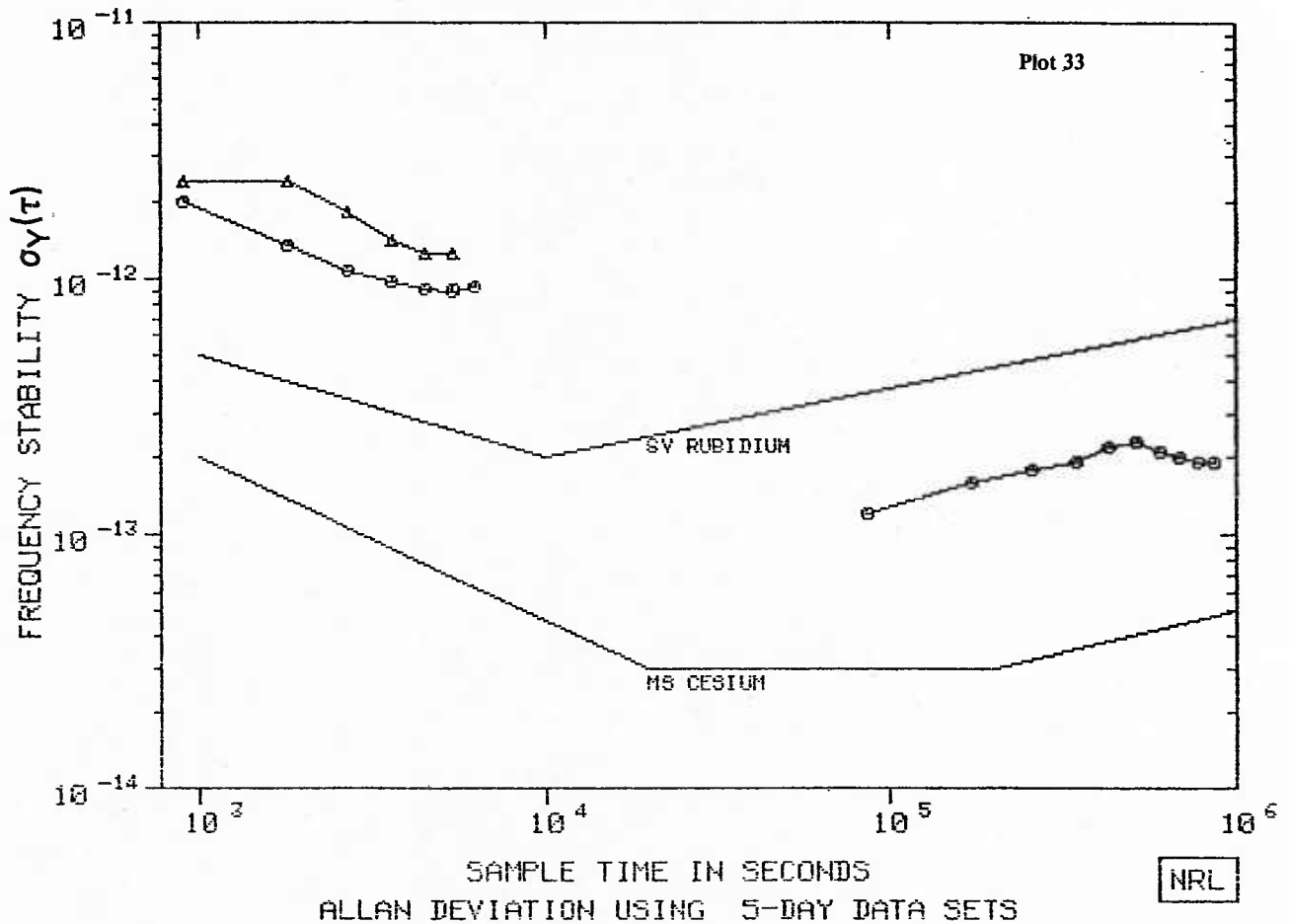


GPS
CLOCK ANALYSIS
GUAM VS NAVSTAR-4

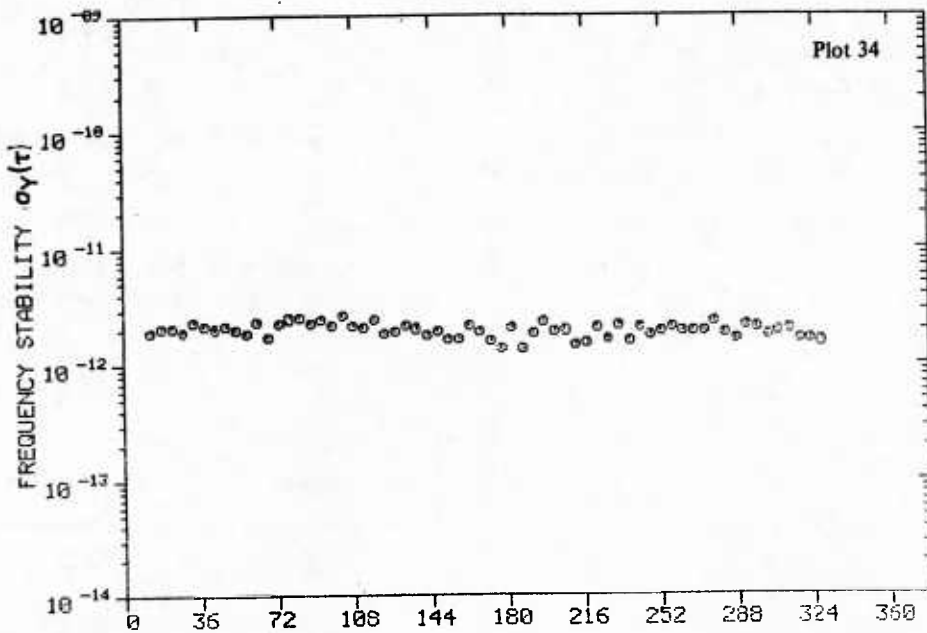


| | τ (HRS) | .25 | .50 | .75 | 1.00 | 1.25 | 1.50 | 1.75 | 2.00 | | |
|-----------|-----------------|------|------|------|------|------|------|------|------|------|------|
| ○ H82-405 | σ (PP13) | 20.1 | 13.6 | 10.8 | 9.8 | 9.2 | 9.0 | 9.3 | 9.3 | | |
| | AVG PTS | 59 | 52 | 39 | 31 | 24 | 19 | 14 | 9 | | |
| △ H93-405 | σ (PP13) | 23.9 | 24.1 | 18.1 | 14.2 | 12.7 | 12.6 | 11.2 | 10.4 | | |
| | AVG PTS | 39 | 38 | 29 | 21 | 16 | 12 | 9 | 5 | | |
| | τ (DAYS) | 1 | 2 | 3 | 4 | 5 | 6 | 7 | 8 | 9 | 10 |
| ○ HAW-482 | σ (PP14) | 12.0 | 16.0 | 18.0 | 19.0 | 22.0 | 23.0 | 21.0 | 20.0 | 19.0 | 19.0 |
| | TOT PTS | 292 | 271 | 266 | 270 | 263 | 260 | 308 | 260 | 260 | 262 |

GPS CLOCK ANALYSIS HAWAII VS NAVSTAR-4



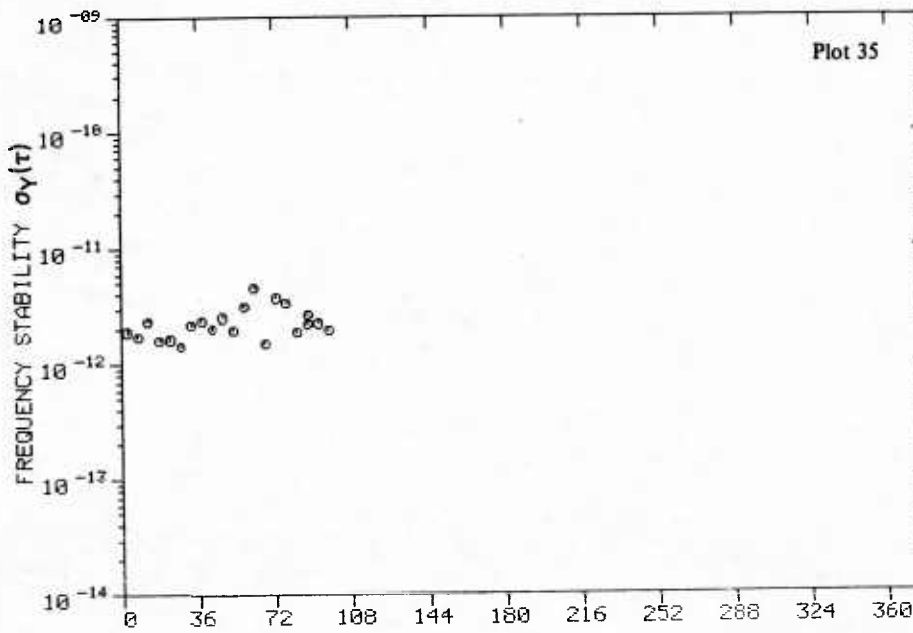
GPS
CLOCK ANALYSIS
HAWAII VS NAVSTAR-4



SAMPLE TIME 900 SEC
5-DAY DATA SETS

NRL

GPS
CLOCK ANALYSIS
HAWAII VS NAVSTAR-4

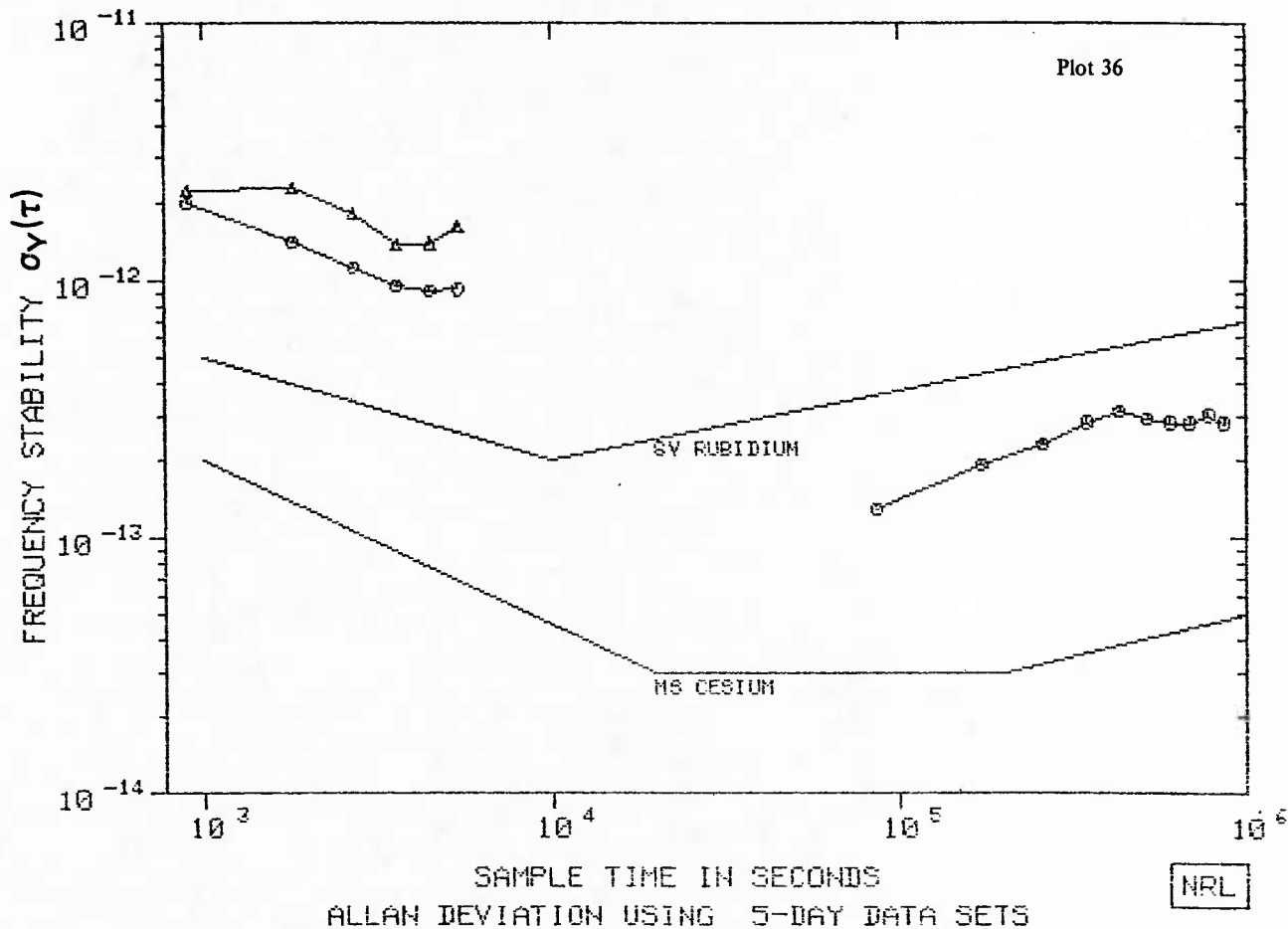


SAMPLE TIME 900 SEC
5-DAY DATA SETS

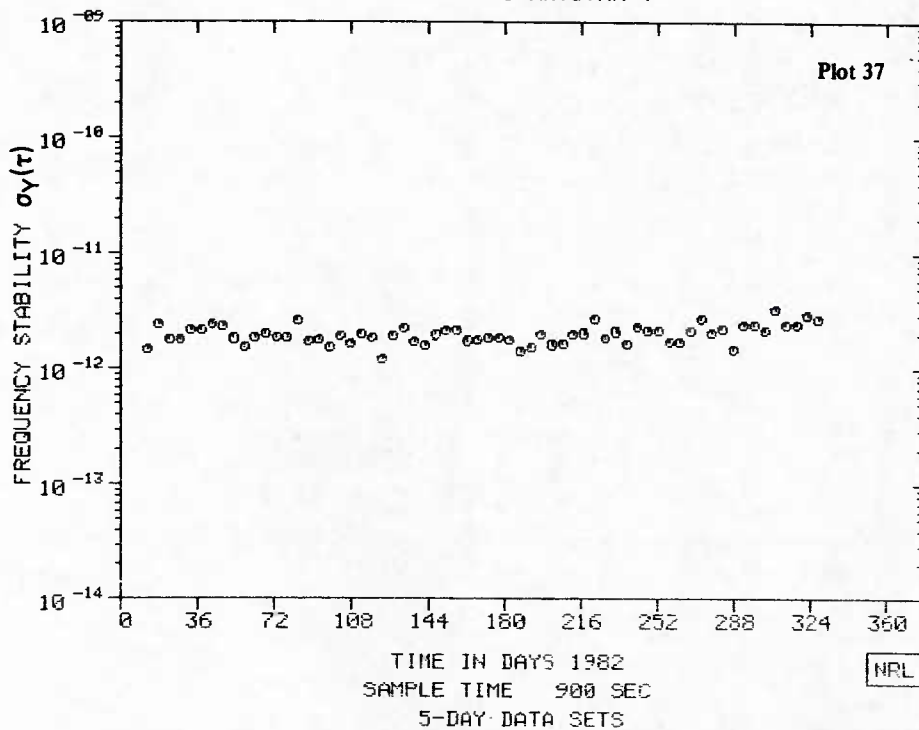
NRL

| | τ (HRS) | .25 | .50 | .75 | 1.00 | 1.25 | 1.50 | 1.75 | 2.00 | | |
|-----------|-----------------|------|------|------|------|------|------|------|------|------|------|
| ● A82-405 | σ (PP13) | 20.0 | 14.2 | 11.3 | 9.6 | 9.2 | 9.3 | 9.6 | 7.9 | | |
| | AVG PTS | 61 | 55 | 44 | 37 | 27 | 17 | 9 | 3 | | |
| ▲ A83-405 | σ (PP13) | 22.3 | 22.9 | 18.2 | 13.9 | 14.0 | 15.2 | 13.1 | 13.7 | | |
| | AVG PTS | 57 | 57 | 47 | 38 | 28 | 18 | 9 | 2 | | |
| | τ (DAYS) | 1 | 2 | 3 | 4 | 5 | 6 | 7 | 8 | 9 | 10 |
| ● ALK-482 | σ (PP14) | 13.0 | 19.0 | 23.0 | 28.0 | 31.0 | 29.0 | 28.0 | 28.0 | 30.0 | 28.0 |
| | TOT PTS | 272 | 260 | 248 | 239 | 220 | 200 | 227 | 190 | 195 | 180 |

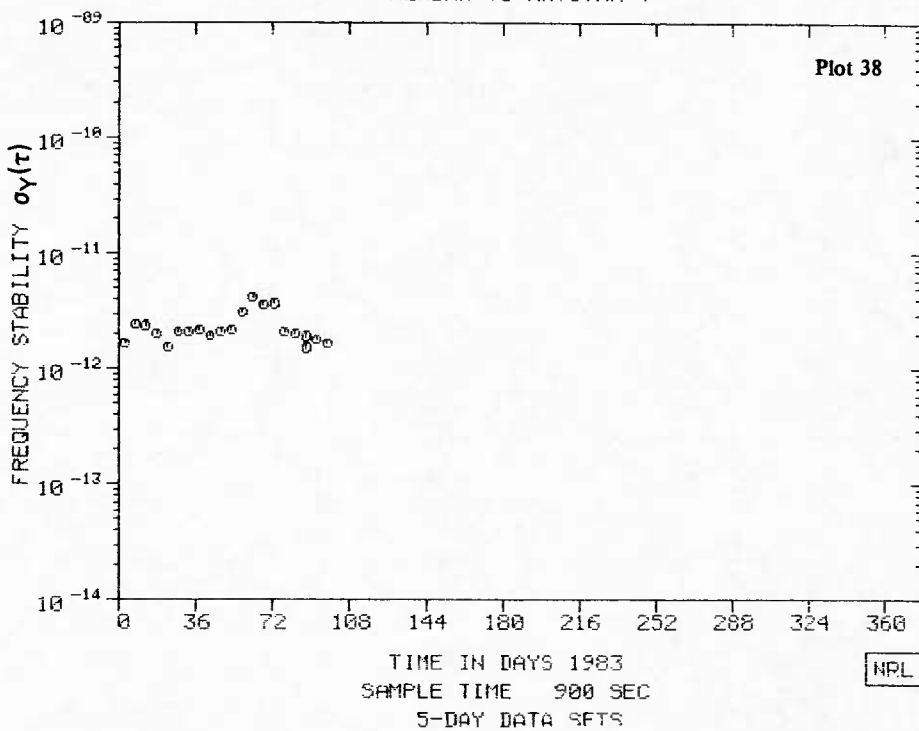
GPS
CLOCK ANALYSIS
ALASKA VS NAVSTAR-4



GPS
CLOCK ANALYSIS
ALASKA VS NAVSTAR-4

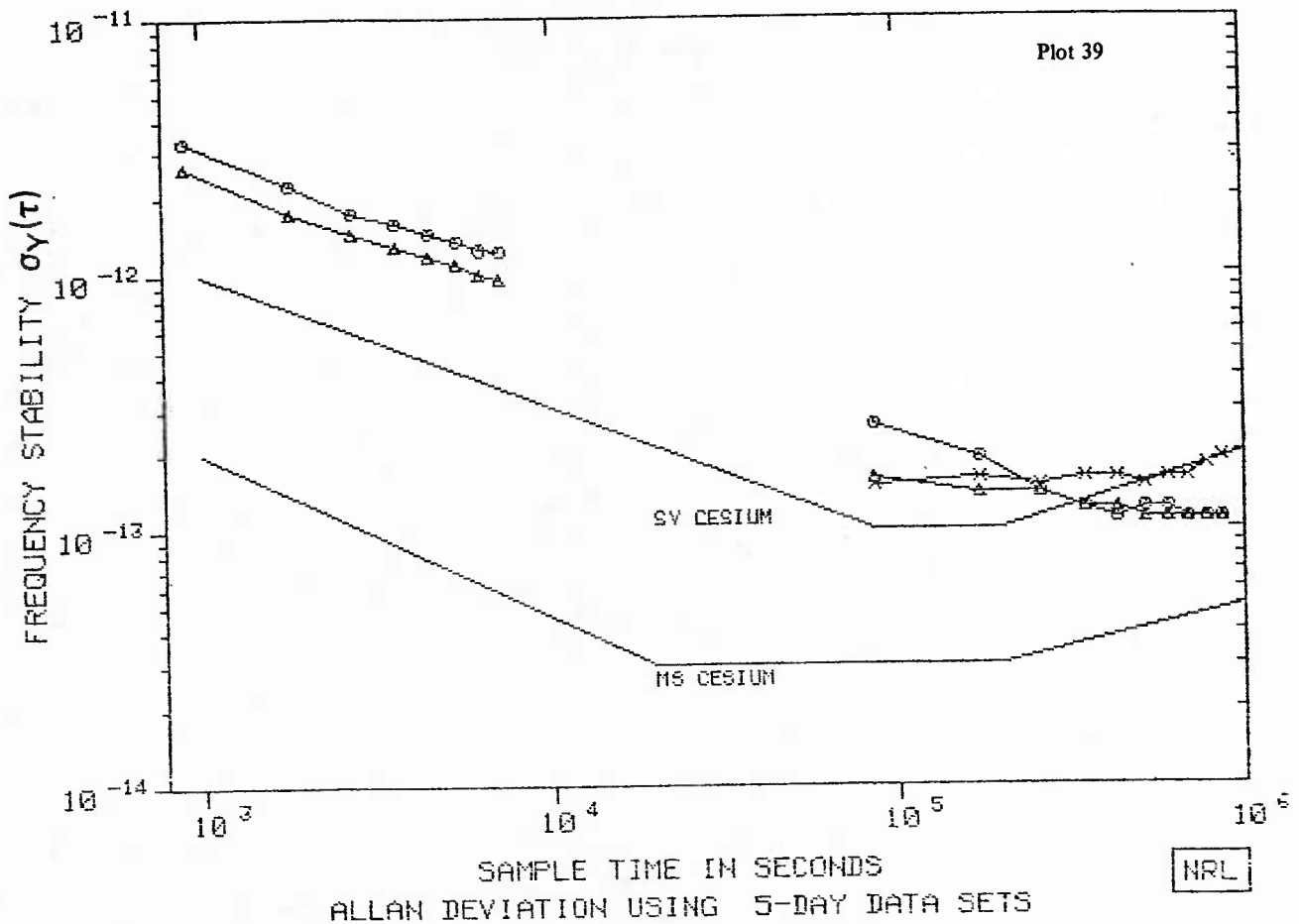


GPS
CLOCK ANALYSIS
ALASKA VS NAVSTAR-4

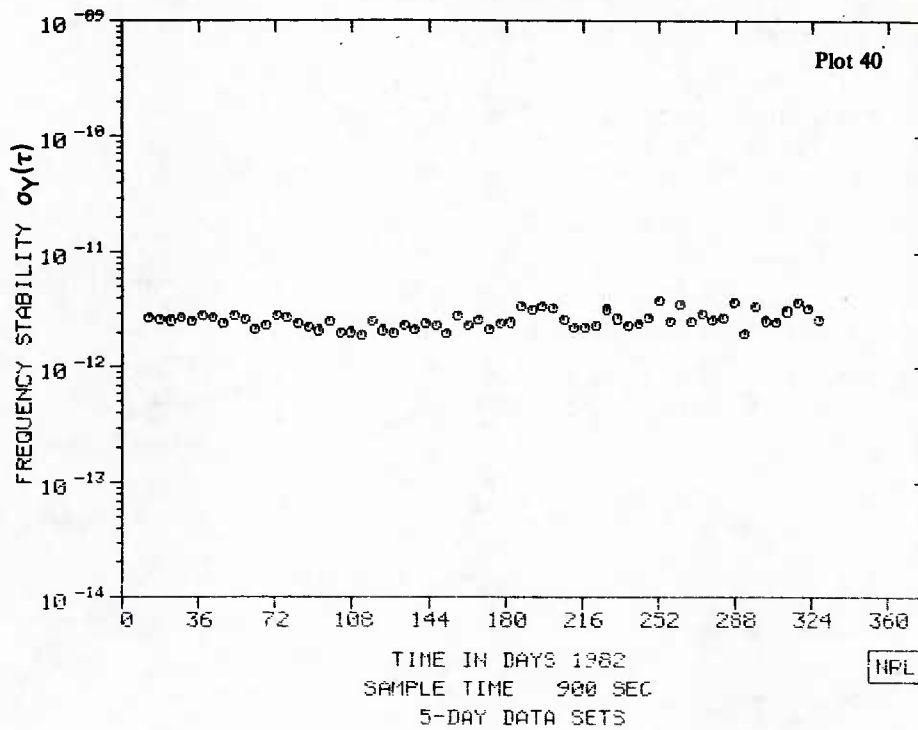


| | τ (HRS) | .25 | .50 | .75 | 1.00 | 1.25 | 1.50 | 1.75 | 2.00 | | |
|-----------|-----------------|------|------|------|------|------|------|------|------|------|------|
| o V83-595 | σ (PP13) | 33.4 | 22.6 | 17.5 | 15.8 | 14.5 | 13.4 | 12.5 | 12.3 | | |
| | AVG PTS | 68 | 67 | 60 | 55 | 49 | 42 | 34 | 27 | | |
| Δ V82-585 | σ (PP13) | 26.4 | 17.6 | 14.4 | 12.8 | 11.7 | 10.9 | 10.0 | 9.6 | | |
| | AVG PTS | 78 | 76 | 69 | 63 | 55 | 47 | 39 | 31 | | |
| | τ (DAYS) | 1 | 2 | 3 | 4 | 5 | 6 | 7 | 8 | 9 | 10 |
| o VAN-583 | σ (PP14) | 26.0 | 19.0 | 14.0 | 12.0 | 11.0 | 12.0 | 12.0 | 11.0 | 11.0 | 11.0 |
| | TOT PTS | 60 | 53 | 49 | 47 | 51 | 49 | 42 | 41 | 36 | 36 |
| Δ VAN-582 | σ (PP14) | 16.0 | 14.0 | 14.0 | 12.0 | 12.0 | 11.0 | 11.0 | 11.0 | 11.0 | 11.0 |
| | TOT PTS | 197 | 200 | 194 | 196 | 193 | 187 | 200 | 179 | 180 | 178 |
| x VAN-581 | σ (PP14) | 15.0 | 16.0 | 15.0 | 16.0 | 16.0 | 15.0 | 16.0 | 16.0 | 18.0 | 19.0 |
| | TOT PTS | 147 | 134 | 132 | 129 | 134 | 135 | 153 | 127 | 115 | 122 |

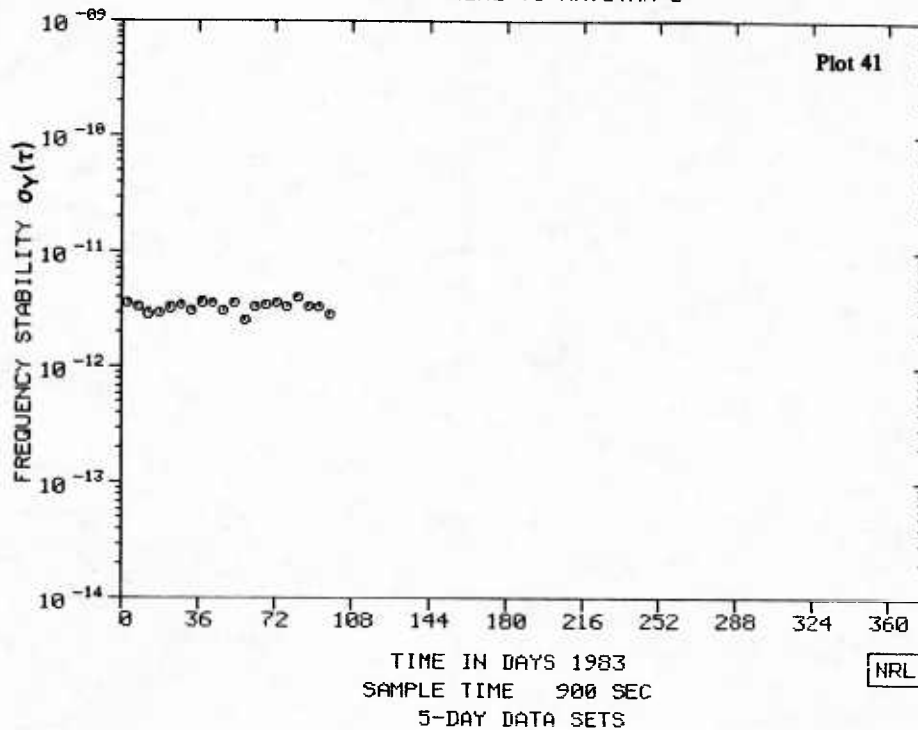
GPS
CLOCK ANALYSIS
VANDENBERG VS NAVSTAR-5



GPS
CLOCK ANALYSIS
VANDENBERG VS NAVSTAR-5



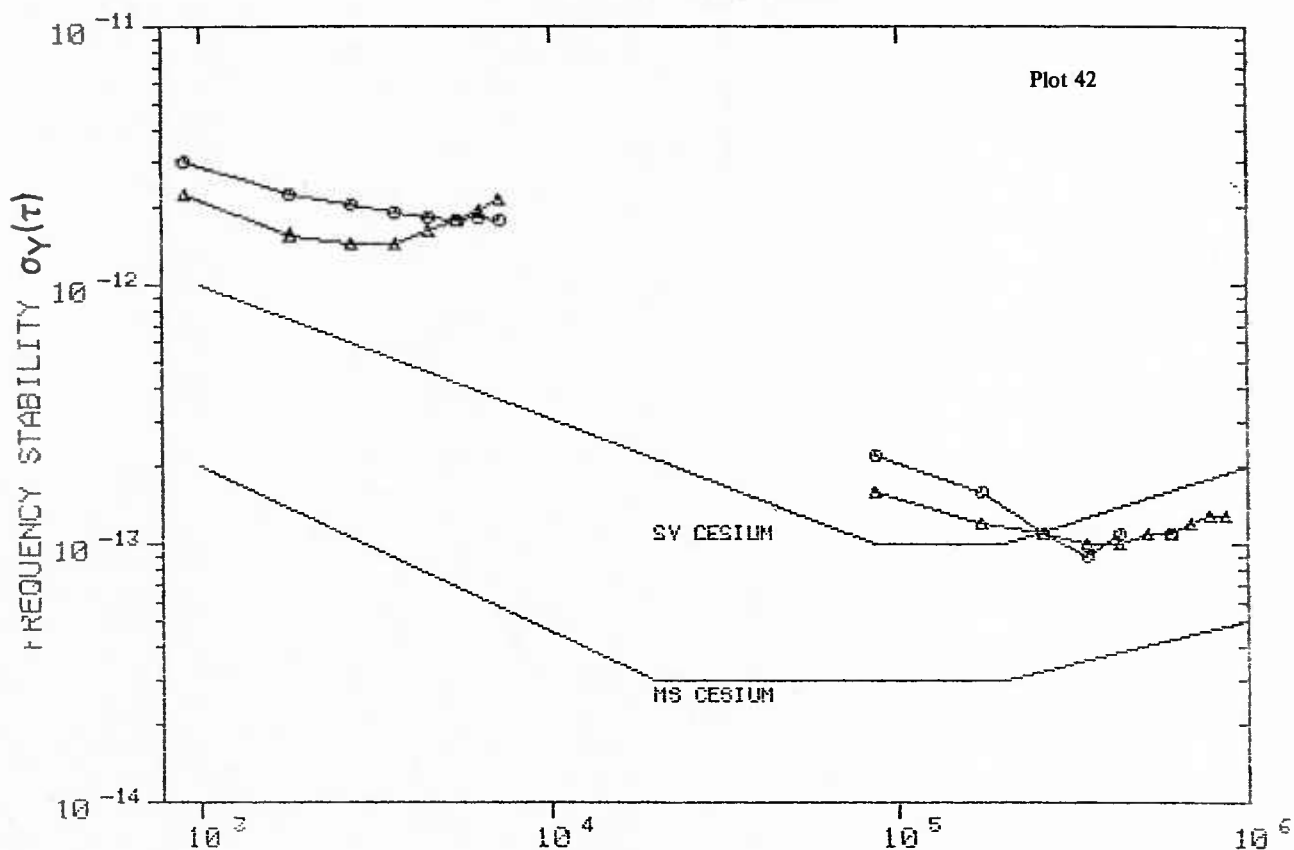
GPS
CLOCK ANALYSIS
VANDENBERG VS NAVSTAR-5



| | τ (HRS) | 25 | .50 | .75 | 1.00 | 1.25 | 1.50 | 1.75 | 2.00 | | |
|-----------|-----------------|------|------|------|------|------|------|------|------|------|------|
| ○ G93-505 | σ (PP13) | 30.1 | 22.4 | 20.3 | 19.2 | 18.1 | 17.9 | 18.1 | 17.8 | | |
| | AVG PTS | 47 | 44 | 39 | 33 | 28 | 23 | 19 | 13 | | |
| △ G82-505 | σ (PP13) | 22.3 | 15.7 | 14.4 | 14.6 | 16.4 | 17.9 | 19.5 | 21.4 | | |
| | AVG PTS | 47 | 44 | 39 | 35 | 29 | 23 | 18 | 13 | | |
| | τ (DAYS) | 1 | 2 | 3 | 4 | 5 | 6 | 7 | 8 | 9 | 10 |
| ○ GUA-583 | σ (PP14) | 22.0 | 16.0 | 11.0 | 9.0 | 11.0 | 9.0 | 11.0 | 12.0 | 12.0 | 12.0 |
| | TOT PTS | 24 | 23 | 23 | 20 | 14 | 9 | 12 | 7 | 5 | 4 |
| △ GUA-582 | σ (PP14) | 16.0 | 12.0 | 11.0 | 10.0 | 10.0 | 11.0 | 11.0 | 12.0 | 13.0 | 13.0 |
| | TOT PTS | 99 | 86 | 80 | 73 | 61 | 61 | 67 | 49 | 34 | 30 |

GPS CLOCK ANALYSIS

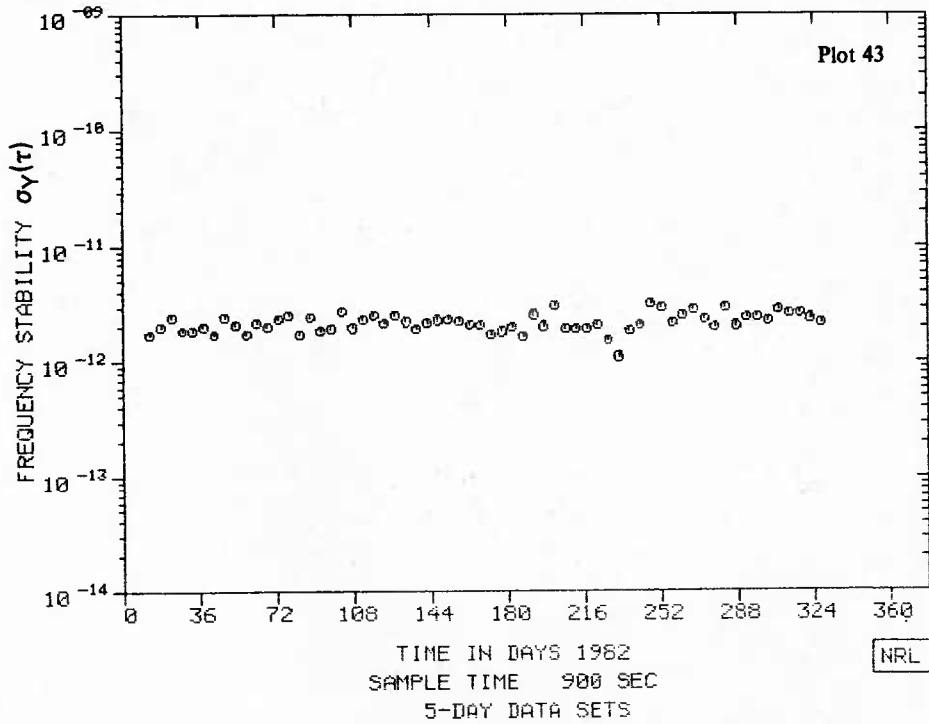
GUAM VS NAVSTAR-5



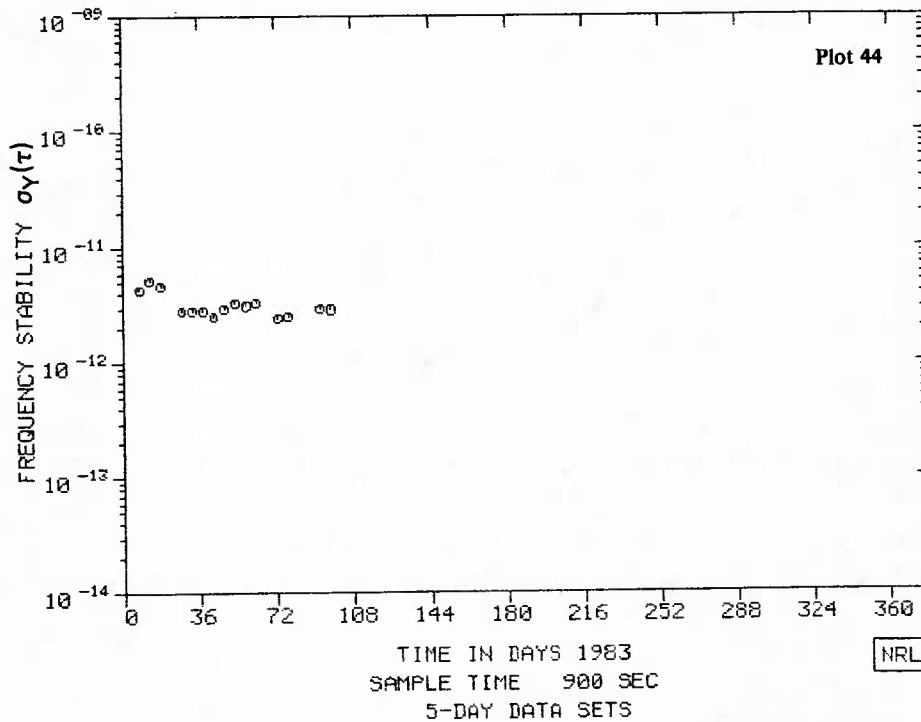
SAMPLE TIME IN SECONDS
ALLAN DEVIATION USING 5-DAY DATA SETS



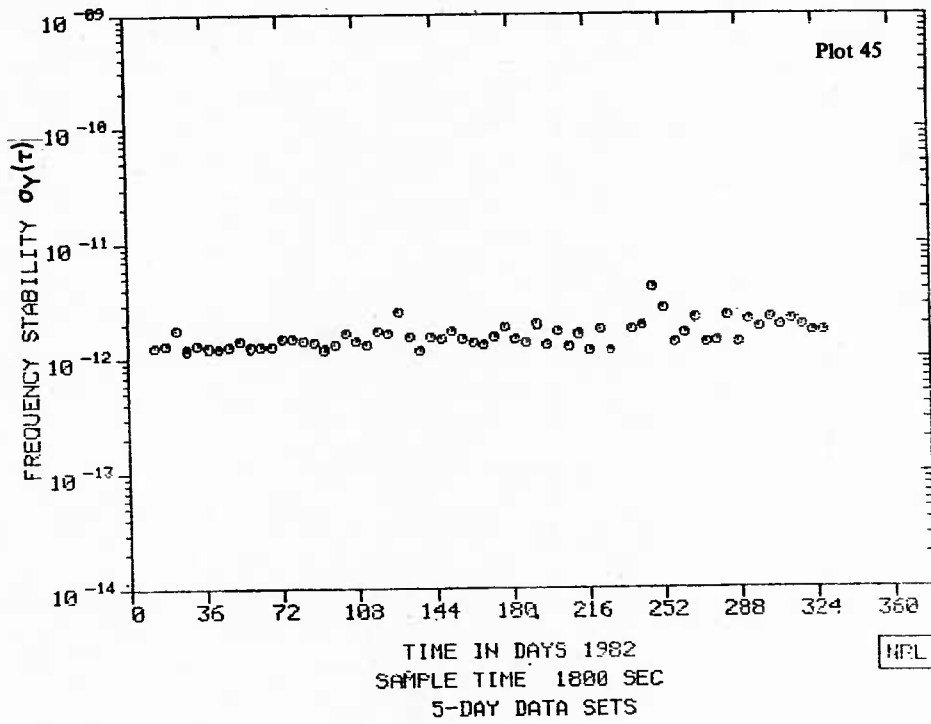
GPS
CLOCK ANALYSIS
GUAM VS NAVSTAR-5



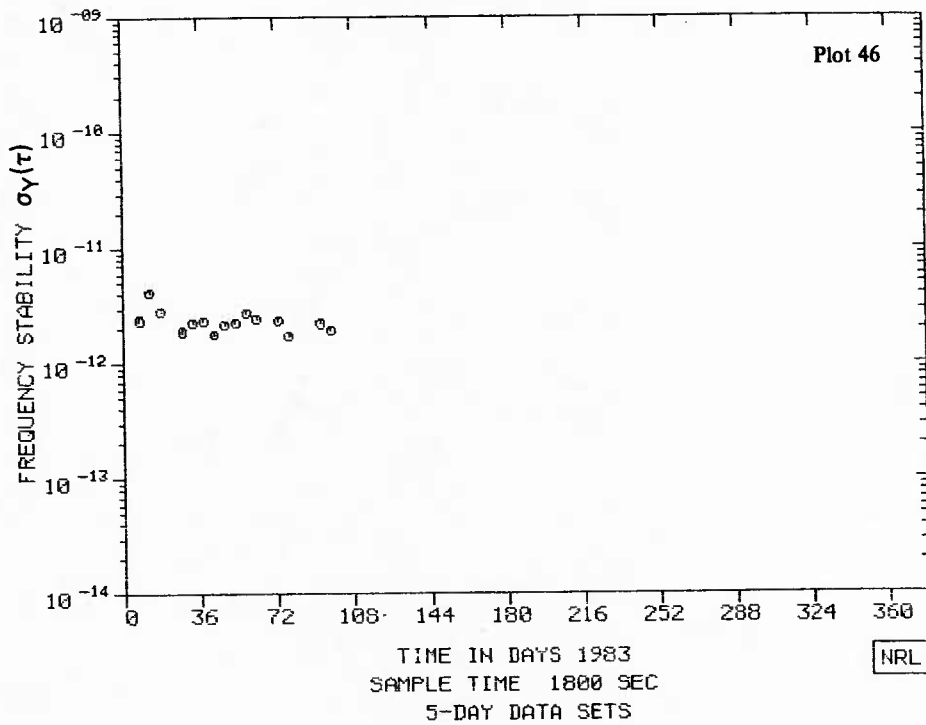
GPS
CLOCK ANALYSIS
GUAM VS NAVSTAR-5



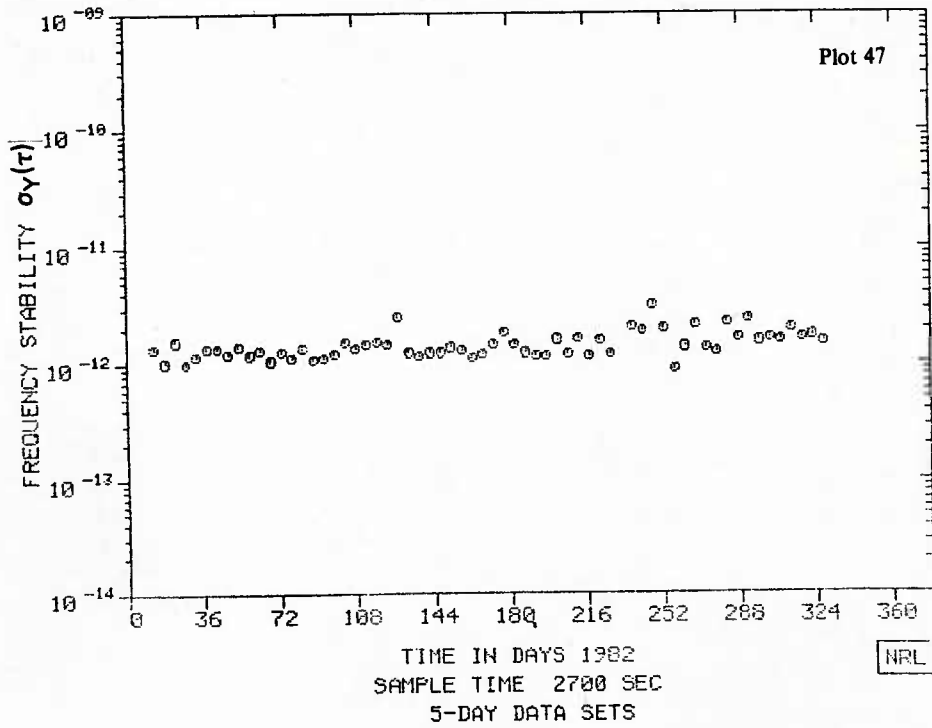
GPS
CLOCK ANALYSIS
GUAM VS NAVSTAR-5



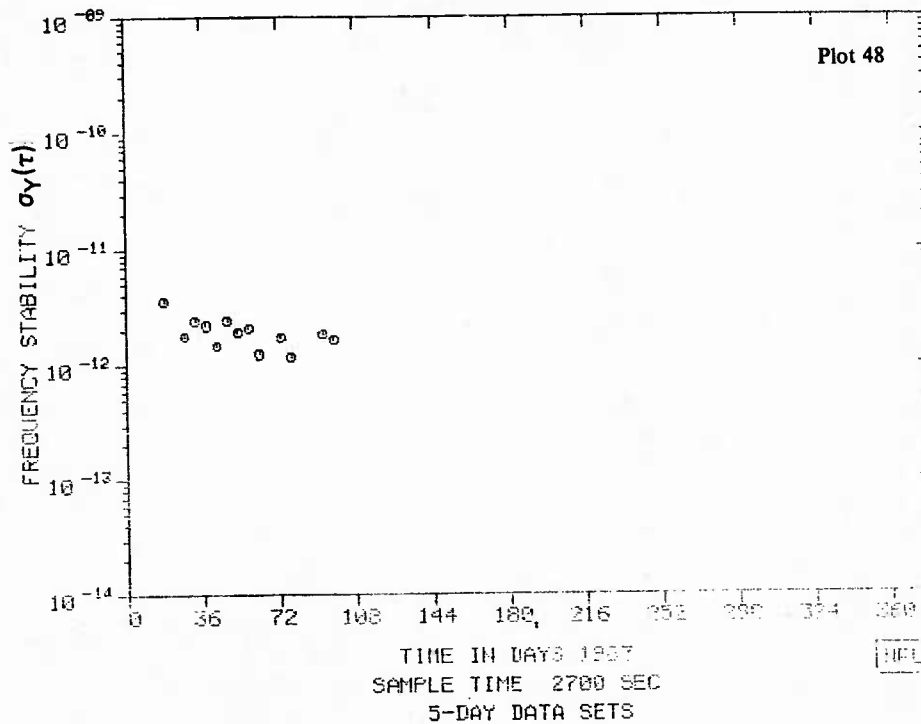
GPS
CLOCK ANALYSIS
GUAM VS NAVSTAR-5



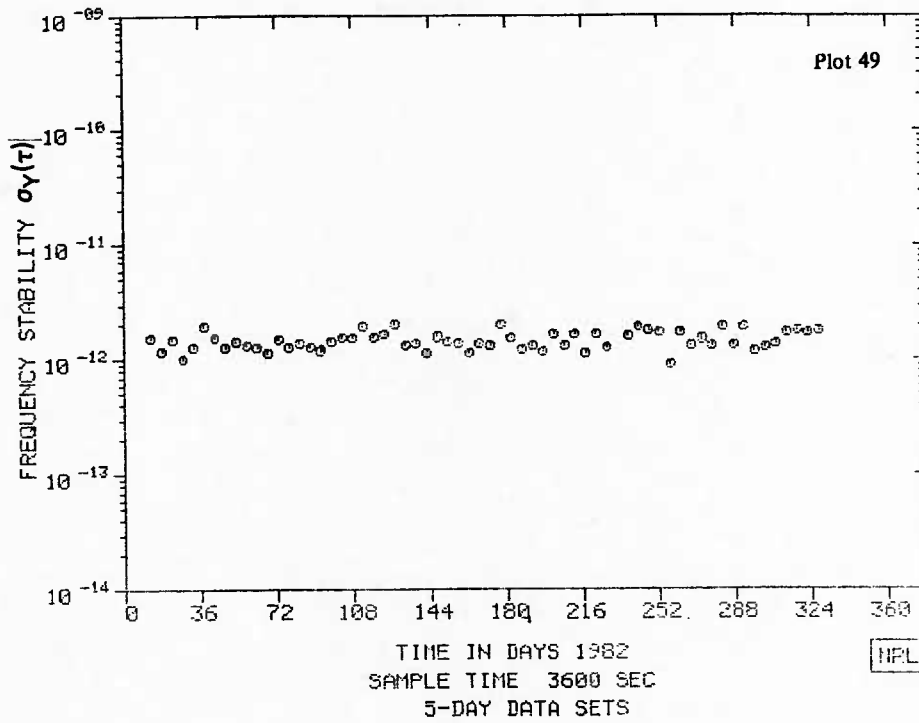
GPS
CLOCK ANALYSIS
GUAM VS NAVSTAR-5



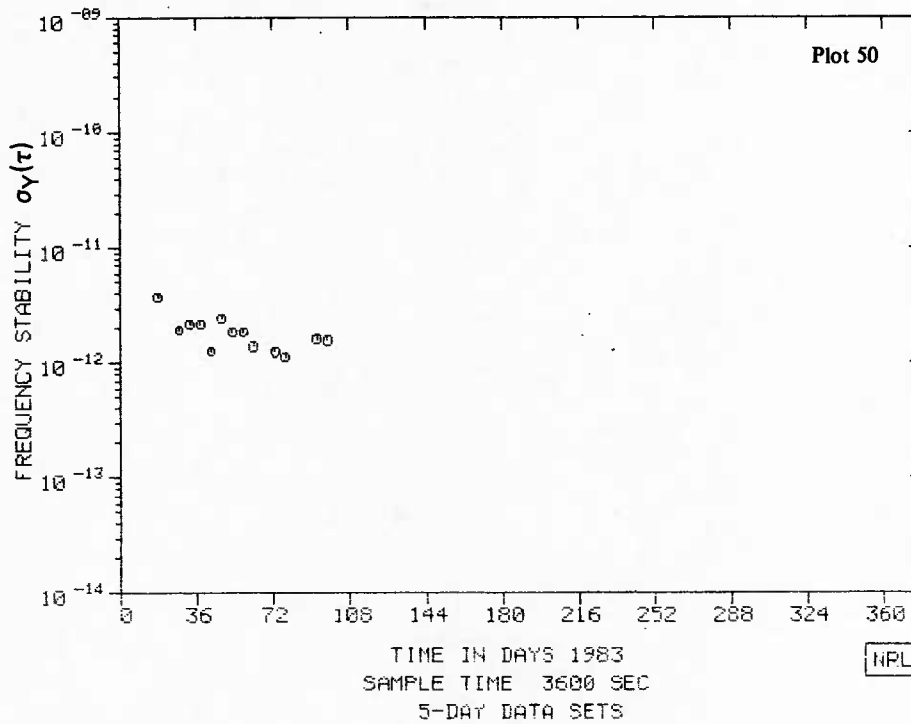
GPS
CLOCK ANALYSIS
GUAM VS NAVSTAR-5



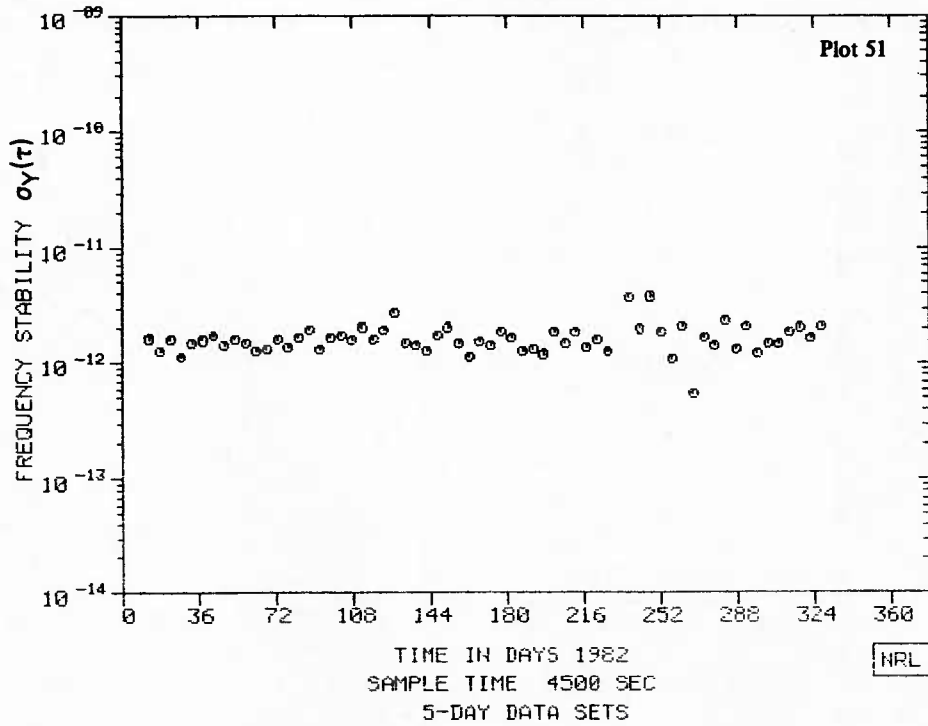
GPS
CLOCK ANALYSIS
GUAM VS NAVSTAR-5



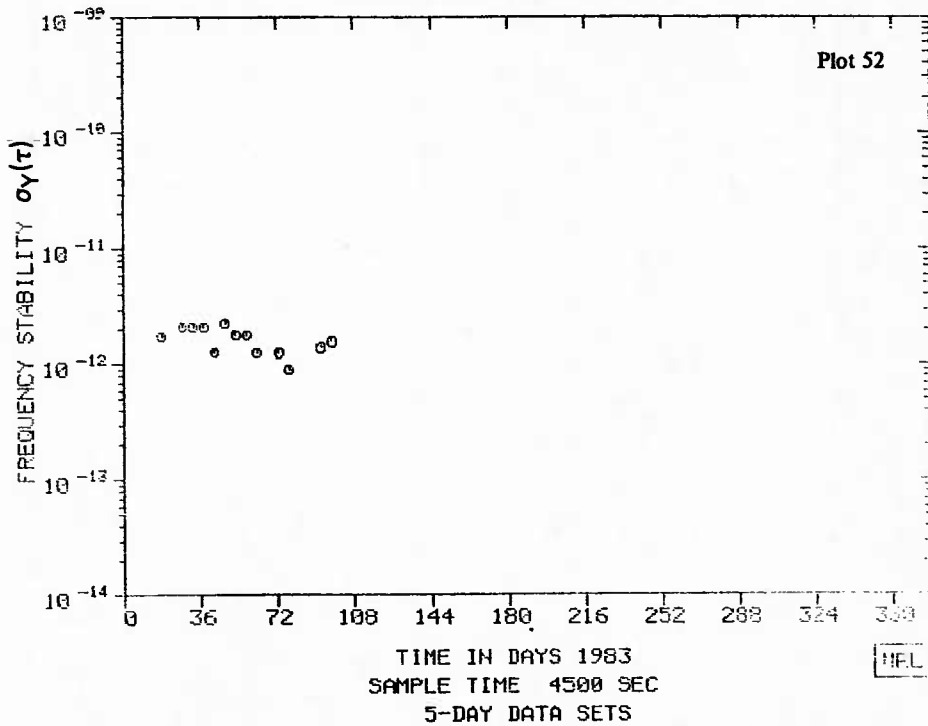
GPS
CLOCK ANALYSIS
GUAM VS NAVSTAR-5



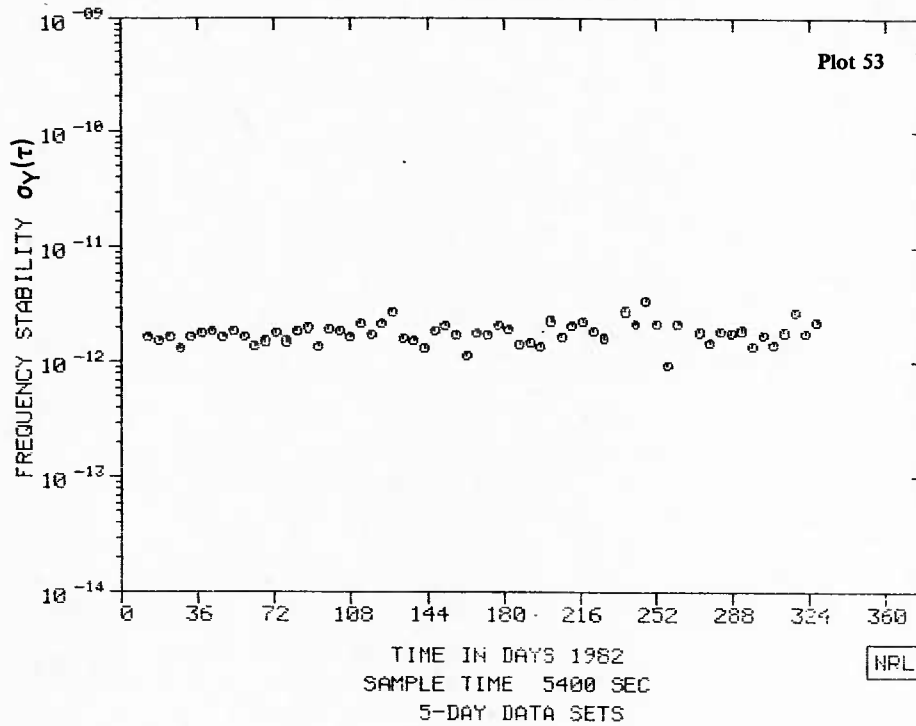
GPS
CLOCK ANALYSIS
GUAM VS NAVSTAR-5



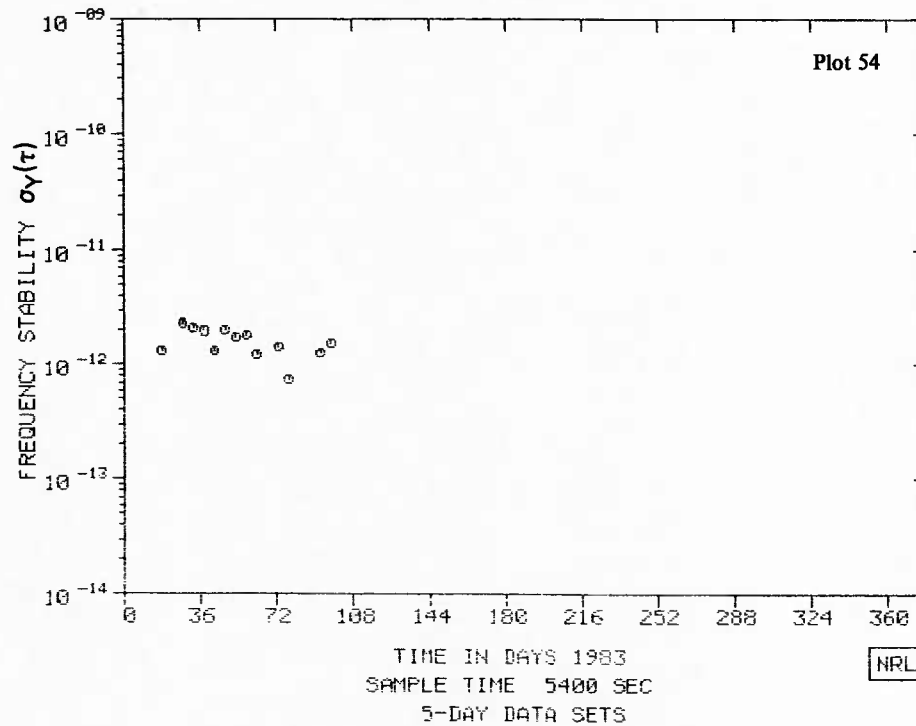
GPS
CLOCK ANALYSIS
GUAM VS NAVSTAR-5



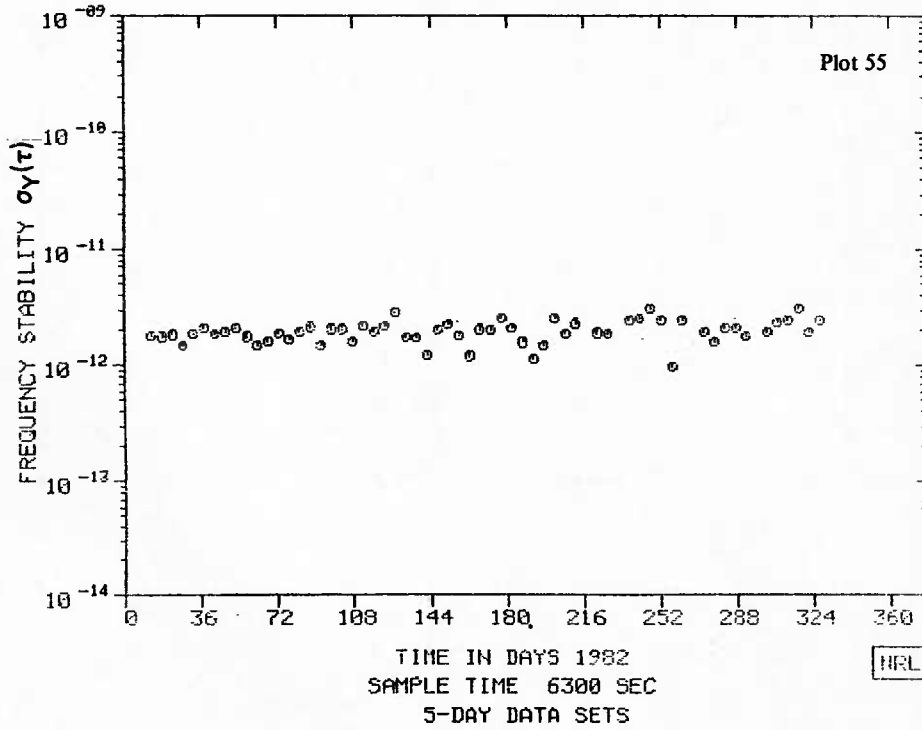
GPS
CLOCK ANALYSIS
GUAM VS NAVSTAR-5



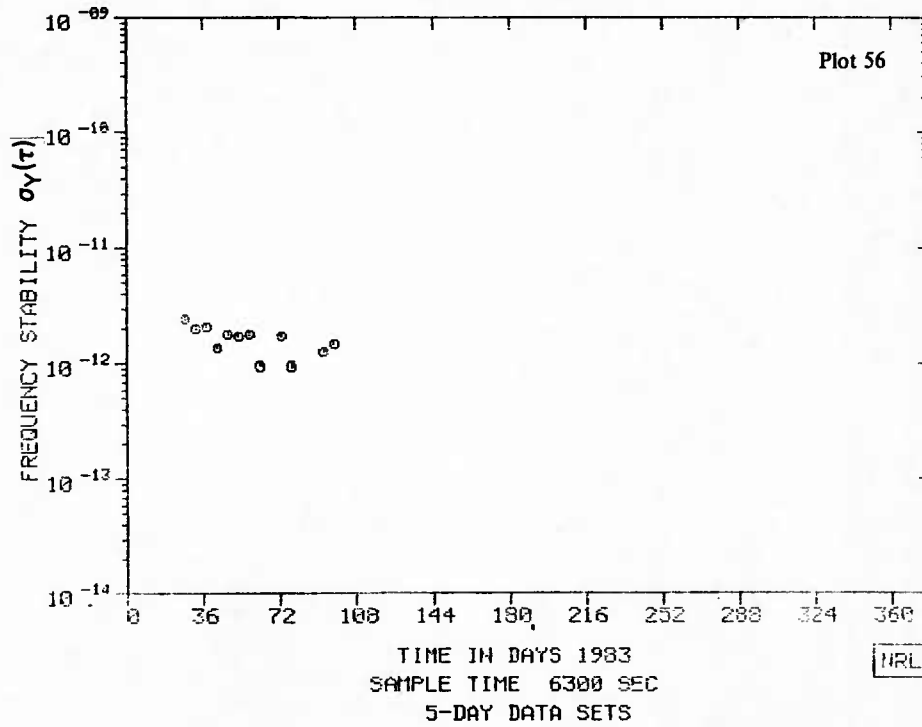
GPS
CLOCK ANALYSIS
GUAM VS NAVSTAR-5



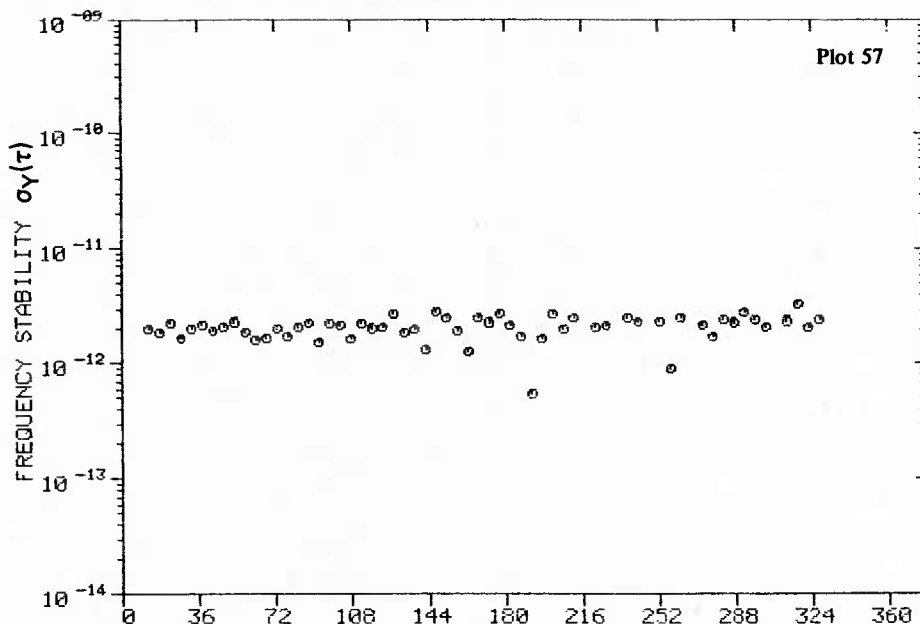
GPS
CLOCK ANALYSIS
GUAM VS NAVSTAR-5



GPS
CLOCK ANALYSIS
GUAM VS NAVSTAR-5



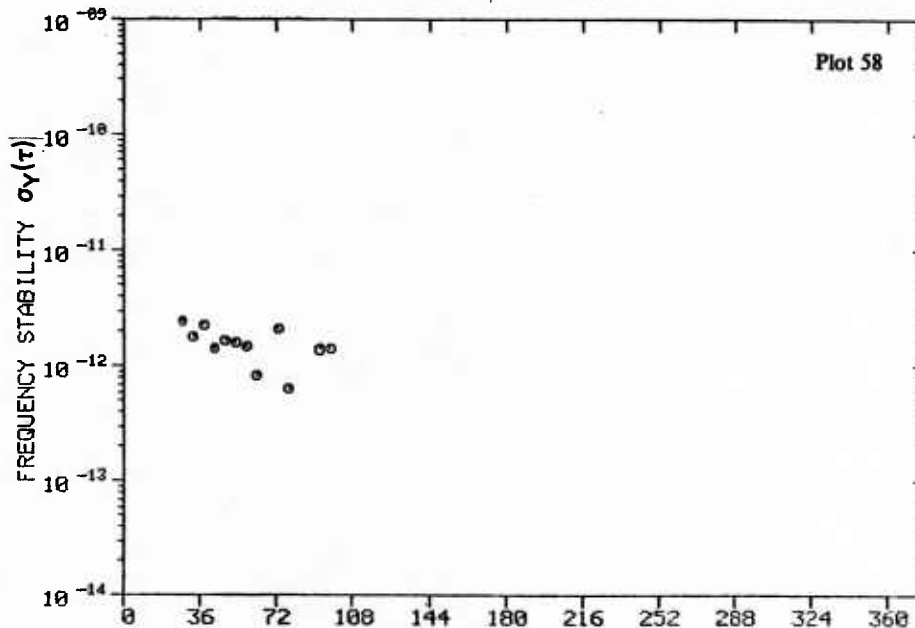
GPS
CLOCK ANALYSIS
GUAM VS NAVSTAR-5



TIME IN DAYS 1982
SAMPLE TIME 7200 SEC
5-DAY DATA SETS

NRL

GPS
CLOCK ANALYSIS
GUAM VS NAVSTAR-5

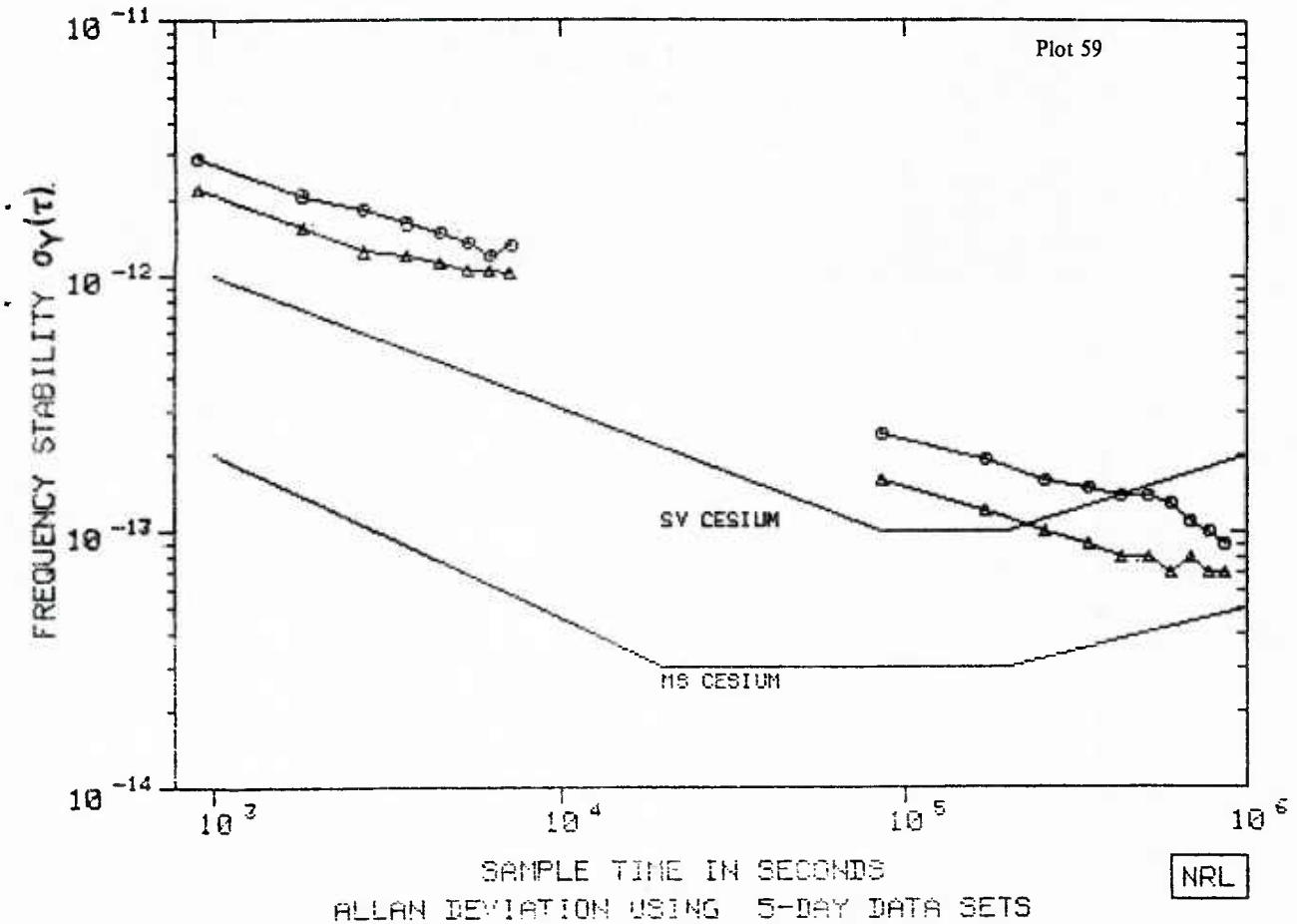


TIME IN DAYS 1983
SAMPLE TIME 7200 SEC
5-DAY DATA SETS

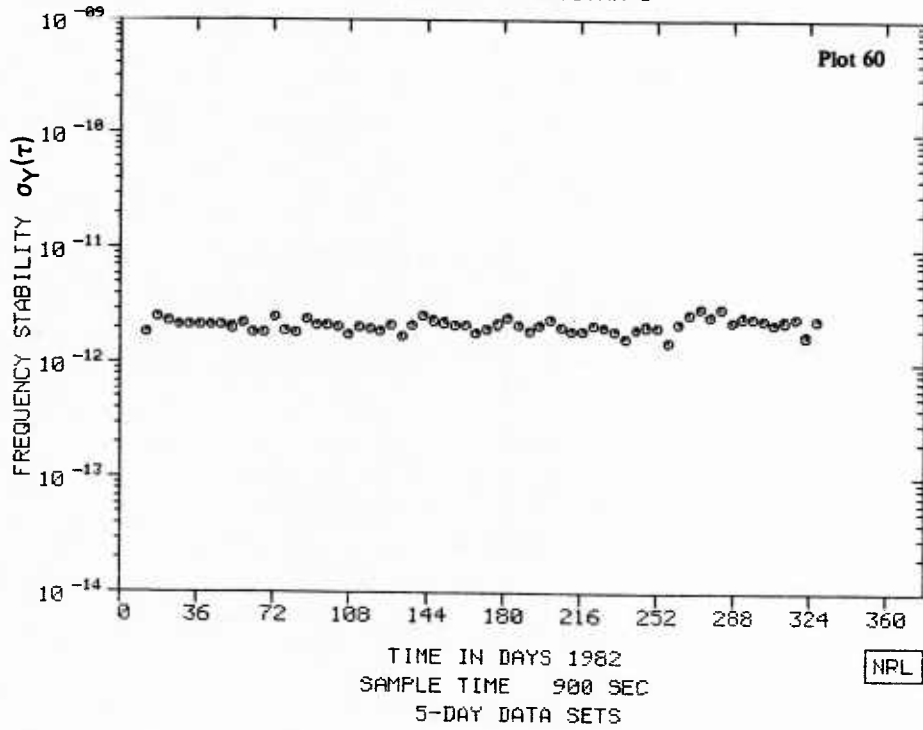
NRL

| | τ (HRS) | .25 | .50 | .75 | 1.00 | 1.25 | 1.50 | 1.75 | 2.00 | | |
|-----------|-----------------|------|------|------|------|------|------|------|------|------|-----|
| ○ H93-595 | σ (PP13) | 28.9 | 20.7 | 18.1 | 15.1 | 14.8 | 13.4 | 12.1 | 13.3 | | |
| | AVG PTS | 69 | 66 | 54 | 45 | 34 | 27 | 19 | 13 | | |
| ▲ H82-505 | σ (PP13) | 21.9 | 15.5 | 12.5 | 12.1 | 11.2 | 10.6 | 10.5 | 10.3 | | |
| | AVG PTS | 67 | 65 | 54 | 45 | 35 | 27 | 21 | 13 | | |
| | τ (DAYS) | 1 | 2 | 3 | 4 | 5 | 6 | 7 | 9 | 9 | 10 |
| ○ HAW-523 | σ (PP14) | 24.0 | 19.0 | 15.0 | 15.0 | 14.0 | 14.0 | 13.0 | 11.0 | 10.0 | 9.0 |
| | TOT PTS | 100 | 88 | 72 | 67 | 58 | 54 | 53 | 44 | 40 | 40 |
| ▲ HAW-522 | σ (PP14) | 16.0 | 12.0 | 10.0 | 9.0 | 8.0 | 8.0 | 7.0 | 8.0 | 7.0 | 7.0 |
| | TOT PTS | 289 | 271 | 263 | 260 | 244 | 239 | 254 | 238 | 218 | 209 |

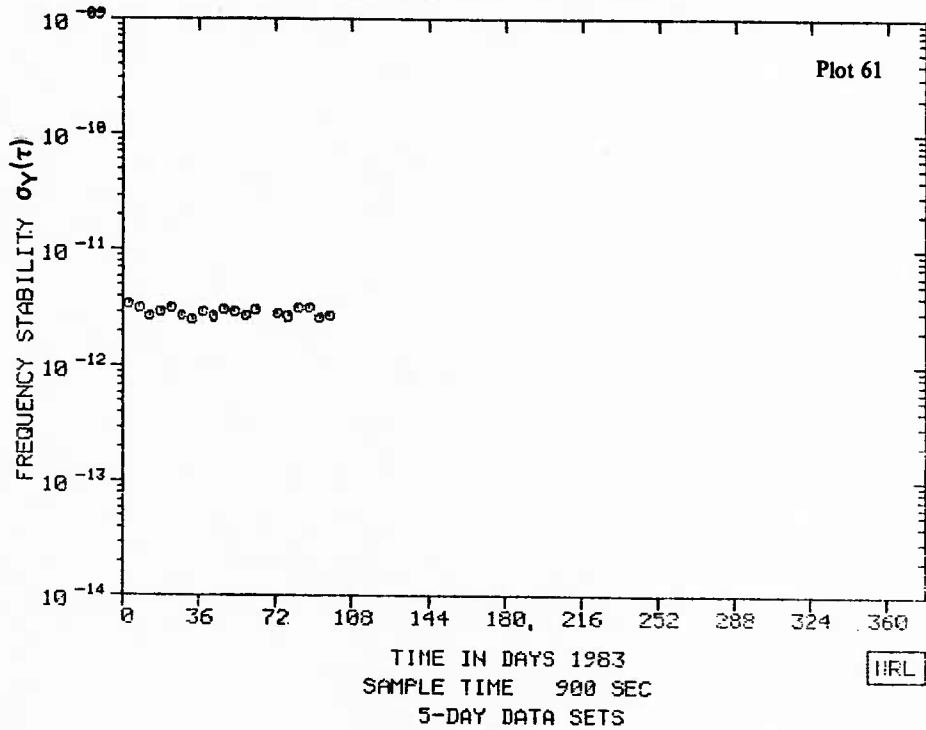
GPS
CLOCK ANALYSIS
HAWAII VS NAVSTAR-5



GPS
CLOCK ANALYSIS
HAWAII VS NAVSTAR-5



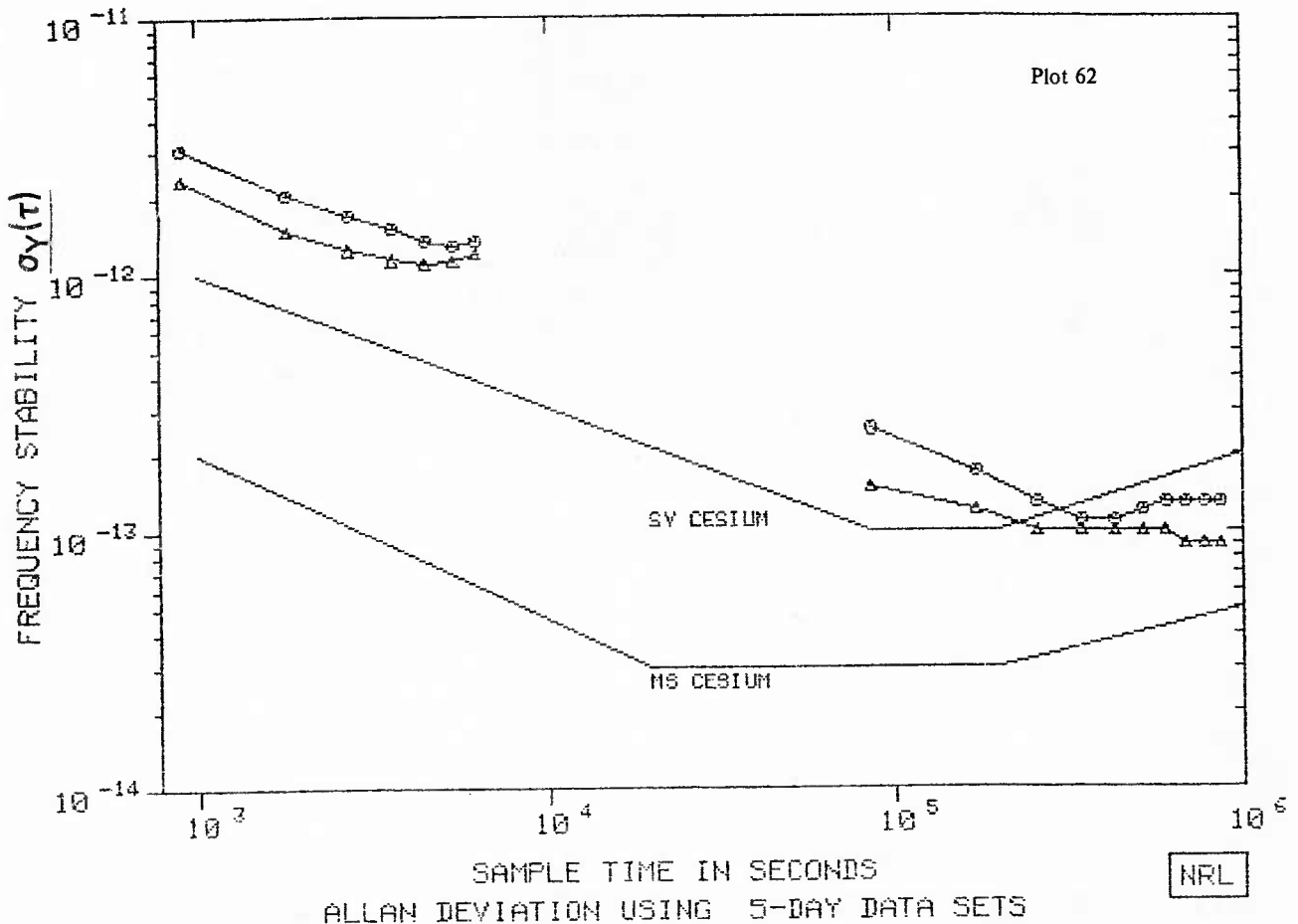
GPS
CLOCK ANALYSIS
HAWAII VS NAVSTAR-5



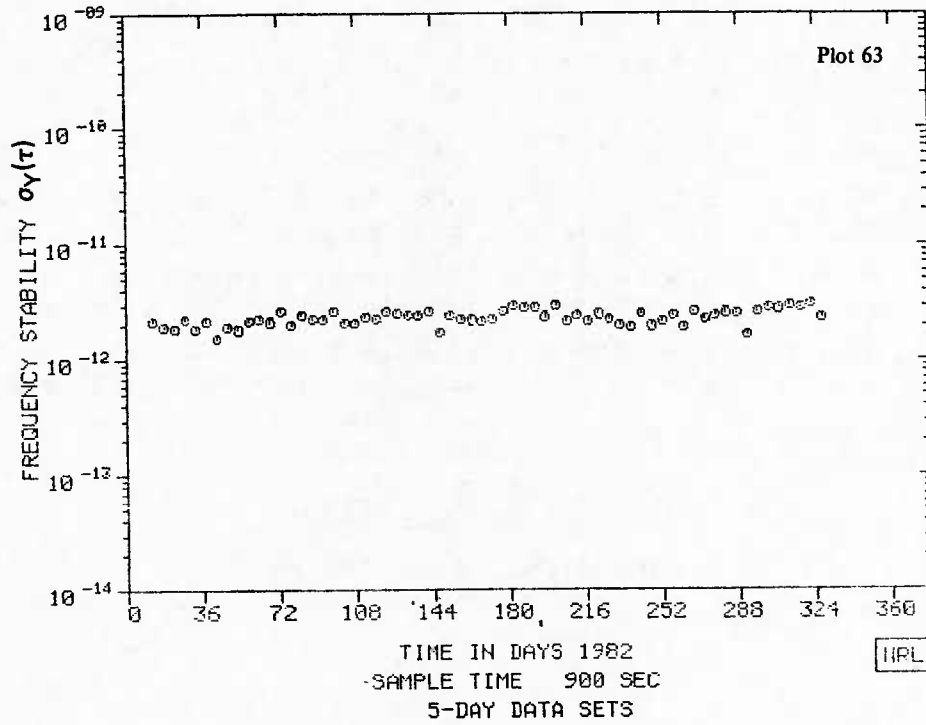
McCASKILL, BUISSON, AND STEBBINS

| | τ (HRS) | .25 | .50 | .75 | 1.00 | 1.25 | 1.50 | 1.75 | 2.00 | | |
|------------------|-----------------|------|------|------|------|------|------|------|------|------|------|
| o A83-505 | σ (PP13) | 30.7 | 20.5 | 16.9 | 15.2 | 13.4 | 13.0 | 13.5 | 13.5 | | |
| | AVG PTS | 75 | 70 | 59 | 51 | 38 | 27 | 16 | 9 | | |
| Δ A82-505 | σ (PP13) | 23.3 | 14.9 | 12.5 | 11.4 | 11.0 | 11.2 | 12.1 | 13.7 | | |
| | AVG PTS | 77 | 71 | 59 | 51 | 39 | 27 | 15 | 9 | | |
| | τ (DAYS) | 1 | 2 | 3 | 4 | 5 | 6 | 7 | 8 | 9 | 10 |
| o ALK-583 | σ (PP14) | 25.0 | 17.0 | 13.0 | 11.0 | 11.0 | 12.0 | 13.0 | 13.0 | 13.0 | 13.0 |
| | TOT PTS | 89 | 80 | 75 | 72 | 65 | 61 | 64 | 54 | 49 | 45 |
| Δ ALK-582 | σ (PP14) | 15.0 | 12.0 | 10.0 | 10.0 | 10.0 | 10.0 | 10.0 | 9.0 | 9.0 | 9.0 |
| | TOT PTS | 291 | 276 | 255 | 263 | 249 | 238 | 260 | 231 | 224 | 215 |

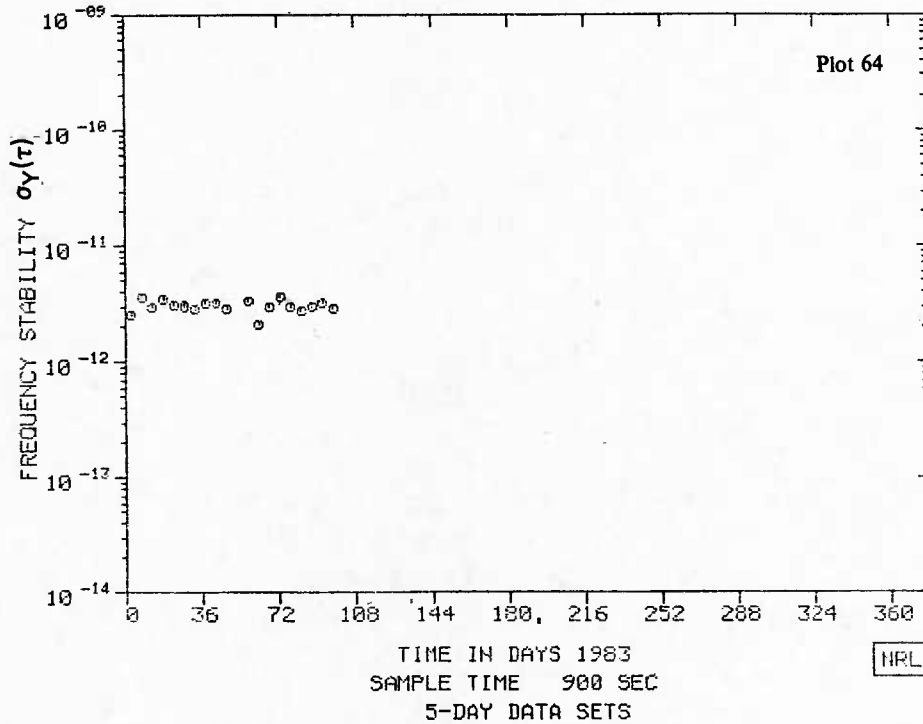
GPS
CLOCK ANALYSIS
ALASKA VS NAVSTAR-5



GPS
CLOCK ANALYSIS
ALASKA VS NAVSTAR-5



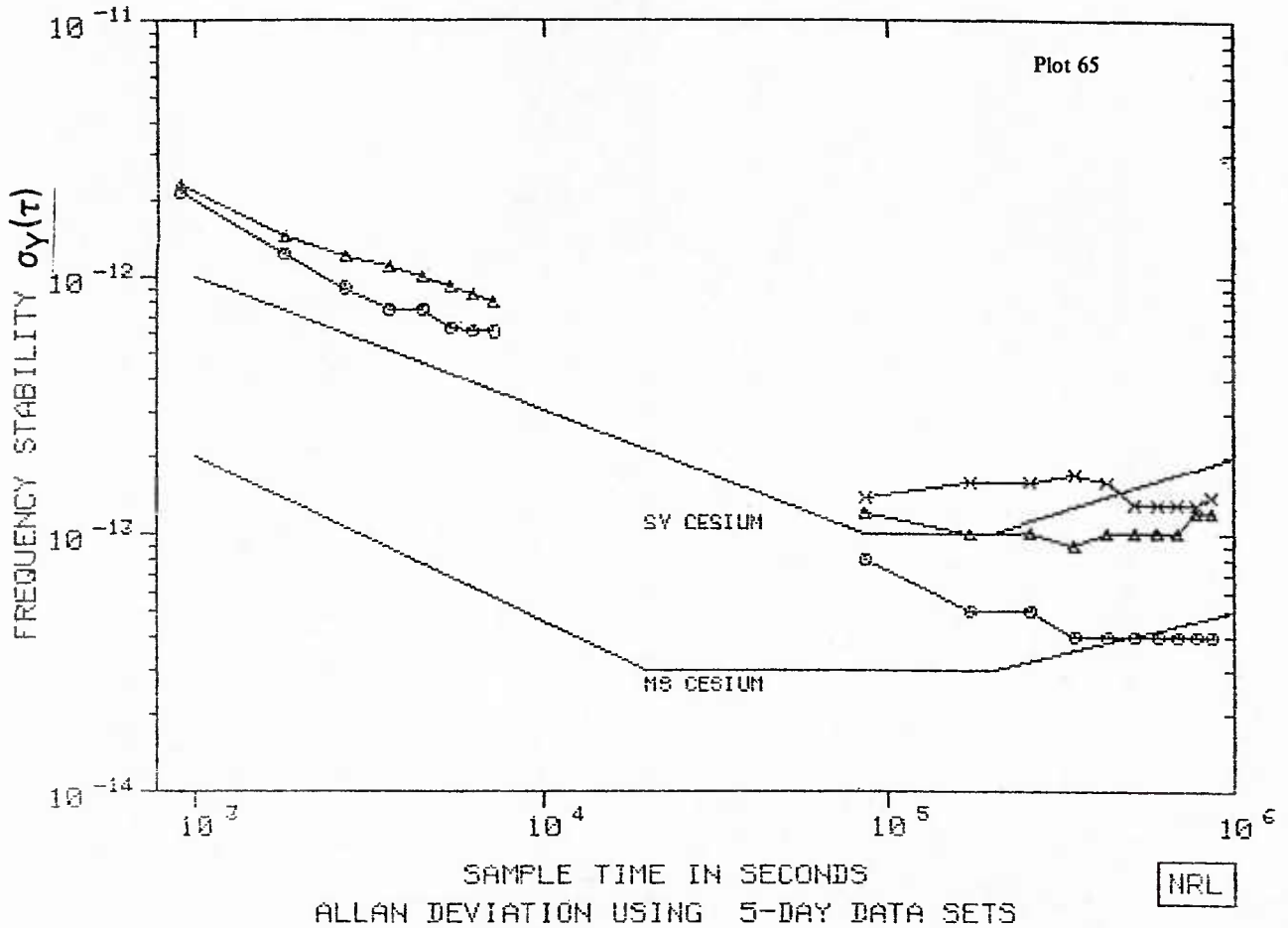
GPS
CLOCK ANALYSIS
ALASKA VS NAVSTAR-5



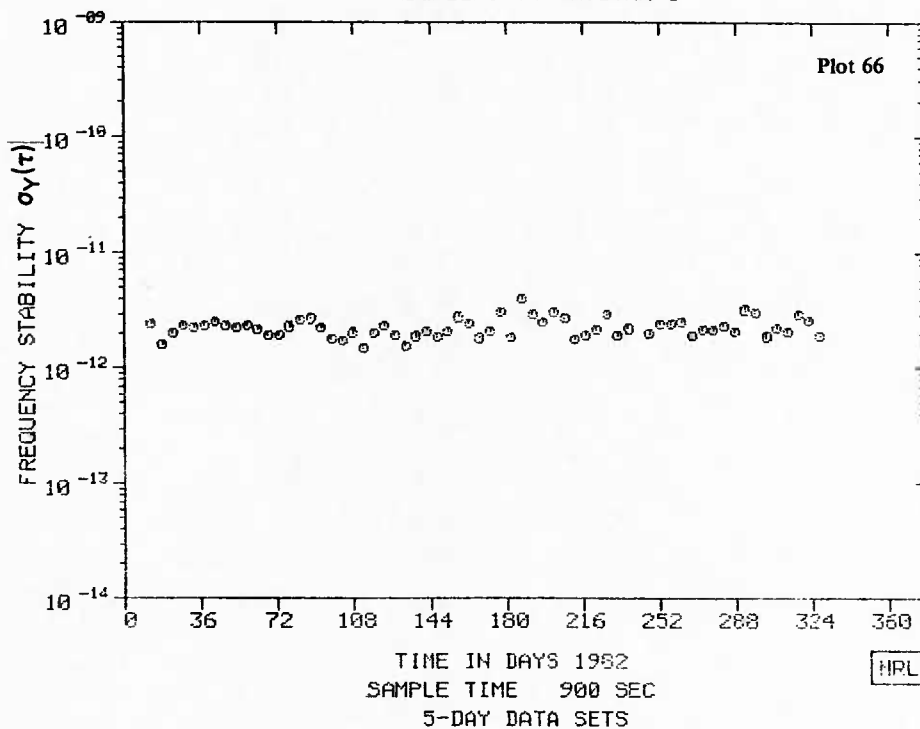
McCASKILL, BUISSON, AND STEBBINS

| | τ (HRS) | .25 | .50 | .75 | 1.00 | 1.25 | 1.50 | 1.75 | 2.00 | | |
|------------------|-----------------|------|------|------|------|------|------|------|------|------|------|
| o Y83-685 | σ (PP13) | 21.4 | 12.3 | 9.0 | 7.5 | 7.4 | 6.4 | 6.2 | 6.1 | | |
| | AVG PTS | 62 | 68 | 63 | 60 | 51 | 43 | 35 | 25 | | |
| Δ Y82-685 | σ (PP13) | 23.0 | 14.5 | 12.1 | 10.9 | 10.1 | 9.2 | 8.5 | 7.9 | | |
| | AVG PTS | 60 | 59 | 55 | 56 | 48 | 40 | 33 | 25 | | |
| | τ (DAYS) | 1 | 2 | 3 | 4 | 5 | 6 | 7 | 8 | 9 | 10 |
| o VAN-683 | σ (PP14) | 8.0 | 5.0 | 5.0 | 4.0 | 4.0 | 4.0 | 4.0 | 4.0 | 4.0 | 4.0 |
| | TOT PTS | 91 | 89 | 87 | 87 | 84 | 82 | 82 | 82 | 78 | 76 |
| Δ VAN-682 | σ (PP14) | 12.0 | 10.0 | 10.0 | 9.0 | 10.0 | 10.0 | 10.0 | 10.0 | 12.0 | 12.0 |
| | TOT PTS | 186 | 194 | 184 | 189 | 185 | 179 | 197 | 177 | 175 | 180 |
| x VAN-681 | σ (PP14) | 14.0 | 16.0 | 16.0 | 17.0 | 16.0 | 13.0 | 13.0 | 13.0 | 13.0 | 14.0 |
| | TOT PTS | 189 | 174 | 157 | 166 | 161 | 157 | 168 | 151 | 147 | 145 |

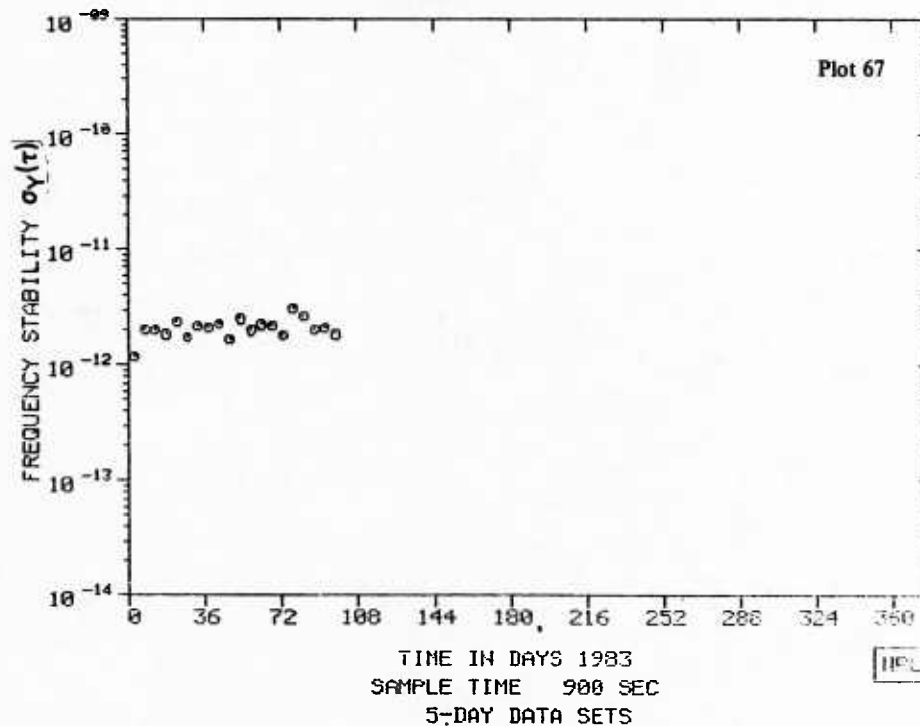
GPS
CLOCK ANALYSIS
VANDENBERG VS NAVSTAR-6



GPS
CLOCK ANALYSIS
VANDENBERG VS NAVSTAR-6



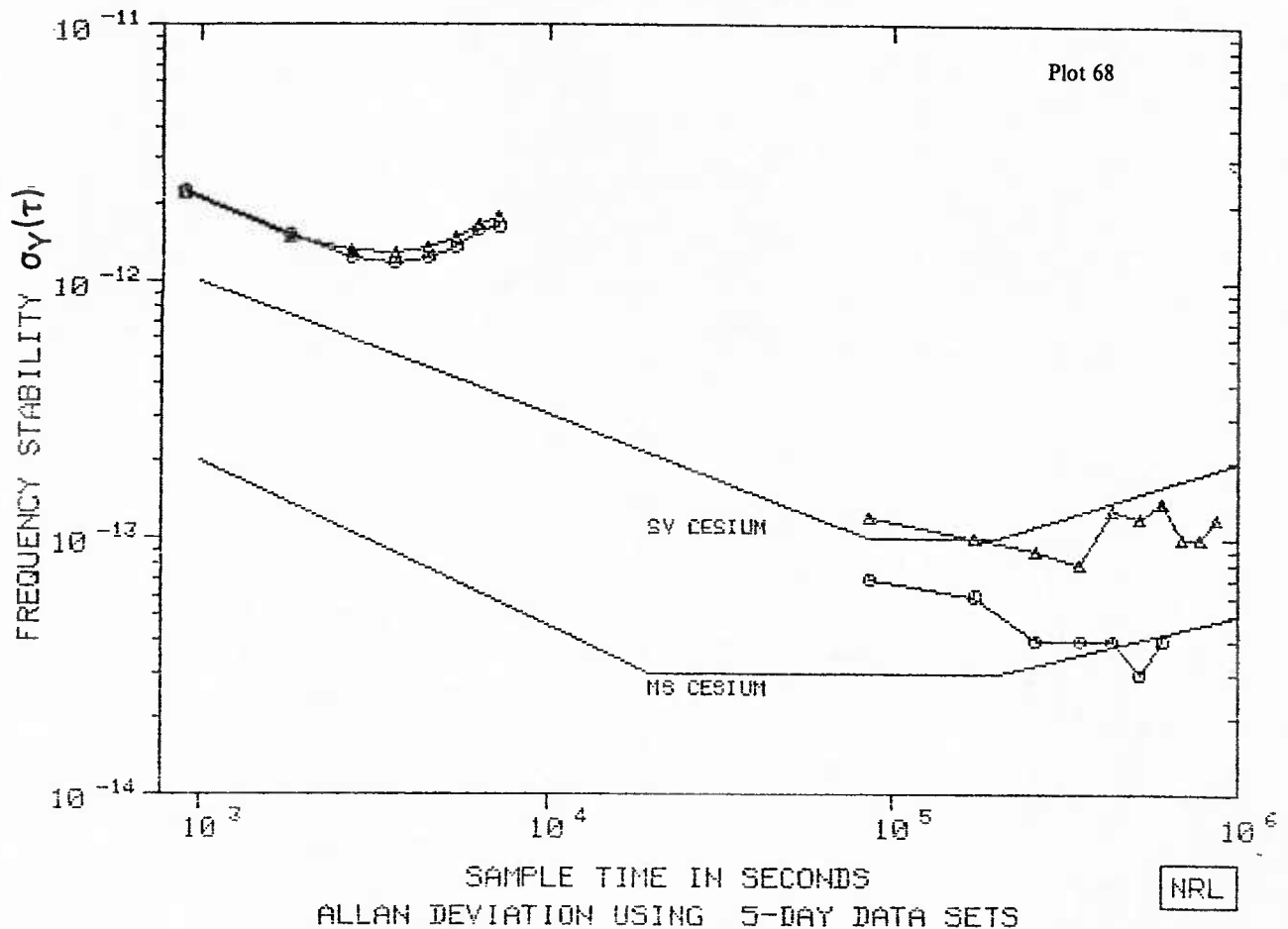
GPS
CLOCK ANALYSIS
VANDENBERG VS NAVSTAR-6



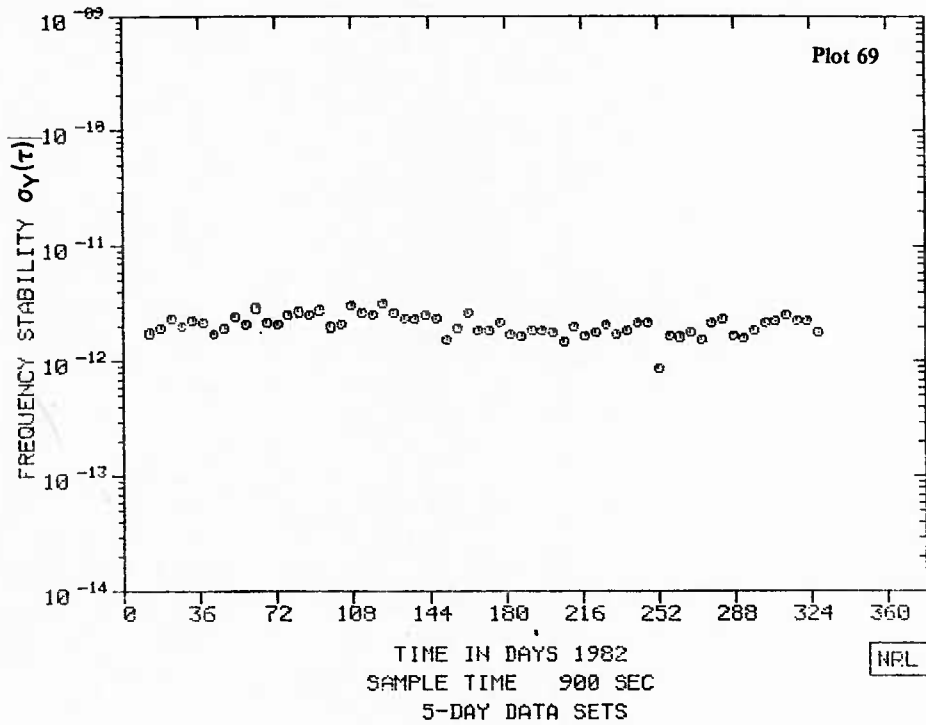
McCASKILL, BUISSON, AND STEBBINS

| | τ (HRS) | .25 | .50 | .75 | 1.00 | 1.25 | 1.50 | 1.75 | 2.00 | | |
|-----------|-----------------|------|------|------|------|------|------|------|------|------|------|
| ⊙ G83-605 | σ (PP13) | 22.2 | 15.3 | 12.3 | 11.7 | 12.3 | 13.6 | 16.0 | 15.3 | | |
| | AVG PTS | 50 | 46 | 39 | 38 | 32 | 25 | 20 | 14 | | |
| △ G82-605 | σ (PP13) | 22.0 | 14.8 | 13.2 | 12.9 | 13.5 | 14.9 | 16.5 | 17.7 | | |
| | AVG PTS | 57 | 53 | 47 | 42 | 35 | 27 | 21 | 15 | | |
| | τ (DAYS) | 1 | 2 | 3 | 4 | 5 | 6 | 7 | 8 | 9 | 10 |
| ⊙ GUA-683 | σ (PP14) | 7.0 | 6.0 | 4.0 | 4.0 | 4.0 | 3.0 | 4.0 | 4.0 | 4.0 | 4.0 |
| | TOT PTS | 47 | 37 | 32 | 24 | 21 | 17 | 14 | 9 | 8 | 4 |
| △ GUA-682 | σ (PP14) | 12.0 | 10.0 | 9.0 | 8.0 | 13.0 | 12.0 | 14.0 | 10.0 | 10.0 | 12.0 |
| | TOT PTS | 155 | 133 | 126 | 109 | 96 | 90 | 87 | 62 | 52 | 45 |

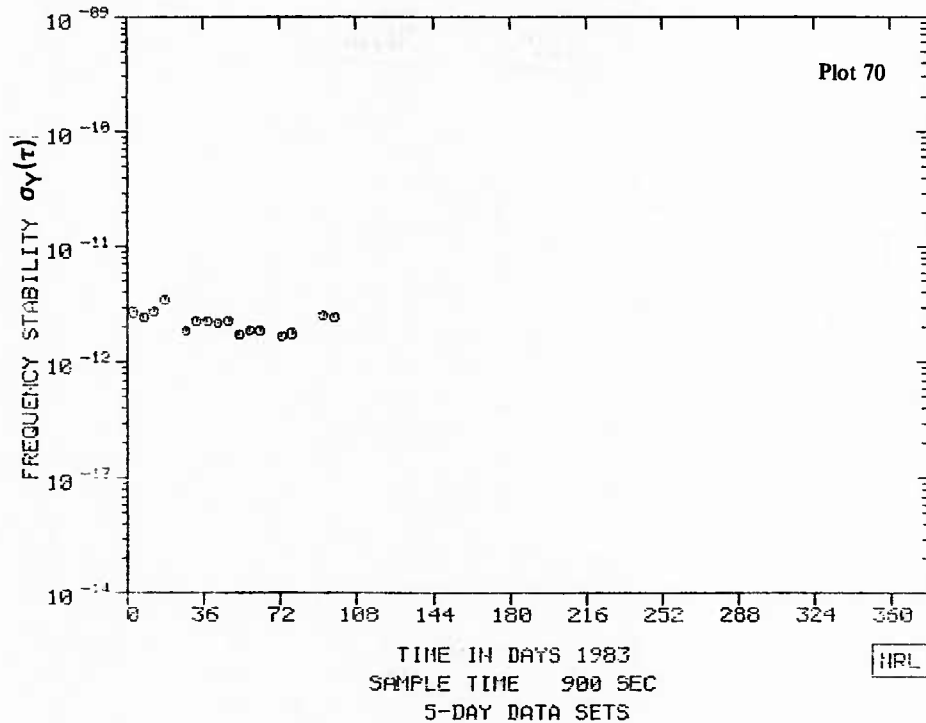
GPS
CLOCK ANALYSIS
GUAM VS NAVSTAR-6



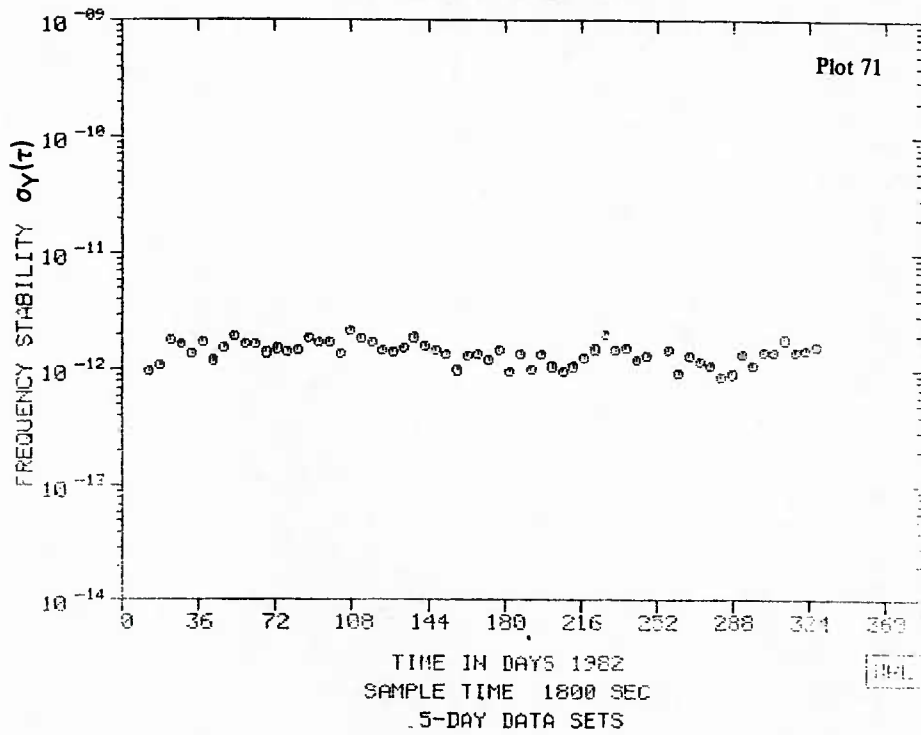
GPS
CLOCK ANALYSIS
GUAM VS NAVSTAR-6



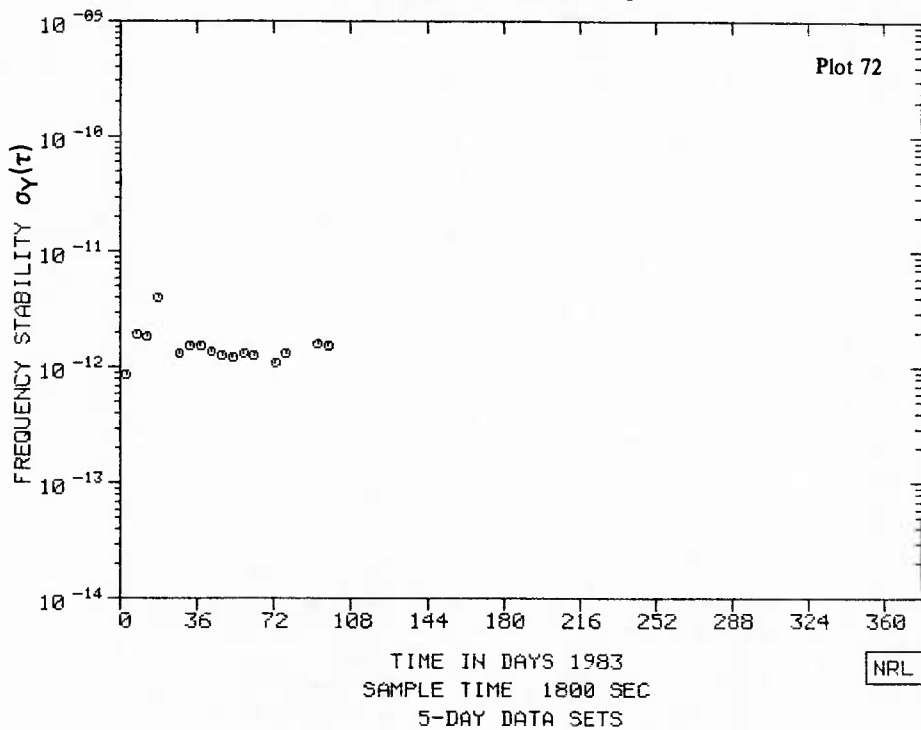
GPS
CLOCK ANALYSIS
GUAM VS NAVSTAR-6



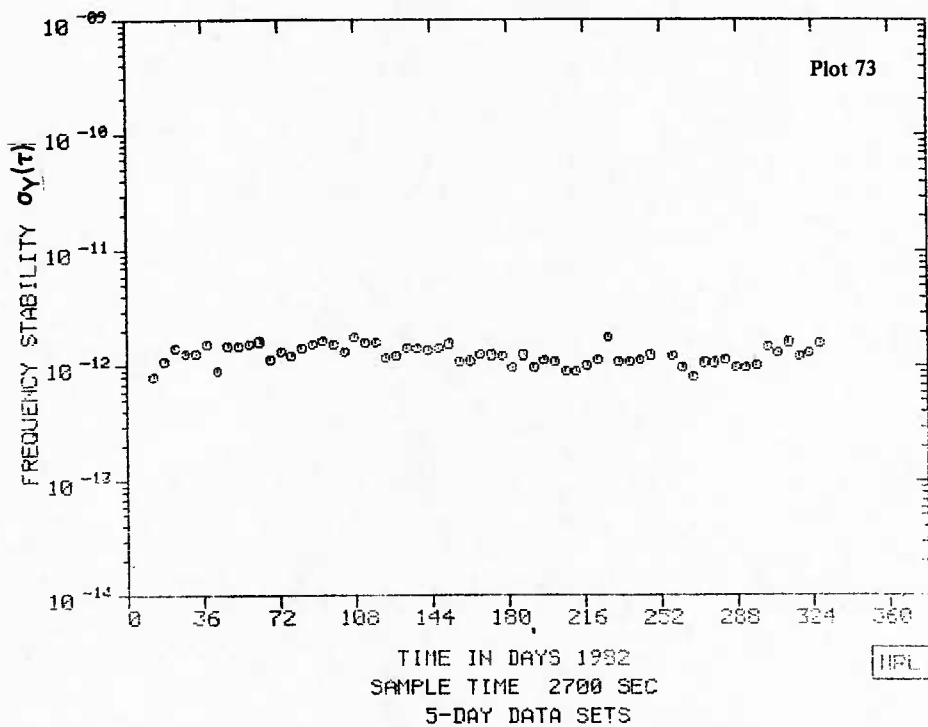
GPS
CLOCK ANALYSIS
GUAM VS NAVSTAR-6



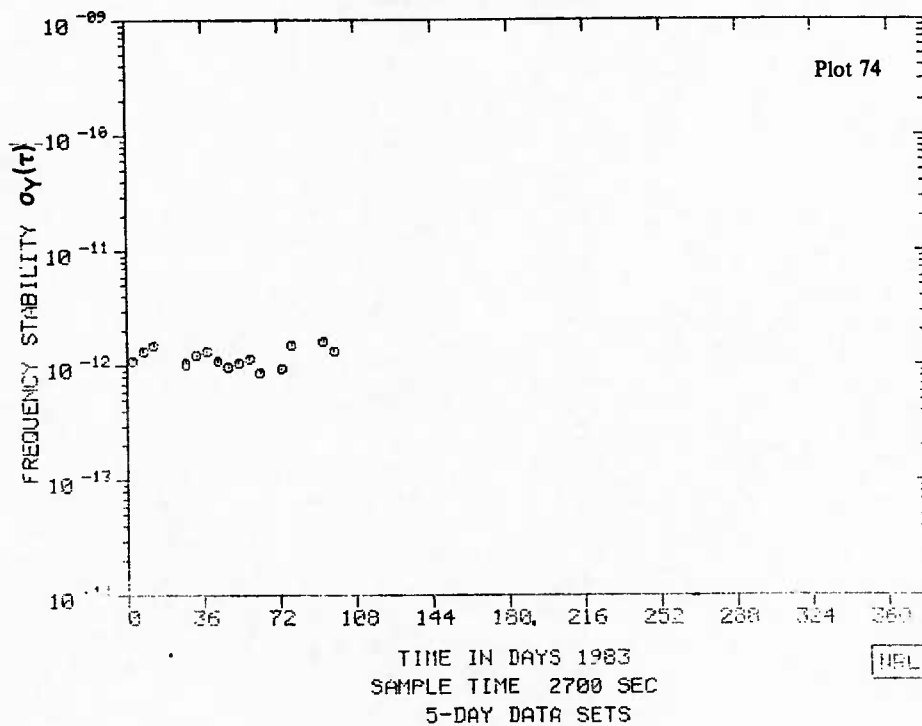
GPS
CLOCK ANALYSIS
GUAM VS NAVSTAR-6



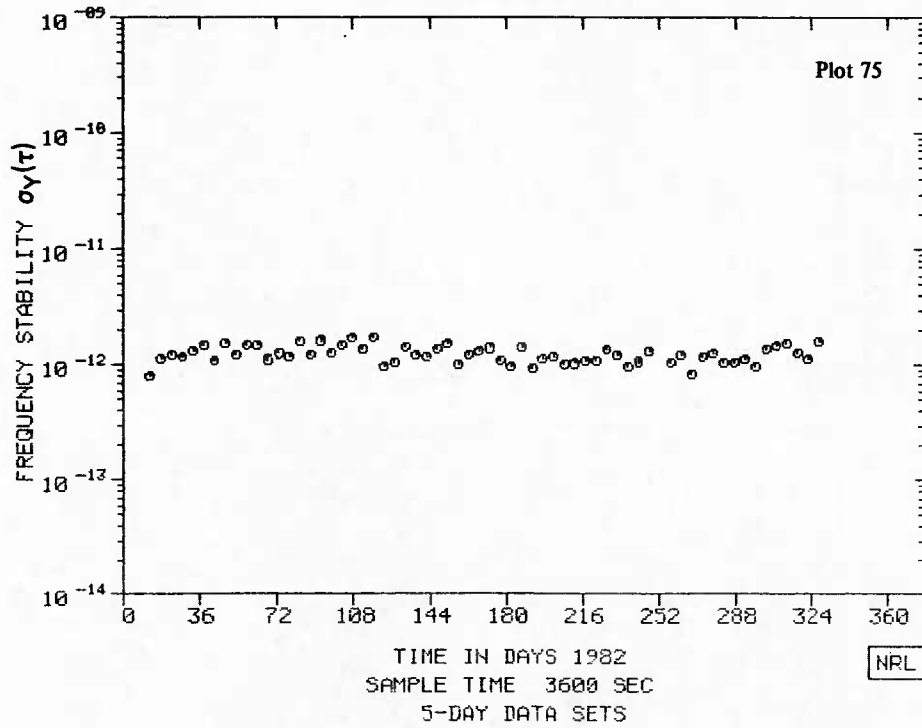
GPS
CLOCK ANALYSIS
GUAM VS NAVSTAR-6



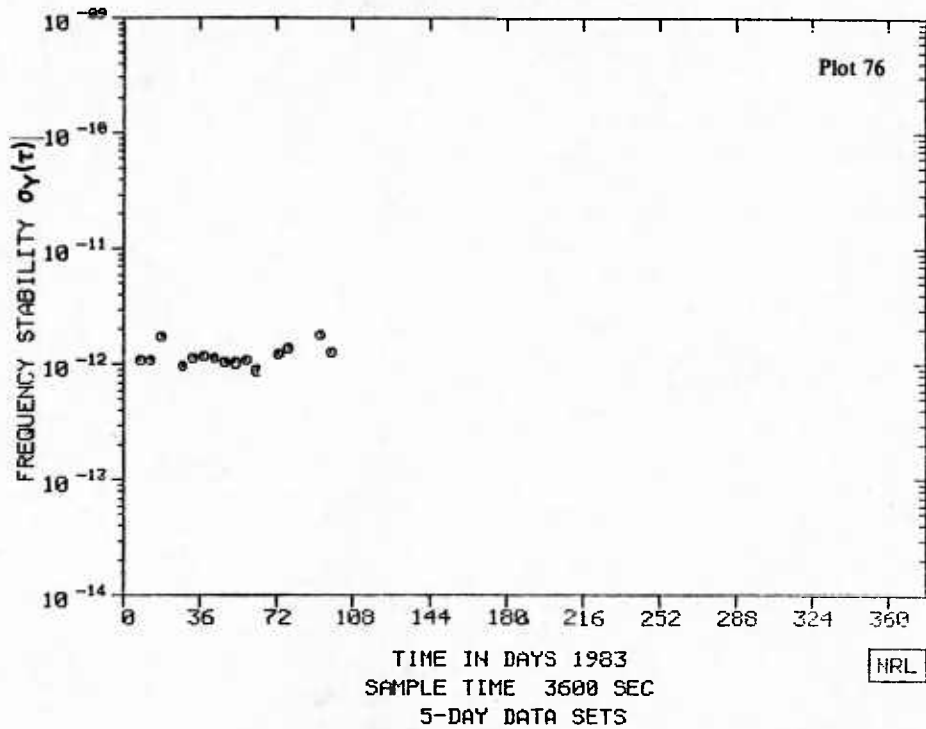
GPS
CLOCK ANALYSIS
GUAM VS NAVSTAR-6



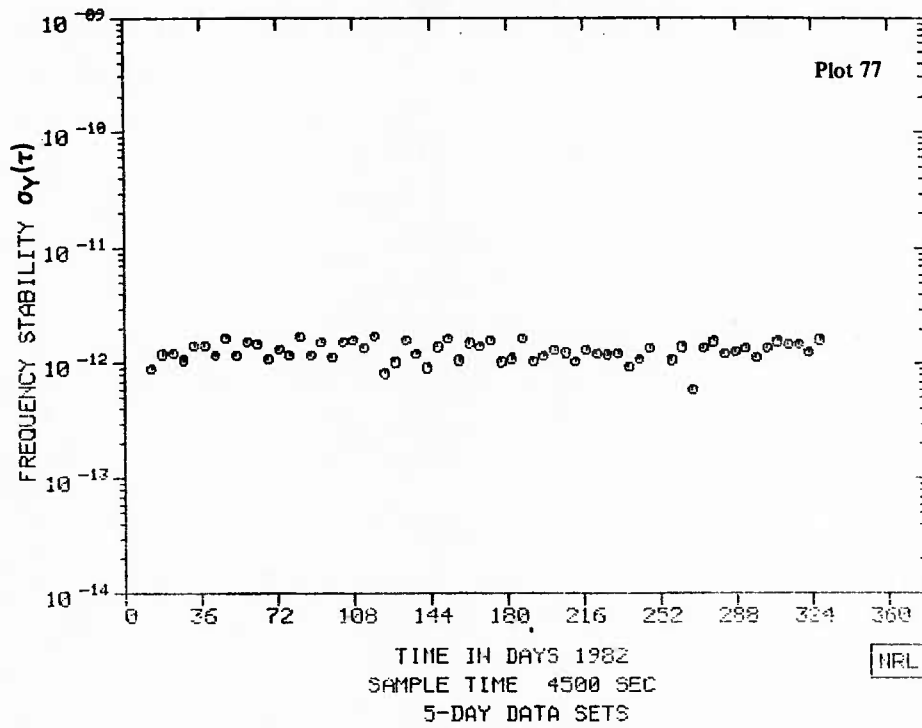
GPS
CLOCK ANALYSIS
GUAM VS NAVSTAR-6



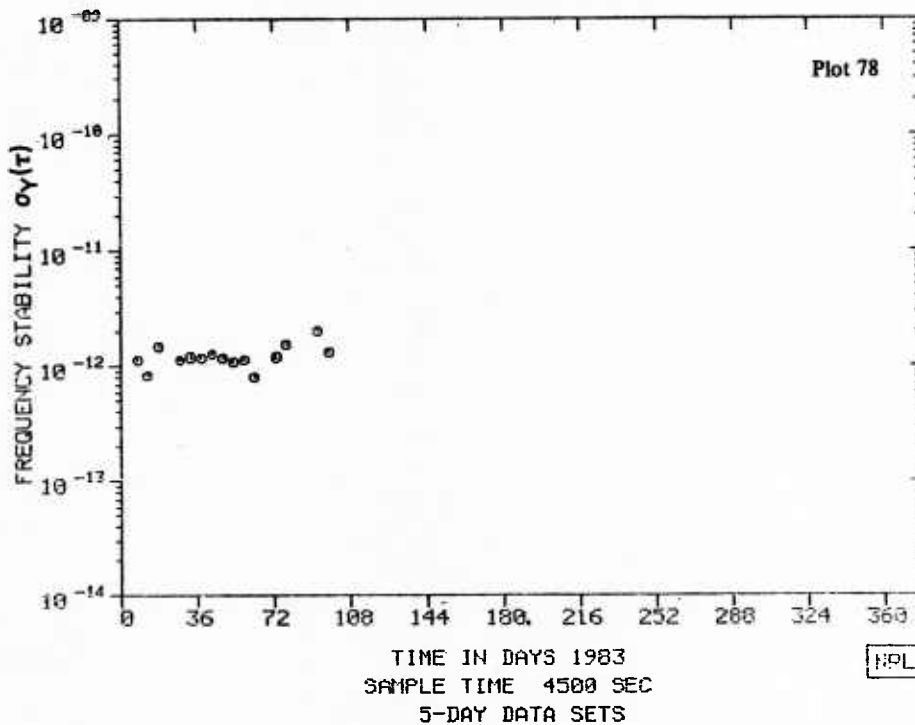
GPS
CLOCK ANALYSIS
GUAM VS NAVSTAR-6



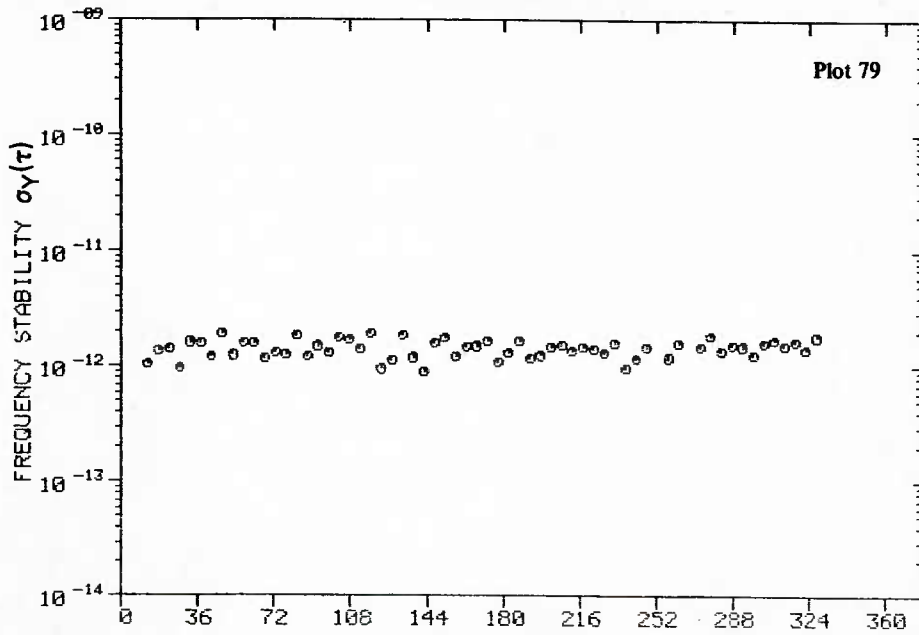
GPS
CLOCK ANALYSIS
GUAM VS NAVSTAR-6



GPS
CLOCK ANALYSIS
GUAM VS NAVSTAR-6



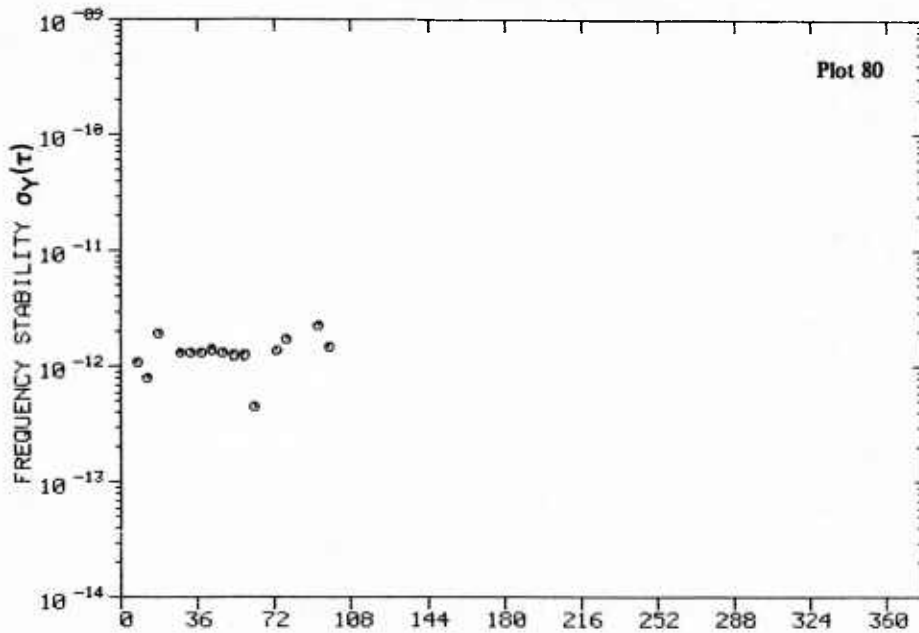
GPS
CLOCK ANALYSIS
GUAM VS NAVSTAR-6



SAMPLE TIME 5400 SEC
5-DAY DATA SETS

NRL

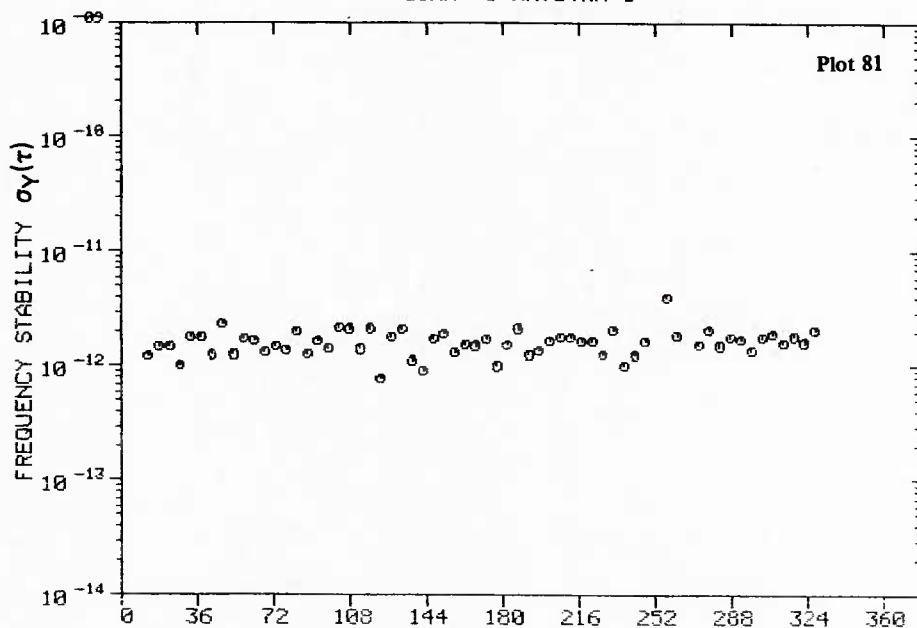
GPS
CLOCK ANALYSIS
GUAM VS NAVSTAR-6



SAMPLE TIME 5400 SEC
5-DAY DATA SETS

NRL

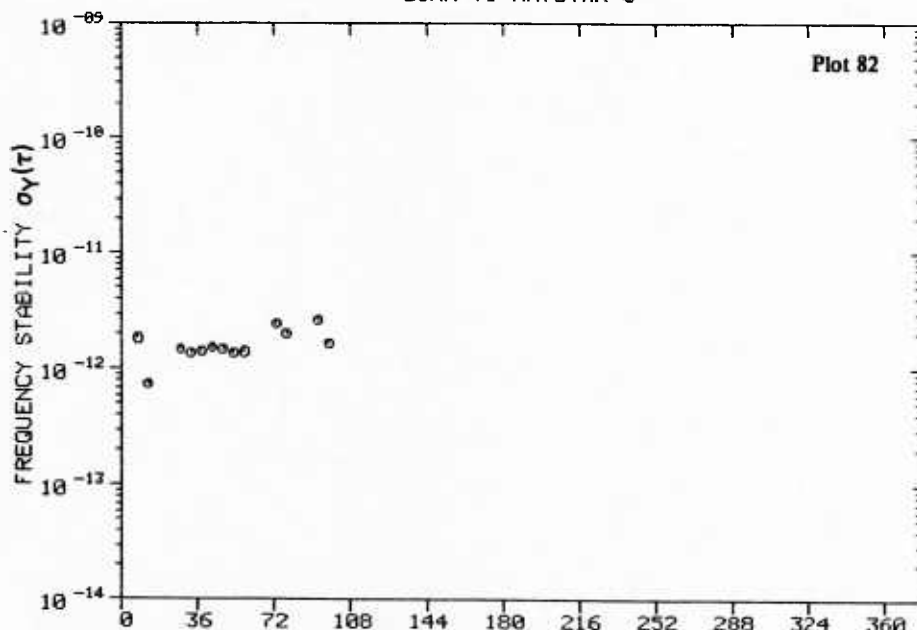
GPS
CLOCK ANALYSIS
GUAM VS NAVSTAR-6



TIME IN DAYS 1982
SAMPLE TIME 6300 SEC
5-DAY DATA SETS

NRL

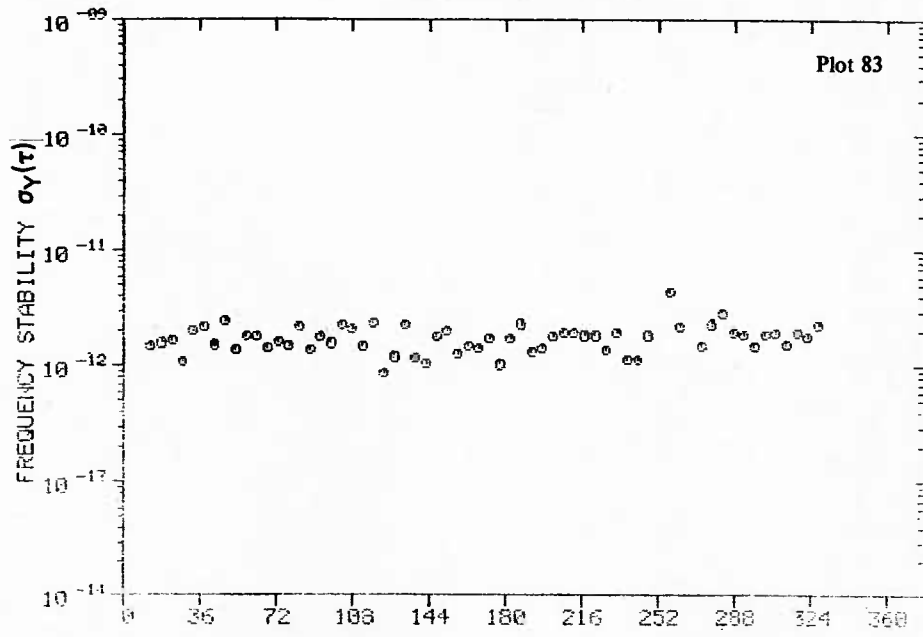
GPS
CLOCK ANALYSIS
GUAM VS NAVSTAR-6



TIME IN DAYS 1983
SAMPLE TIME 6300 SEC
5-DAY DATA SETS

NRL

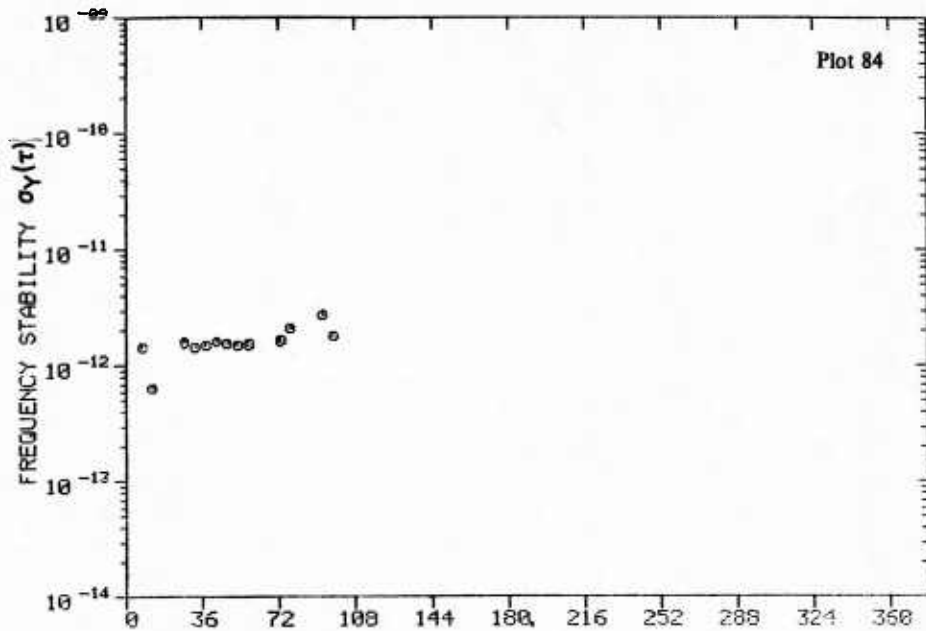
GPS
CLOCK ANALYSIS
GUAM VS NAVSTAR-6



TIME IN DAYS 1982
SAMPLE TIME 7200 SEC
5-DAY DATA SETS

NRL

GPS
CLOCK ANALYSIS
GUAM VS NAVSTAR-6

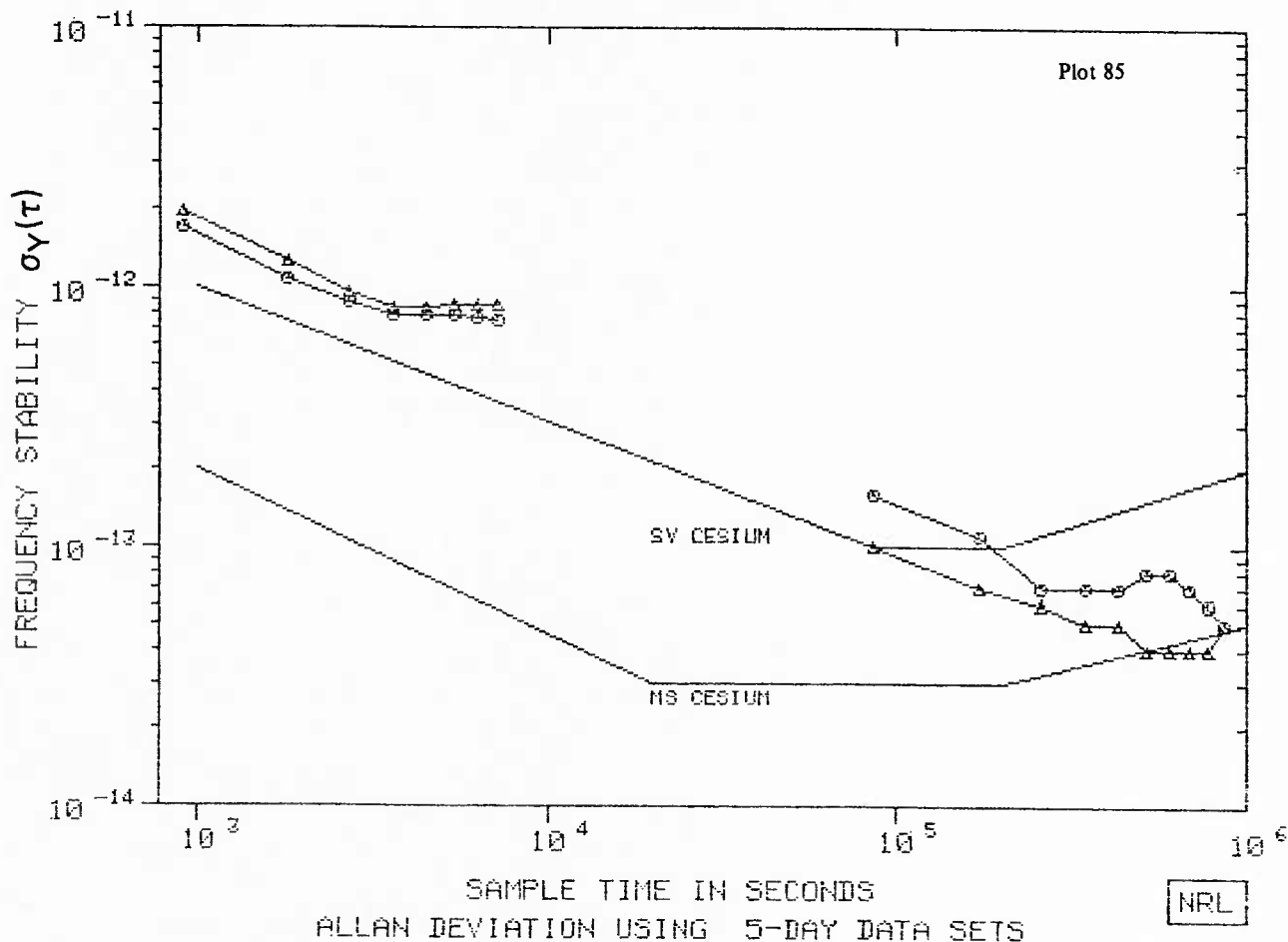


TIME IN DAYS 1983
SAMPLE TIME 7200 SEC
5-DAY DATA SETS

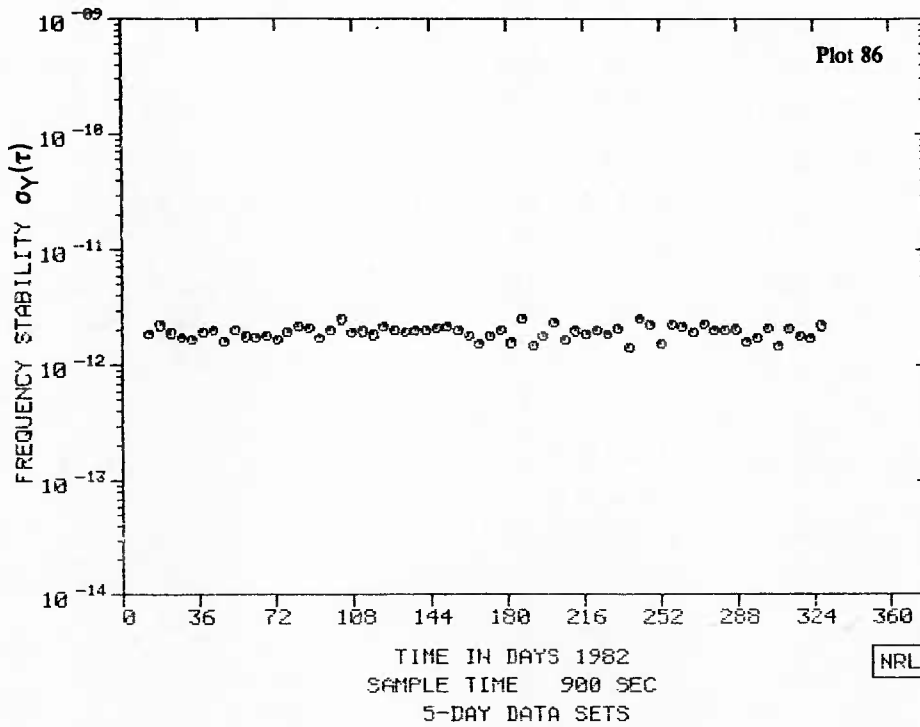
NPL

| | τ (HRS) | .25 | .50 | .75 | 1.00 | 1.25 | 1.50 | 1.75 | 2.00 | | |
|-----------|-----------------|------|------|-----|------|------|------|------|------|-----|-----|
| ○ H83-685 | σ (PP13) | 17.0 | 10.7 | 8.7 | 7.9 | 7.8 | 7.8 | 7.6 | 7.5 | | |
| | AVG PTS | 89 | 94 | 88 | 86 | 77 | 69 | 62 | 53 | | |
| △ H82-685 | σ (PP13) | 19.4 | 12.6 | 9.6 | 8.4 | 8.4 | 8.5 | 8.5 | 8.5 | | |
| | AVG PTS | 94 | 120 | 94 | 89 | 81 | 73 | 64 | 57 | | |
| | τ (DAYS) | 1 | 2 | 3 | 4 | 5 | 6 | 7 | 8 | 9 | 10 |
| ○ HAW-683 | σ (PP14) | 16.0 | 11.0 | 7.0 | 7.0 | 7.0 | 8.0 | 8.0 | 7.0 | 6.0 | 5.0 |
| | TOT PTS | 62 | 54 | 44 | 43 | 37 | 35 | 34 | 33 | 27 | 24 |
| △ HAW-682 | σ (PP14) | 10.0 | 7.0 | 6.0 | 5.0 | 5.0 | 4.0 | 4.0 | 4.0 | 4.0 | 5.0 |
| | TOT PTS | 175 | 169 | 161 | 157 | 150 | 146 | 152 | 139 | 132 | 128 |

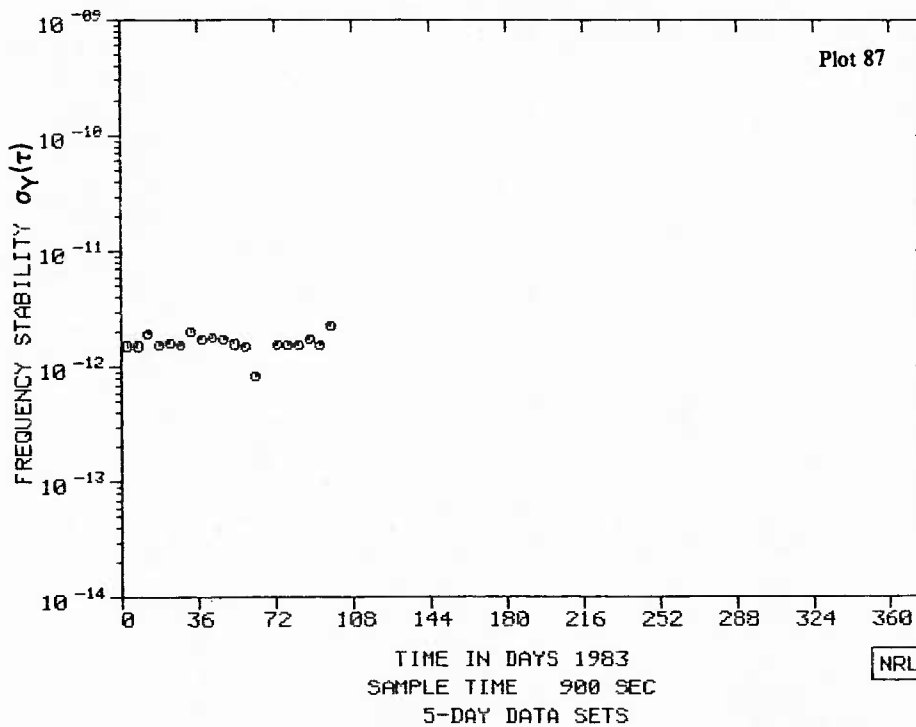
GPS
CLOCK ANALYSIS
HAWAII VS NAVSTAR-6



GPS
CLOCK ANALYSIS
HAWAII VS NAVSTAR-6

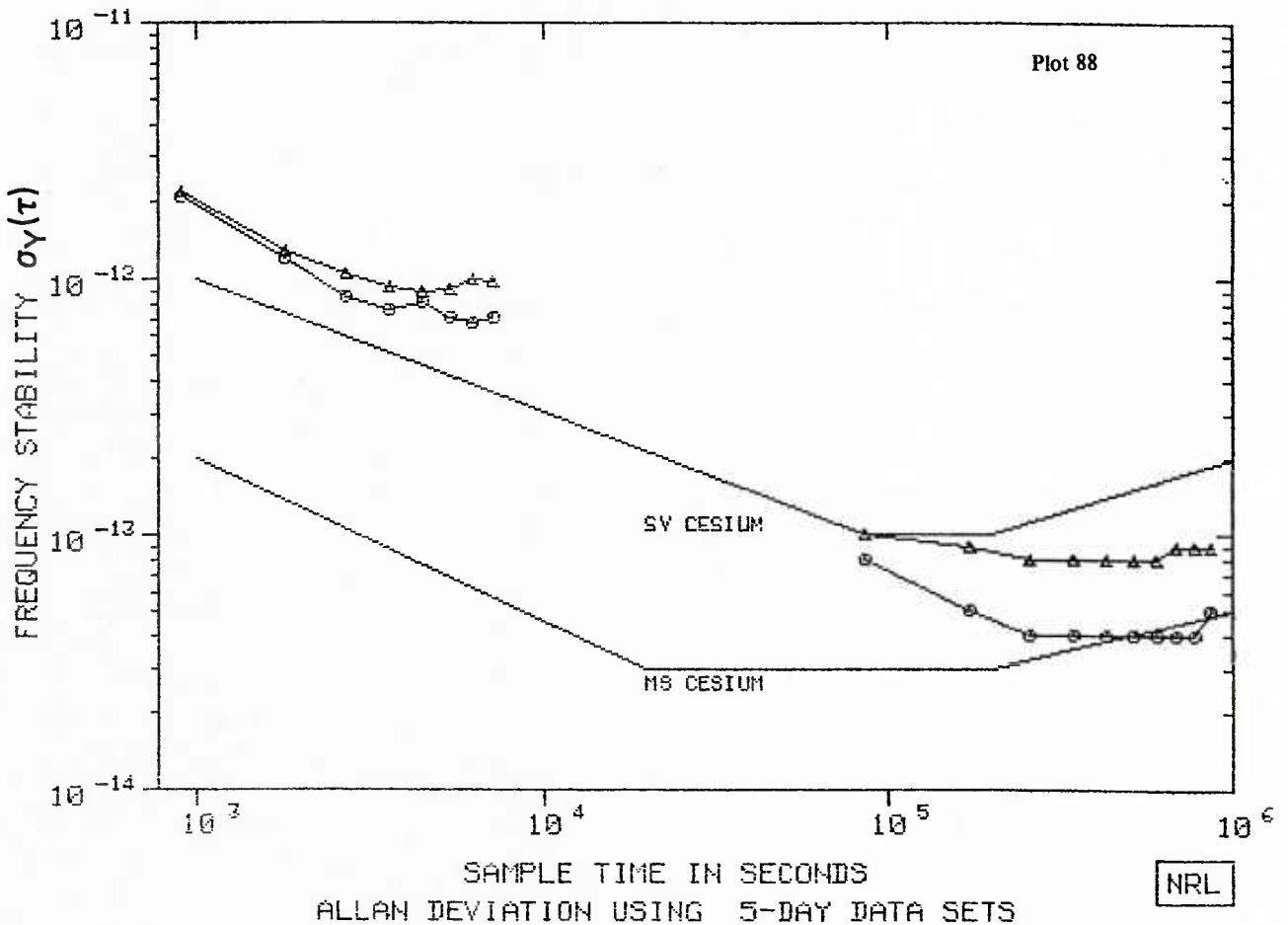


GPS
CLOCK ANALYSIS
HAWAII VS NAVSTAR-6

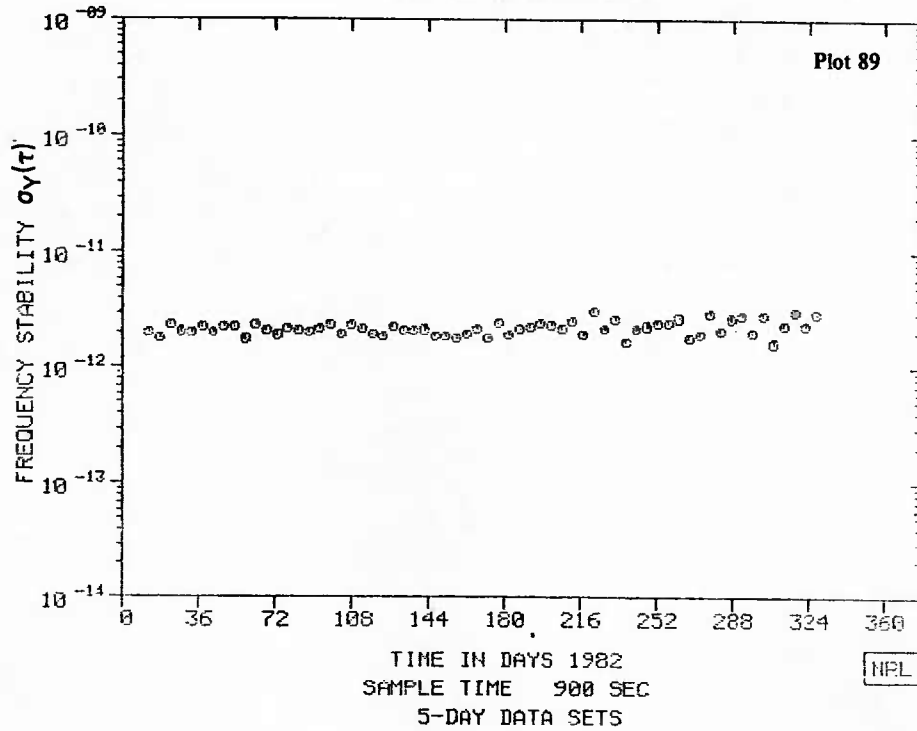


| | τ (HRS) | .25 | .50 | .75 | 1.00 | 1.25 | 1.50 | 1.75 | 2.00 | | |
|-----------|-----------------|------|------|------|------|------|------|------|------|-----|-----|
| ● A83-685 | σ (PP13) | 21.0 | 12.2 | 8.6 | 7.6 | 8.2 | 7.0 | 6.8 | 7.1 | | |
| | AVG PTS | 67 | 69 | 61 | 55 | 45 | 38 | 31 | 23 | | |
| ▲ A82-605 | σ (PP13) | 21.9 | 12.9 | 10.5 | 9.4 | 8.9 | 9.1 | 9.9 | 9.9 | | |
| | AVG PTS | 62 | 56 | 47 | 45 | 35 | 30 | 24 | 18 | | |
| | τ (DAYS) | 1 | 2 | 3 | 4 | 5 | 6 | 7 | 8 | 9 | 10 |
| ● ALK-683 | σ (PP14) | 8.0 | 5.0 | 4.0 | 4.0 | 4.0 | 4.0 | 4.0 | 4.0 | 4.0 | 5.0 |
| | TOT PTS | 78 | 77 | 69 | 67 | 67 | 60 | 61 | 52 | 50 | 49 |
| ▲ ALK-682 | σ (PP14) | 10.0 | 9.0 | 8.0 | 8.0 | 8.0 | 8.0 | 8.0 | 9.0 | 9.0 | 9.0 |
| | TOT PTS | 235 | 225 | 210 | 203 | 190 | 191 | 211 | 168 | 170 | 159 |

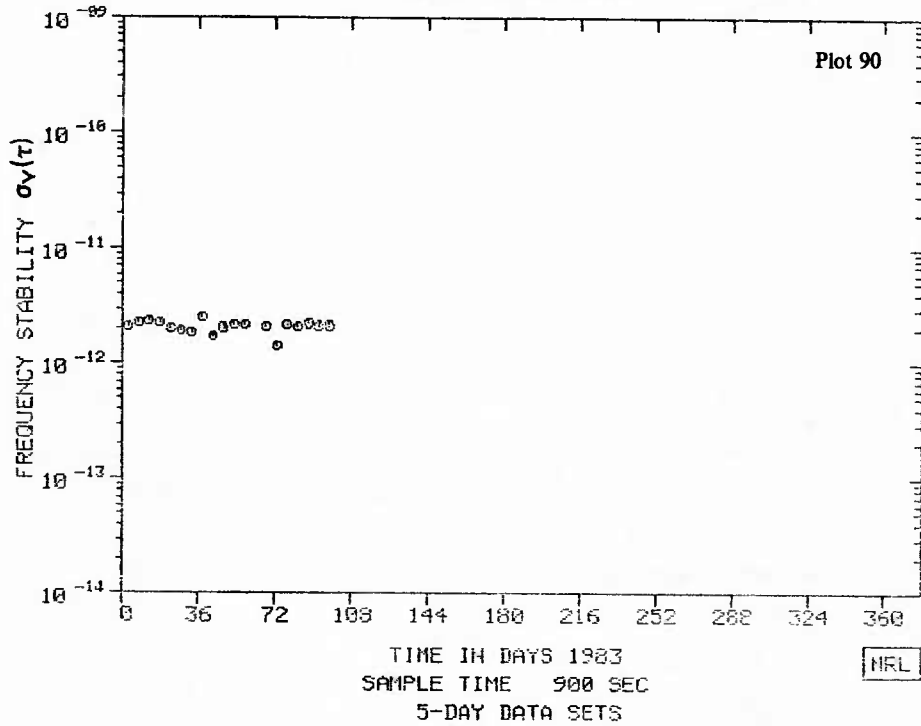
GPS
CLOCK ANALYSIS
ALASKA VS NAVSTAR-6



GPS
CLOCK ANALYSIS
ALASKA VS NAVSTAR-6



GPS
CLOCK ANALYSIS
ALASKA VS NAVSTAR-6



U211610

DEPARTMENT OF THE NAVY

NAVAL RESEARCH LABORATORY
Washington, D.C. 20375

OFFICIAL BUSINESS

PENALTY FOR PRIVATE USE, \$300

SUPERINTENDENT
U.S. NAVAL POSTGRADUATE SCHOOL
ATTN: TECHNICAL LIBRARY
MONTEREY, CA 93940



POSTAGE AND FEES PAID
DEPARTMENT OF THE NAVY
DoD-316
THIRD CLASS MAIL



U S F O T O